T-4504

A THERMODYNAMIC STUDY OF THE FORMATION OF GASEOUS HYDROXIDES OF VANADIUM, MOLYBDENUM AND TUNGSTEN

by

José Luis Sánchez Osio

A thesis submitted to the Faculty and Board of Trustees of the Colorado School of Mines in partial fulfillment of the requirements for the degree of Doctor of Philosophy (Metallurgical and Materials Engineering).

Golden, Colorado

Date 12/06/93

Signed: José Luis Sánchez Osio

José Luis Sánchez Osio

Approved: John P. Hager

Dr. John. P. Hager

Golden, Colorado

Date 12/5/93

J. J. Moore

Dr. John. J. Moore
Department Head
Metallurgical and Materials Engineering

ABSTRACT

The formation of volatile hydroxides of vanadium, molybdenum and tungsten has been investigated using the transpiration technique. It was established that the principal hydroxide species formed in the presence of $V_2O_5(s)$, $MoO_3(s)$ and $WO_3(s)$ are $VO(OH)_3$, $MO_2(OH)_2$ and $WO_2(OH)_2$, respectively, according to:

$$(1) \quad V_2O_5(s) + 3\,H_2O(g) = 2\,VO(OH)_3(g)$$

$$(2) \quad MoO_3(s) + H_2O(g) = MoO_2(OH)_2(g)$$

$$(3) \quad WO_3(\alpha,\beta) + H_2O(g) = WO_2(OH)_2(g)$$

The vapor pressures of these volatile hydroxides were measured as a function of temperature, water pressure, oxygen pressure and flowrate. The results have been used to determine their Gibbs free energy of reaction as a function of temperature, according to the above reactions:

$$(1) \quad \Delta G^{\circ} = 57{,}938 - 14.46\,T \quad \text{(cal/mole)} \quad 560\text{-}650\ ^{\circ}C$$
$$\Delta G^{\circ} = 242{,}413 - 60.50\,T \quad \text{(J/mole)}$$

$$(2) \quad \Delta G^{\circ} = 31{,}143 - 19.57\,T \quad \text{(cal/mole)} \quad 580\text{-}702\ ^{\circ}C$$
$$\Delta G^{\circ} = 130{,}302 - 81.88\,T \quad \text{(J/mole)}$$

$$
\begin{aligned}
(3)\quad \Delta G^{o}_{\alpha} &= 39{,}733 - 18.00\ T \quad (\text{cal/mole}) \qquad 699\text{-}778\ ^{o}C\\
\Delta G^{o}_{\alpha} &= 166{,}243 - 75.31\ T \quad (\text{J/mole})\\
\Delta G^{o}_{\beta} &= 40{,}162 - 18.40\ T \quad (\text{cal/mole}) \qquad 778\text{-}985\ ^{o}C\\
\Delta G^{o}_{\beta} &= 168{,}038 - 76.99\ T \quad (\text{J/mole})
\end{aligned}
$$

The enhancement of the vapor pressure of V_2O_3(s) in the presence of water vapor was also studied. For this oxide of vanadium, however, no evidence of vapor transport was observed.

The generated thermodynamic knowledge has been used to devise process conditions for the extraction and recovery of Mo, V and W in feedstocks and wastes through vapor transport. The results showed that for V_2O_5(s), significant pressures of the volatile hydroxides are realized at temperatures at least at 1250 °C and water vapor pressures of 5 atm. In the case of MoO_3(s), on the other hand, it was determined that high vapor pressures of the molybdenum hydroxides are obtained at temperatures slightly below the melting point (795 °C) and water pressures of 1 atm. For the case of WO_3(s), it was established that high vapor pressures of the volatile hydroxides were achieved at temperatures of 1150 °C and water vapor pressures of 1 atm.

Finally, in order to minimize losses of MoO_3(s) and WO_3(s) based materials, when exposed to water vapor, it is recommended to operate at temperatures below 500 °C for molybdenum, and below 700 °C for tungsten. Moreover, based on the observation that volatile vanadium hydroxides significantly attack silica, the use of substrates other than quartz is recommended, where catalysts are to be used in the presence of V_2O_5(s) and water vapor.

The results of this study also served to resolve the disagreements found in the literature for the enhanced vapor transport of V, Mo and W in the presence of water vapor.

TABLE OF CONTENTS

LIST OF TABLES

LIST OF FIGURES

ACKNOWLEDGMENTS

The author would like to express his appreciation to his advisor Dr. John P. Hager for his invaluable guidance and support throughout the period of this research. Also, the author would like to extend especial thanks of his comitee members Dr. G. Martins, Dr. J. Ely, Dr. J. Moore and Dr. R. Cohen, for their contributions in resolving some technical and experimental problems encounter during this investigation.

Financial support for this research was provided by the U.S. Bureau of Mines Generic Mineral Technology Center for Pyrometallurgy, under grants G1175129, G1105129, G1115129 and G1125229.

Thanks are also expressed to Guy Frederickson, Jerry Downey, Carlos da Silva, Lindor Geraldo, Jae-Ho Lee and Jason Sallee for their friendship and assistance. Special thanks to my wife Alicia and my brother Alberto for their continuous enthusiasm and support.

DEDICATION

The author dedicates this thesis to his parents Alberto and Bertha Sánchez who he has admired and respected all his life.

I. INTRODUCTION

The vapor transport of refractory metals from feedstocks and wastes does not appear to be a feasible extraction method based on the data available in the JANAF tables[2] and the USBM bulletin # 672[1]. However, unusual vapor transport of transition metals have been observed by some investigators[12,14,15,16,47], in the presence of water vapor. They suggest that, although the hydrates of transition metals usually decompose when heated above 300 °C, the metals can form bonds with gaseous water molecules strong enough to dislodge the oxides from their crystal lattices[45].

The findings of these investigators are interesting, and suggest the possibility of exploring the formation of volatile hydroxides as a means of selectively extracting refractory metals and their oxides from feedstocks and wastes. However, their results still remain inconclusive due to the discrepancies in the reported molecularity of the volatile hydroxides formed, as well as in the magnitudes of the observed apparent vapor pressures. In the patent by Chambers[17], for example, a high recovery of vanadium is reported (56 wt. % in 2 hrs at 745 °C), while other investigators observed significantly more modest vapor pressures, under similar conditions.

Given the inconclusive results on the formation of volatile hydroxides and the exciting possibility of devising new extractive processes based on the enhancement of the volatility of refractory metals, a systematic study on the formation of volatile hydroxides was undertaken with two objectives, in mind. The first objective was to generate accurate and conclusive fundamental thermodynamic data on the enhancement of the volatility of at least three refractory metals, known to form volatile hydroxides. The second objective was to devise new vapor transport schemes for the recovery and extraction of refractory metals.

Four refractory metal oxides were chosen for this study: $V_2O_5(s)$, $V_2O_3(s)$, $MoO_3(s)$ and $WO_3(s)$. These metals oxides were chosen because they are frequently found in wastes from metallurgical process such as slags, and because they are extensively used as catalysts in petrochemical processes under atmospheres containing water vapor.

The transpiration technique was selected for this study because it allows the measurement of vapor pressures under precisely controlled atmospheres. Thus, by specifying an adequate oxygen potential throughout the experiments, the integrity of the condensed phases can be maintained. For each of the chosen metal oxides, experiments were first conducted in the absence of water vapor. The purpose of these experiments was to measure the contribution of the volatile oxides to the total vapor pressure. This was an important consideration because in the transpiration technique only total vapor pressures can be measured. Consequently, in order to quantify the vapor pressures of the volatile hydroxides from the total measured vapor pressure, the contribution of any volatile oxides had to be taken into account. Thus, after the baseline vapor chemistry for each oxide was established, the study of the enhancement of the volatility of the chosen metal oxides in the presence of water vapor was undertaken.

As a result of this investigation, the vapor transport chemistries of V_2O_5(s), V_2O_3(s), MoO_3(s), and WO_3(s) in the presence of water vapor have finally been resolved. Also, based on the fundamental thermodynamic data generated in the present investigation, new vapor transport chemistries for the extraction, recovery, and conservation of vanadium, molybdenum, and tungsten, are proposed.

II. LITERATURE REVIEW

A comprehensive literature review was conducted to identify and review the available data necessary to characterize and quantify the vapor transport chemistries of $V_2O_5(s)$, $V_2O_3(s)$, $MoO_3(s)$, and $WO_3(s)$. From this review, the stability ranges of these oxides were first established in order to determine the experimental conditions that would assure their integrity throughout the experiments. If conditions too reducing were used, the condensed phase would disproportionate into a lower oxide and oxygen. Thus the measured vapor pressures would be of a compound other than the one of interest. On the other hand, if the sample was not in its highest oxidation state and conditions too oxidizing were imposed, it would oxidize to a different compound. Such is the case of $V_2O_3(s)$, which requires a reducing atmosphere to maintain its integrity.

Once the stability ranges of the condensed phases had been established, the next step was to review the proposed vapor transport chemistries in the absence of water vapor (baseline vapor chemistries) to determine the contribution of the predominant volatile oxides to the total vapor pressure at the temperatures ranges of interest in this study. To account for these contributions was important because in the experimental technique utilized in this investigation (the transpiration technique), only the total vapor pressure can be measured. Thus, in order to obtain the vapor pressure of any of the formed hydroxides, the vapor pressures of the volatile oxides had to be subtracted from the total vapor pressure.

Finally, once the baseline vapor chemistries had been characterized, the third step was to review the available literature on the formation of volatile hydroxides with $V_2O_5(s)$, $V_2O_3(s)$, $MoO_3(s)$, and $WO_3(s)$. The results of this literature review, for each of the above mentioned oxides, are presented in the following sections of this chapter.

2.1 Vanadium Pentoxide

The first objective in this literature review was to establish the stability range of the condensed phases of the vanadium-oxygen system. The thermodynamic data reported in USBM bulletin # 672[1] and the JANAF tables[2] list V(s), VO(s), $V_2O_3(s)$, $V_2O_4(s)$, and $V_2O_5(s)$ as the only stable solid condensed phases. However, the vanadium-oxygen system is far more complicated and a large number of oxide phases have been reported. Matsui and Naito[3] carried out an extensive literature review and reported an updated phase diagram for the V-O system (see Figure 2.1). As can be appreciated, a wide range of stable phases exist between V(s) and $V_2O_5(s)$. The complexity of this system is not surprising because vanadium, being a transition metal with an atomic radius approximately 1.89 times larger than that of oxygen, is highly susceptible to oxygen interstitial dissolution[4].

The thermodynamic properties of the V_2O_{5-x} system ($0 < x < 1$) are thus very complicated and depend on the temperature, oxygen pressure, and composition of the system. At $x < 0.43$ and around 600 °C, for example, the phases that coexist are V_2O_5 and V_6O_{13}. Cooling the system, however, results in the formation of V_3O_7[5]. Vanadium

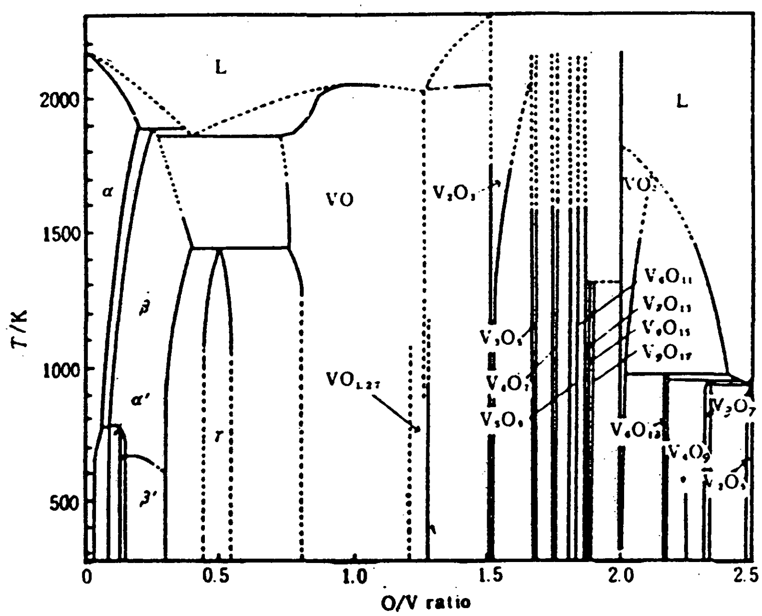

Figure 2.1 Phase diagram for the V-O system[3].

pentoxide is the highest oxide in the V-O system and is a red-yellowish acidic compound with a rhombohedral structure[6]. The O/V homogeneity range for vanadium pentoxide, as reported by Dziembaj and Piwowarczyk, is between 2.49 and 2.5[7]. In their study, they suggested that at the vicinity of 600 °C, the equilibrium reaction for the decomposition of $V_2O_5(s)$ in the presence of oxygen is:

$$V_2O_5(s) = V_6O_{13}(s) + O_2(g) \tag{2.1}$$

From their measurements, assuming $\Delta C_p° = 0$ in the temperature range of 575 to 615 °C, they estimated the values for $\Delta H°$ and $\Delta S°$ as:

$$\Delta H° = -63.50 \pm 0.46 \quad \text{(kcal/mole of } O_2\text{)}$$

$$\Delta S° = -44.84 \pm 0.55 \quad \text{(cal/mole of } O_2\text{)}$$

Using this data and assuming $\Delta C_p° = 0$ (in the absence of additional data) in the range of 550 to 660 °C, equilibrium partial pressures for the decomposition of $V_2O_5(s)$ were calculated and theoretical experimental limits estimated. In this temperature range the calculated decomposition pressures are in the order of 10^{-8} to 10^{-5} atm. These pressures are significantly lower than the pressures used in this investigation ($0.10 < P_{O2} < 1$ atm) for the same temperature range. Therefore, no difficulties were encountered in preventing the decomposition of $V_2O_5(s)$.

2.1.1 Baseline Vapor Chemistry of $V_2O_5(s,l)$

In order to study the vapor transport chemistry of $V_2O_5(s)$ in the presence of water vapor, it was first necessary to identify the principal vapor species formed in the absence of water vapor and determine their contribution to the total vapor pressure. Thus, the baseline vapor chemistry of $V_2O_5(s)$ was first investigated.

Available references were reviewed concerning the vaporization of $V_2O_5(s,l)$. The earliest experiments date back to 1946 with the work of Polyakov[8] who concluded that $V_2O_5(l)$ vaporized congruently as $V_2O_5(g)$ when subjected to a 1 atm oxygen pressure for the temperature range of 700 to 1200 °C. Their results were summarized as:

$$V_2O_5(l) = V_2O_5(g) \tag{2.2}$$

$$\Delta G^\circ = 32{,}266.9 - 12.8\,T \quad \text{(cal/mole of } V_2O_5(g))$$

Berkowitz, Chupka and Inghram[9] qualitatively studied $V_2O_5(s)$ employing a mass spectrometer and found no evidence of $V_2O_5^+$ ions. They observed initial peaks corresponding to $V_4O_{10}(g)$ and $V_4O_8(g)$ with subsequent formation of $V_6O_{14}(g)$, $V_2O_{12}(g)$, and $V_2O_4(g)$. The appearance of the latter three molecules was attributed to the decomposition of the $V_2O_5(s)$. Due to their inability to maintain a constant composition of the condensed phase (an indication that $V_2O_5(s)$ did not vaporize congruently), they were unable to make quantitative determinations. Their observation that $V_2O_5(s)$ did not vaporize congruently is in agreement, however, with the observations of Frantseva and Semenov[10] that $V_2O_3(s)$ is the only vanadium oxide that vaporizes congruently.

Farber, Uyy, and Srivastava[11] also studied the vapor transport chemistry of $V_2O_5(s)$ with an effusion-mass spectrometer in the temperature range of 730 to 932 °C. They observed the same behavior as Berkowitz et al. and in order to obtain quantitative data, they ran several experiments for only a few minutes each (until the vapor pressures of $V_4O_{10}(g)$ and $V_4O_8(g)$ became unstable). Farber et al.'s results were summarized as:

$$2V_2O_5(s) = V_4O_{10}(g) \tag{2.3}$$

$$\Delta G^\circ = 23{,}439.53 + 4.07\ T \quad \text{(cal/mole of } V_4O_{10}(g))$$

$$2V_2O_5(s) = V_4O_8(g) + O_2(g) \tag{2.4}$$

$$\Delta G^\circ = 110{,}348.17 - 39.86\ T \quad \text{(cal/mole of } V_4O_8(g))$$

The ΔG° equations shown above were derived based on the reported free energy function (gef) data. The calculated values of ΔG° were correlated with temperature by the method of least square linear regression. Although it would have been preferred to correlate the Sigma function (see page 73) with temperature, heat capacity data could not be located for $V_4O_{10}(g)$ and $V_4O_8(g)$.

Yannopoulos[12] studied the vapor transport chemistry of V_2O_5(s,l) using a transpiration apparatus at a temperature range of 639 to 899 °C. He did not observe, within his detection limits, any volatilization.

Semenov et al.[13], also using a transpiration apparatus with oxygen as the carrier gas, measured the volatilization of V_2O_5(l) in the temperature range of 942 to 1257 °C. They proposed congruent volatilization according to:

$$2V_2O_5(l) = V_4O_{10}(g) \tag{2.5}$$

$$\Delta G^\circ = 27{,}021.64 + 1.65\ T\ (\text{cal/mole of } V_4O_{10})$$

Suito and Gaskell[14] studied the volatilization above liquid mixtures of V_2O_5 and V_2O_4 over the temperature range of 900 to 1099 °C using a transpiration apparatus. They observed congruent volatilization of the melt, as well as a dependance of the gaseous species on the oxygen potential and melt composition. From their experimental work they proposed two simultaneous reactions for the vaporization of V_2O_5(s):

$$VO_2(s) = VO_2(g) \tag{2.6}$$

$$\Delta G^\circ = 32{,}930 - 1.55\ T\ (\text{cal/mole of } VO_2(g))$$

$$VO_{2.5}(l) + \frac{1}{4}O_2(g) = VO_3(g) \tag{2.7}$$

$$\Delta G^\circ = 39{,}610 - 7.7\ T\ (\text{cal/mole } VO_3(g))$$

Also, they proposed the following reaction for the gas phase:

$$VO_2(g) + \frac{1}{2}O_2(g) = VO_3(g) \tag{2.8}$$

$$\Delta G° = -2{,}210 - 2.33\ T\ \text{(cal/mole } VO_3(g))$$

The JANAF tables[2] and USBM bulletin 672[1] report the existence of two gaseous vanadium oxides, VO(g) and VO_2(g). The calculated total vapor pressure for these gaseous species above V_2O_5(s) at 600 °C and 1 atmosphere of O_2, is in the order of 10^{-20} atm. These remarkably low vapor pressures suggest a practically null volatilization of vanadium pentoxide at the conditions studied in this investigation.

A table presenting the apparent vapor pressures at selected temperatures by the different investigators was constructed for comparison purposes (see Table 2.1). It was observed from this comparison that, except for the work of Polyakov (extremely high vapor pressure) and the calculated pressures from USBM bulletin 672 and JANAF tables (extremely low vapor pressure), the reported apparent vapor pressures from the different researchers were comparable in magnitude.

Since the purpose of this investigation was to study the vapor transport chemistry of solid V_2O_5 (mp. 677 °C), the working temperatures used were around 600°C. As seen from Table 2.1, when the work of the different investigators was extrapolated to 600 °C, the calculated vapor pressures, except for the work of Polyakov, were in the range of $10^{-8.6}$ to $10^{-6.8}$. These pressures are extremely low and would be difficult to detect in the transpiration apparatus used in this study, whose sensitivity limit was $10^{-6.6}$ atm. Such was the case of Yannopoulos who, as mentioned earlier, was not able to detect any volatilization of V_2O_5(s,l) using the transpiration technique.

Table 2.1 Comparison of the Vapor Pressures Reported by the Different Investigators for V_2O_5, Pressures in Atmospheres

Investigators	T °C	P_{O2}	Log $P_{Apparent}$	Main Reactions Proposed
Polyakov[8]	600	_	-5.64$^{(1)}$	$V_2O_5(s) = V_2O_5(g)$
	700	_	-4.35	
	900	_	-3.39	
	1000	_	-2.75	
	1100	_	-2.29	
	1200	_	-1.93	
Berkowitz et al.[8, 9]		not reported		$2\ V_2O_5(s) = V_4O_{10}(g)$
Farber et al.[11]	600	not	-6.76$^{(1)}$	$2\ V_2O_5(s) = V_4O_{10}(g)$
	730	controlled	-6.01	
	907		-5.25	
	932		-5.14	
Yannopoulos[12]	639-839	0.06 - 0.25	below detection	
Semenov et al.[13]	600	_	-7.74$^{(1)}$	$2\ V_2O_5(s) = V_4O_{10}(g)$
	942	_	-5.22	
	1100	_	-4.66	
	1257	_	-4.22	
Suito and Gaskell[14]	600	0.21	-8.56$^{(1)}$	$VO_{2.5}(l) + 1/4\ O_2(g) = VO_3(g)$
	900	0.21	-5.68	
	1025	0.21	-5.05	
	1099	0.21	-4.70	
USBM bulletin 672[1] and JANAF tables[2]	600	1	-19.79	$V_2O_5(s) = 2\ VO_2(g) + 1/2\ O_2(g)^{(2)}$

(1) Extrapolated values using ΔG^o of fusion for V_2O_5 when applicable.
(2) Proposed reaction based on species reported.

This conclusion was important since it allowed the direct measurement of the partial pressures of the hydroxide species formed above $V_2O_5(s)$ in the presence of water vapor with no interference from the volatile oxides. However, to provide a final check on the contribution of these gaseous oxides to the measured vapor pressure in the absence of $H_2O(g)$, baseline vapor pressure measurements with $V_2O_5(s)$ were made.

2.1.2 Enhancement of the Volatility of $V_2O_5(s,l)$ in the Presence of Water Vapor

Increased volatility of $V_2O_5(s)$ using water vapor was studied by Glemser and Muller[15]. Using a transpiration apparatus in the temperature range of 500 to 650 °C and using O_2 as the carrier gas, they concluded that the enhancement in vapor pressure was due to the formation of $V_2O_3(OH)_4(g)$ according to:

$$V_2O_5(s) + 2H_2O(g) = V_2O_3(OH)_4(g) \qquad (2.9)$$

$$\Delta G^\circ = 21{,}321 + 14.83\ T \text{ (cal/mole of } V_2O_5(s))$$

Since all their reported data was for a single carrier gas flow rate, no evidence was given that they worked in a flowrate independent regime. Thus, it is not clear as to whether or not the measurements were made under equilibrium conditions.

Yannopoulos[12] conducted experiments using both $V_2O_5(s)$ and $V_2O_5(l)$ as his condensed phases. He used a transpiration apparatus with mixtures of O_2 and H_2O as carrier gas in the temperature range of 639 to 899 °C. He concluded that the enhancement of the vapor transport was due to the formation of $VO(OH)_3(g)$ according to:

$$V_2O_5(s,l) + 3H_2O(g) = 2VO(OH)_3(g) \tag{2.10}$$

$$\Delta G^\circ = 44{,}010 + 1.03\ T \quad (\text{cal/mole of } V_2O_5(s,l))$$

It is important to note that although Yannopoulos conducted experiments with both $V_2O_5(s)$ and $V_2O_5(l)$, his measurements were made primarily above liquid V_2O_5. Moreover his measurements above solid V_2O_5 were carried out at only one temperature. Thus it is questionable, from a statistical point of view, as to whether or not the reported Gibbs free energy equation reflects the actual trends in the solid phase.

Yannopoulos' work was later criticized by Suito and Gaskell[14] for his use of silica boats. They argued that his melts were silica saturated and that consequently, he was unable to detect any difference in volatilization due to oxygen variation.

Taniguchi and Ooue[16] conducted experiments with solid V_2O_5 in the temperature range of 465 to 620 °C, also using a transpiration apparatus. In agreement with Yannopoulos, they also concluded that $VO(OH)_3$ was the molecularity of the gaseous species formed according to:

$$V_2O_5(s,l) + 3H_2O(g) = 2VO(OH)_3(g) \tag{2.11}$$

$$\Delta G^\circ = 41{,}643 + 1.45\ T \quad (\text{cal/mole of } V_2O_5(s))$$

The formation of volatile vanadium hydroxides was also investigated by Suito and Gaskell[14]. Using a transpiration apparatus in the temperature range of 900 to 1099 °C, they concluded that the main volatile hydroxides formed above VO_2 and $VO_{2.5}$ melts were $VO(OH)_2$ and $VO_2(OH)_2$ according to:

$$VO_2(s) + H_2O(g) = VO(OH)_2(g) \tag{2.12}$$

$$\Delta G^\circ = 50{,}150 - 14.77\ T\ (\text{cal/mole of } VO_2(g))$$

$$V_2O_5(l) + 2H_2O(g) + \frac{1}{2}O_2(g) = 2VO_2(OH)_2(g) \tag{2.13}$$

$$\Delta G^\circ = 43{,}250 + 7.06\ T\ (\text{cal/mole of } V_2O_5(l))$$

In comparing their work with that of the other investigators, Suito and Gaskell emphasized their observations of congruent volatilization and oxygen dependance of the melt composition. The other previously mentioned authors reported no oxygen dependance and only one gaseous hydroxide species formed above $V_2O_5(l)$.

A graphical comparison of the work reported by the different investigators is presented in Figure 2.2. The reported equations for the proposed Gibbs free energies of the predominant reactions were plotted as a function of temperature within the working temperature range of each investigator.

Although the investigators worked at different temperature ranges, it was evident that where their ranges overlapped, except for the work of Taniguchi et al. and that of Yannopoulos, there was no agreement on the molecularity of the predominant volatile hydroxide. Moreover, even when they agreed in the molecularity, the values of the ΔG°

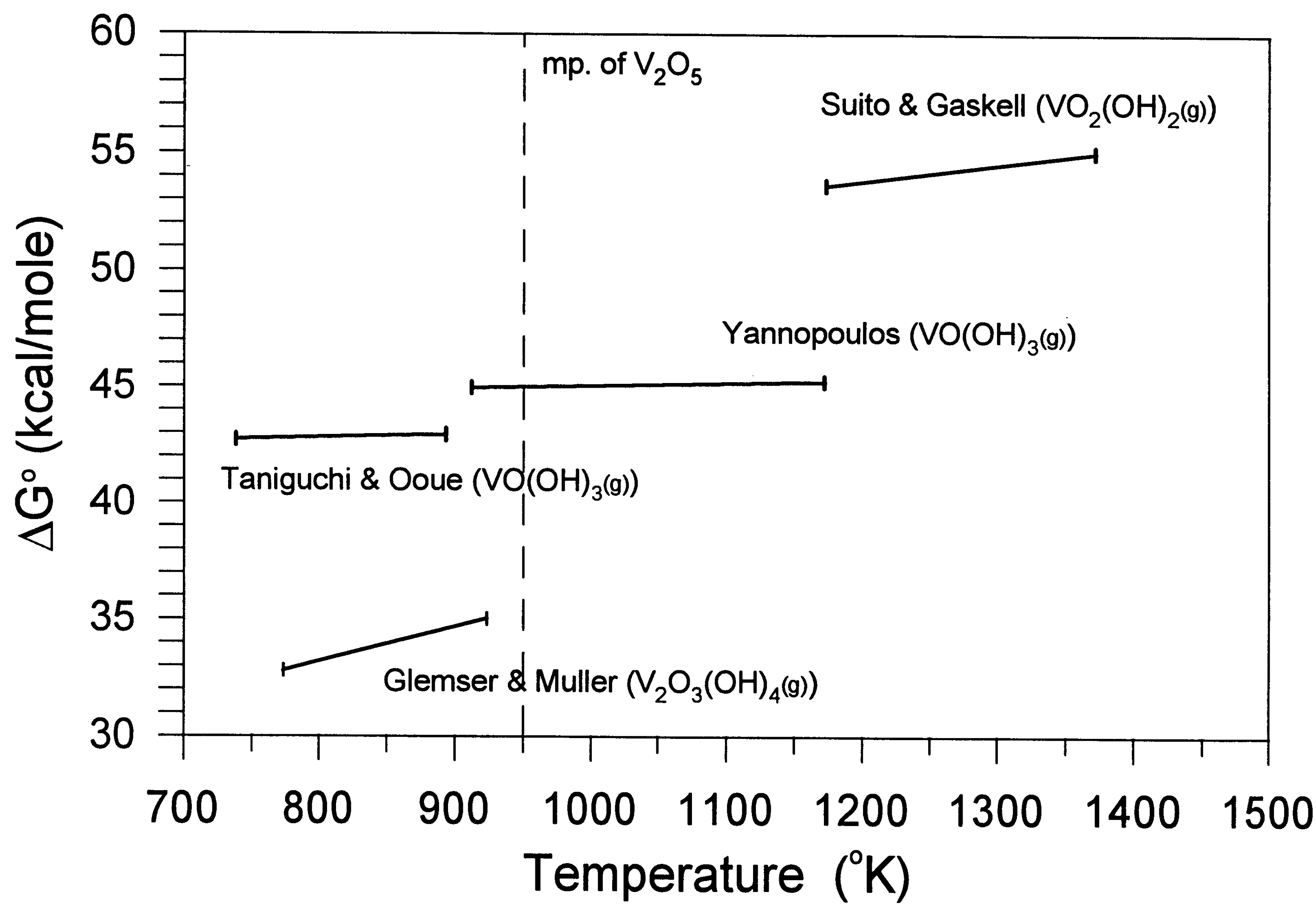

Figure 2.2 Gibbs free energy of reaction as a function of temperatures as reported in the literature, according to reactions (2.9), (2.11), and (2.13).

of reaction and, consequently , the vapor pressures, differed considerably.

Other interesting observations on the volatilization of vanadium pentoxide in the presence of water vapor were appreciated in the patent by Chambers[17]. He suggested that vanadium can be transpired from slags and other vanadium bearing materials at temperatures as low as 600 °C. He attributed the high volatility to the formation of volatile hydroxides. Although he did not report a specific molecularity for the vapor species formed nor any mechanisms of vaporization, he observed a dependance on the oxygen potential and a linear relationship with the water vapor pressure. He also reported extractions of around 56 wt.% of the original V_2O_5 in 2 hrs at 745 °C. This suggested remarkably high vapor pressures of the gaseous species formed, compared to the work reported by the previously mentioned investigators.

It was evident from the literature review, as well from the pilot plant data obtained by McNulty[18], that the known vapor chemistries on vanadium were not complete and that the reported experimental investigations, due to the disagreements between the different researchers, were inconclusive.

It was the objective of the present investigation to sort out the molecularity of the predominant gaseous hydroxides formed above $V_2O_5(s)$ in the presence of water vapor. Moreover, in view of the large discrepancies among the Gibbs free energy values reported by the different investigators, independent measurements of the Gibbs free energy for the transport reaction at different temperatures were conducted.

2.2 Vanadium Trioxide

Vanadium trioxide is a black solid compound with an structure similar to that of α-corundum and is considered to be basic[19]. Its range of homogeneity, as reported by Stringer,[6] goes from $VO_{1.44}$ to $VO_{1.65}$ depending on the temperature; actually, the range narrows with decreasing temperature[20].

Oxygen dissociation pressures for the $VO_{1.5}$ and $VO_{1.67}$ system were measured by Anderson[21] by varying the oxygen partial pressure at a number of relatively high temperatures (1173 to 1423 °K). The proposed oxidation reaction is shown in the following equation:

$$\frac{1}{2}V_2O_3(s) + \frac{1}{12}O_2(g) = \frac{1}{3}V_3O_5(s) \tag{2.14}$$

The measured vapor pressures for the lower and higher limits of the temperature range were Log P_{O2} (atm) = -12.1 and Log P_{O2} (atm) = -8.49 respectively.

Masakata and Katsura[20] also studied the thermodynamic properties of V_2O_3 but at higher temperatures (1400 to 1700 °K). They reported Gibbs free energies of oxidation for $V_2O_3(s)$ according to:

$$1/2\,V_2O_3(s) + 1/12\,O_2(g) = 1/3\,V_3O_5(s) \tag{2.15}$$

$$\frac{d(\log K)}{d(1/T)} = (1.85 \pm 0.05)\times 10^3 \quad (\text{cal/0.5 mole of } V_2O_3(s)) \tag{2.16}$$

An extrapolation of this work to compare it with the work of Anderson resulted in a dissociation pressure of Log P_{O2} (atm) = -11.8 at 1173 °K. It was appreciated that, given the uncertainty of the extrapolation, the agreement between the two investigations was good (Log P_{O2} (atm) = -11.8 versus -12.1).

Since no information for the oxidation of V_2O_3(s) was found at lower temperatures (600 to 900 °C), and given the proximity of the extrapolation to the values reported by Anderson at lower temperatures, Masataka and Katsura's equation was used to estimate the oxygen partial pressures for the oxidation of V_2O_3(s) in the present work. For the above temperature range, the calculated equilibrium oxygen pressures were:

$$600\ °C : \text{Log } P_{O2} \text{ (atm)} = -18.33$$

$$900\ °C : \text{Log } P_{O2} \text{ (atm)} = -11.83$$

These values were used to define the <u>upper</u> P_{O2} limit for the transpiration experiments on V_2O_3(s).

For the vanadium rich boundary of the homogeneity region of V_2O_3(s), no categorical information was found. In their review of the literature, Matsui and Naito[3] suggested that above 1000 °K the condensed phases in equilibrium are VO(s) and V_2O_3(s); whereas at lower temperatures, the phases in equilibrium are, according to Figure 2.1, $VO_{1.27}$(s) and V_2O_3(s). Since no thermodynamic data were located for the latter equilibrium, the equilibrium VO(s) and V_2O_3(s) was taken as the vanadium rich boundary of V_2O_3(s) and the decomposition oxygen pressures calculated from the data reported in the JANAF tables. In the temperature range of 600 to 900 °C, the calculated decomposition pressures for the low and high limits of the temperature range studied were:

$$600\ ^\circ C:\ \text{Log}\ P_{O2}\ (\text{atm}) = -34.0$$
$$900\ ^\circ C:\ \text{Log}\ P_{O2}\ (\text{atm}) = -23.2$$

These values were used to define the lower P_{O2} limit for the transpiration experiments on $V_2O_3(s)$. These partial pressures are five to ten orders of magnitude lower than the working oxygen pressures used in this investigation. Due to the low magnitude of the oxygen pressures needed for this experiments, an equilibrated mixture of CO(g) and $CO_2(g)$ was used as the carrier gas to accurately control the oxygen potential throughout the experiments according to:

$$CO(g) + \frac{1}{2}O_2(g) = CO_2(g) \tag{2.17}$$

$$\text{Log}\frac{P_{CO_2}}{P_{CO}} = \text{LogK} + \frac{1}{2}\text{LogP}_{O_2} \tag{2.18}$$

The equilibrium P_{CO2}/P_{CO} ratios for the upper and lower limits of the stability range of $V_2O_3(s)$ are presented in Table 2.2.

Table 2.2 Equilibrium P_{CO2}/P_{CO} Ratios for the Upper and Lower Limits of the Stability Range of $V_2O_3(s)$

Temperature (°C)	Log P_{CO2}/P_{CO}	
	VO / V_2O_3	V_2O_3 / V_3O_5
600	-4.63	3.21
900	-3.56	2.15

2.2.1 Baseline Vapor Chemistry of $V_2O_3(s)$

As in the case of vanadium pentoxide, in order to study the vapor chemistry of $V_2O_3(s)$ in the presence of water vapor, it was first necessary to identify the principal vapor species formed in the absence of water and determine their contribution to the total vapor pressure.

All the thermodynamic studies on the volatilization of $V_2O_3(s)$ found in the literature were carried out through high temperature mass spectrometric methods, in the range of 1000 to 2000 °K.

Frantseva and Semenov[10] studied the evaporation above $VO_{1.5}(s)$ and $VO_{1.52}(s)$ in the temperature range of 1400 to 2000 °K, and determined the gas composition and the partial pressures of the components. They found that, at these temperatures, $V_2O_3(s)$ volatilizes congruently as $VO(g)$ and $VO_2(g)$, with equal distributions, as the condensed phase composition approaches stoichiometry. Although they detected significant V^+ intensities, they attributed them to VO^+ and VO_2^+ fragmentation due to the high ionization energies used (70 eV); V^+ did not appear at ionization energies of 12 eV. The derived relationship for the partial pressure of either VO(g) or VO_2(g) as a function of temperature above stoichiometric V_2O_3(s) was presented as:

$$\mathrm{Log}\,P_i\ (\mathrm{atm}) = \frac{-27{,}900}{T} + 8.46 \tag{2.19}$$

Although P_{VO} was equal to P_{VO2} when in equilibrium with $VO_{1.5}$, slight differences in the distribution of VO(g) and VO_2(g) were observed above $VO_{1.52}$(s). The proposed equations for the partial pressures of each component were:

$$\mathrm{Log}\,P_{VO_2}\ (\mathrm{atm}) = \frac{-27{,}470}{T} + 8.34 \tag{2.20}$$

$$\mathrm{Log}\,P_{VO}\ (\mathrm{atm}) = \frac{-28{,}730}{T} + 8.86 \tag{2.21}$$

Frantseva and Semenov also compared their work with that of Killingbeck[22]. They found that the effective pressures of the two works were similar. However, the gaseous species proposed by Killingbeck was V_2O_3(g).

Farber, Uy, and Srivastava[11] determined the heats of formation at 298 °K for VO(g) and VO_2(g) above V_2O_3(s) and reported their free energy functions at 2200 and 2300 °K. Using this information, along with complementary thermodynamic data from the JANAF[2] tables, and making Frantseva and Semenov's assumption of equal gaseous distribution above $VO_{1.5}(s)$, the total effective pressures above $V_2O_3(s)$ were calculated for comparative purposes. The calculated effective pressures at 2200 and 2300 °K were 1.7 E-5 and 5.62 E-5 atm respectively. In their work, Farber et al. confirmed Frantseva and Semenov's observations of the congruent volatilization of $V_2O_3(s)$.

Banchorndhevakul, Matsui, and Naito[3] also studied the vaporization of $V_2O_3(s)$ through mass spectrometric methods, but at low ionizing energies at a temperature range of 1914 to 2182 °K. In their experiments, they used an O/V ratio of 1.501 and observed 3 gaseous species: VO, VO_2, and V, in decreasing order. They reported the following relationships of partial pressure as a function of temperature:

$$\mathrm{Log}\,P_{VO}\ (\mathrm{atm}) = \frac{-\ 26{,}440}{T} + 7.7 \qquad (2.22)$$

$$\mathrm{Log}\,P_{VO_2}\ (\mathrm{atm}) = \frac{-\ 29{,}320}{T} + 8.7 \qquad (2.23)$$

No vapor pressure equation for V(g) is reported due to the large scattering in their results.Therefore, they did not take it into consideration in their thermodynamic studies. They suggested that the stoichiometric condensed phase vaporizes congruently in the form of VO and VO_2. Different from Frantseva and Semenov, they did not find the distribution of the two gaseous compounds to be equal; VO(g) was reported to have a higher partial pressure than $VO_2(g)$. They also noticed that their measured pressures were lower than those of Frantseva and Semenov.

A table presenting the total apparent pressures reported by the different investigators was constructed for comparative purposes (see Table 2.3). The two temperatures selected facilitated the construction of the table (thermodynamic relations from some investigators were not very explicit) but posed some uncertainty on the data due to their extrapolation. Notwithstanding these limitations, the table provided a good indication of the order of magnitude of the vapor pressures as well as the agreement of the data reported by the different investigators.

It was appreciated from Table 2.3 that, although not all the investigators agreed in the molecularity of the volatile hydroxides formed, their agreement in the magnitude of the total vapor pressures above $V_2O_3(s)$ was remarkable. It was also evident, from this literature review, that the vapor pressures of the vanadium species above $V_2O_3(s)$ were relatively low even at high temperatures. Furthermore, when the vapor pressures were extrapolated to a lower temperature range (600 to 900 °C), the expected vapor pressures were in the range of 10^{-24} to 10^{-15} atm. These orders of magnitude were in agreement with the magnitudes obtained when calculating the vapor pressures of both $VO(g)$ and $VO_2(g)$ above $V_2O_3(s)$ from the data reported in the JANAF[2] tables at this lower temperature range (10^{-23} to 10^{-15} atm).

These calculations suggested that the contribution of the volatile oxides above $V_2O_3(s)$ to the total vapor pressure, at the experimental conditions used in this investigation (600 to 900 °C), were practically null. Therefore, they would not interfere in the measurements of the vapor pressures in the presence of water vapor. However, as in the case of the vanadium pentoxide measurements, baseline experiments were

Table 2.3 Comparison of the Vapor Pressures Reported by the Different Investigators for $V_2O_3(s)$, Pressures in Atmospheres

Investigators	T °K	Log	Main Reaction Proposed
Frantseva and Semenov[10]	2200	-3.92[(1)]	$V_2O_3(s) = VO(g) + VO_2(g)$
	2300	-3.37[(1)]	
Kilingbeck[22]	2200	-4.38[(1)]	$V_2O_3(s) = V_2O_3(g)$
	2300	-3.71[(1)]	
Farber et al.[11]	2200	-4.77	$V_2O_3(s) = VO(g) + VO_2(g)$
	2300	-4.25	
Banchorndhevakul	2200	-4.15[(1)]	$V_2O_3(s) = VO(g) + VO_2(g)$
	2300	-3.61[(1)]	
JANAF Tables[2]	2200	-3.79	$V_2O_3(s) = VO(g) + VO_2(g)$
	2300	-3.27	

(1) Extrapolated value.

conducted to provide a final check on the contribution of the volatile oxides to the measured vapor pressure.

2.2.2 Enhancement of the Volatility of $V_2O_3(s)$ in the Presence of Water Vapor

No information was found in the literature on the enhancement of the volatility of vanadium trioxide in the presence of water vapor. Thus, another objective of the present study was to determine if volatile hydroxides could formed with $V_2O_3(s)$. The study attempted to determine the molecularity and the $\Delta G°$ of formation of any volatile hydroxides formed.

2.3 Molybdenum Trioxide

The oxides that have been reported in the molybdenum-oxygen system are listed in Table 2.4. Not all of these substances, however, have been proven to be stable. In fact, some of them were produced, in a metastable state, by heating stoichiometric mixtures of oxides and metals, followed by rapid quenching[23].

In studying the stability of molybdenum oxides, Magnéli[24,25] originally observed three stable compounds between $MoO_2(s)$ and $MoO_3(s)$ in the temperature range of 650 to 750 °C: $Mo_4O_{11}(s)$, $Mo_8O_{23}(s)$, and $Mo_9O_{26}(s)$. Later, two additional phases were observed by Kihlborg and Magnéli[26]: $Mo_{17}O_{47}(s)$ (at temp. $<$ 560 °C) and $Mo_5O_{14}(s)$ (at temp. $<$ 530 °C). Of these two species, $Mo_5O_{14}(s)$ is probably metastable[27].

Table 2.4 Molybdenum Oxides Reported in the Literature[23]

Name	CAS Registry No.	Formula: Empirical	Formula: Molecular	Crystal structure	Color
trioxide	[*1313-27-5*]	MoO_3	MoO_3	rhombic	white
ζ-oxide	[*12136-82-0*]	$MoO_{2.89}$	$Mo_{18}O_{52}$	triclinic	blue black
β'-oxide	[*12163-89-2*]	$MoO_{2.89}$	Mo_9O_{26}	monoclinic	violet
β-oxide	[*12058-34-3*]	$MoO_{2.84}$	Mo_8O_{23}	monoclinic	violet
θ-oxide	[*12438-84-5*]	$MoO_{2.80}$	Mo_5O_{14}	tetragonal	blue violet
κ-oxide	[*12777-01-4*]	$MoO_{2.78}$	$Mo_{17}O_{47}$	orthorhombic	red blue
η-oxide	[*12033-38-4*]	$MoO_{2.75}$	Mo_4O_{11}	monoclinic	wine red
γ-oxide		$MoO_{2.75}$	Mo_4O_{11}	orthorhombic	wine red
dioxide	[*18868-43-4*]	MoO_2	MoO_2	tetragonal	brown black
sesquioxide	[*1313-29-7*]	$MoO_{1.5}$	Mo_2O_3	amorphous	black
	[*12136-80-0*]	$MoO_{0.33}$	Mo_3O	cubic	metallic

Another study on the stability of oxides in the Mo-O system was conducted by Chang and Phillips[28,29]. They were able to obtain, as single phases, MoO_2(s), Mo_4O_{11}(s), a low temperature Mo_9O_{26}(s), and a high temperature Mo_9O_{26}(s). They reported that the X-ray diffraction patterns for the low temperature Mo_9O_{26}(s) matched the patterns reported by Magnéli; whereas the high temperature form did not. They mentioned, however, that some of the front diffraction lines of the high temperature Mo_9O_{26}(s) corresponded to those of Mo_8O_{23}(s), as reported by Magnéli. In order to confirm the stability of Mo_8O_{23}(s), they conducted additional experiments using a mixture of Mo_9O_{26} and Mo_4O_{11} with a composition equivalent to that of Mo_8O_{23} at 700 °C. They were only able to produce an equilibrated mixture of Mo_9O_{26}(s) and Mo_4O_{11}(s). This inability to maintain Mo_8O_{23}(s), suggested that there was still some uncertainty with respect to the stability of Mo_8O_{23}(s).

In the case of the compounds with lower oxygen content than $MoO_2(s)$, shown in Table 2.4, these have not yet been obtained in a pure state and are poorly described[26]. Attempts by Kihlborg[26] to produce $Mo_3O(s)$ from $MoO_3(s)$ were unsuccessful. Thus, he concluded that the existence of these lower oxides was still questionable.

The phase diagram by Brewer and Lamoreax[30] reported five oxide phases as being stable: $MoO_2(s)$, $Mo_4O_{11}(s)$, $Mo_8O_{23}(s)$, $Mo_9O_{26}(s)$, and $MoO_3(s)$ (see Figure 2.3). Calculations (using the JANAF tables[2]) to determine the oxygen equilibrium pressures for the stability boundaries of these phases, however, gave inconsistent results with the Mo_4O_{11}-Mo_8O_{23} and Mo_8O_{23}-Mo_9O_{26} equilibria. The equilibrium Mo_4O_{11}-Mo_9O_{26}, on the other hand, gave consistent results and was in agreement with the findings Chang and Phillips[29].

Based on the phases reported by Brewer (excluding Mo_8O_{23}) and the thermodynamic data from JANAF, the molybdenum rich stability limit for $MoO_3(s)$ was determined. For the temperature range of interest in this study (550 to 750 °C), the oxygen equilibrium pressures for the coexistence of $MoO_3(s)$ with $Mo_9O_{26}(s)$ are presented in Table 2.5.

It was clear from Table 2.5 that if O_2 pressures higher than 10^{-7} atm were used, $MoO_3(s)$ would not be reduced in the temperature range of 550 to 750 °C. In the present study, oxygen pressures of the order of 10^{-1} atm were used. Thus no problems were encountered in maintaining the integrity of $MoO_3(s)$.

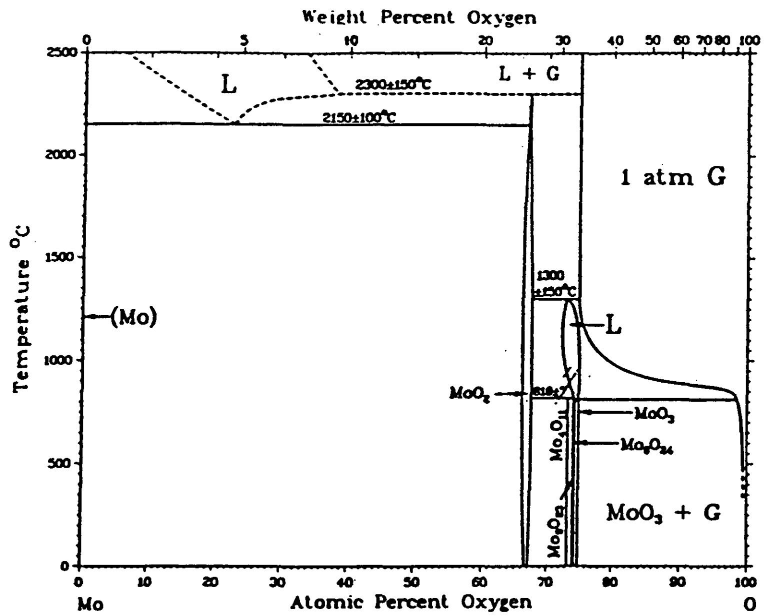

Figure 2.3 Equilibrium phase diagram for the molybdenum-oxygen system[30].

Table 2.5 Equilibrium Oxygen Pressures for the Lower Limit of Stability of $MoO_3(s)$

T °C	P_{O2} (atm)	Log P_{O2}
550	8.32×10^{-12}	-11.08
650	6.03×10^{-10}	-9.22
700	3.63×10^{-09}	-8.44
750	1.82×10^{-08}	-7.74

2.3.1 Baseline Vapor Chemistry of MoO_3(s,l)

Once the stability ranges of the Mo-O system had been established, the next step was to determine the contribution of the volatile oxides to the total vapor pressure. As mentioned earlier, to account for these contributions was important because the vapor pressures of the volatile oxides have to be subtracted form the total vapor pressure to obtain the vapor pressure of any hydroxide formed .

Stability diagrams at three selected temperatures, within the temperature range of interest (550 to 750 °C), were constructed utilizing the stability ranges for the condensed phases obtained in the previous section. To these ranges, lines representing the vapor pressures of the principal volatile oxides have been superimposed. The data were obtained from the JANAF tables[2] with the exception of the data corresponding to $(Mo_3O_9)(g)$. For this species, as will be discussed in the following paragraphs, no categorical data could be obtained. The measurements by Glemser and Haeseler[31] were chosen mainly because they represented an average of the reported data, and because these investigators also were interested in studying the formation of volatile hydroxides (see Figures 2.4 to 2.6).

It was appreciated from these figures, that at 650 °C the partial pressure of Mo_3O_9 was in the order of 10^{-4} atm, and at 750 °C, it was as high as 10^{-3} atm. Since these magnitudes were easily detectable in the transpiration technique, it was evident that an accurate determination of the vapor pressure of $Mo_3O_9(g)$ was necessary in order to be able to measure the vapor pressure of any volatile hydroxides formed above $MoO_3(s)$. A summary of the available literature on the vaporization of $MoO_3(s)$ is presented in the following paragraphs.

The sublimation of $MoO_3(s)$ has been studied by several investigators by different experimental methods. Feiser[32] made indirect determinations of the volatilization of $MoO_3(s,l)$ in the temperature range of 883 to 1428 °K. Having measured the boiling point

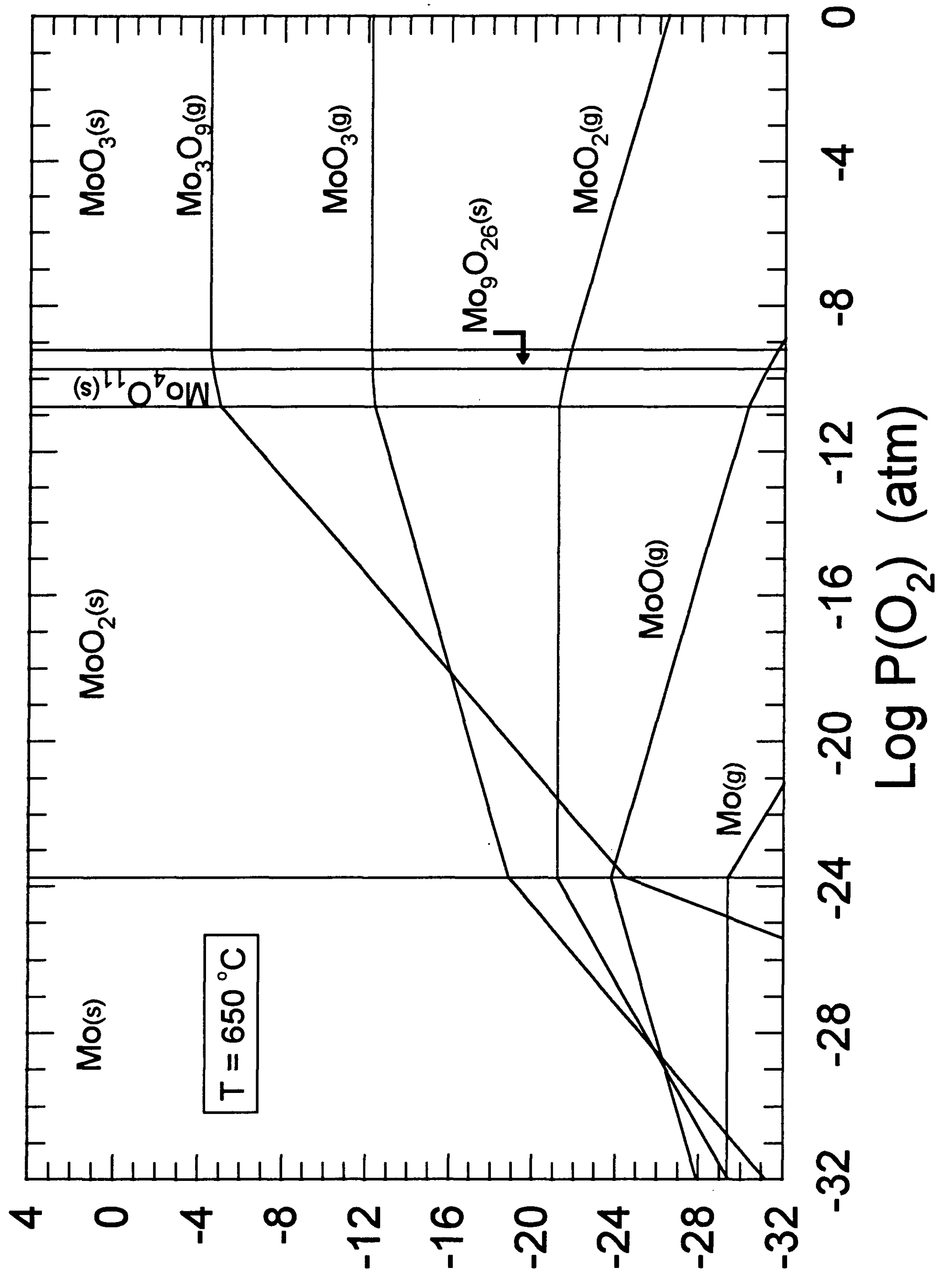

Figure 2.4 Stability diagram for the Mo-O system at 650 °C.

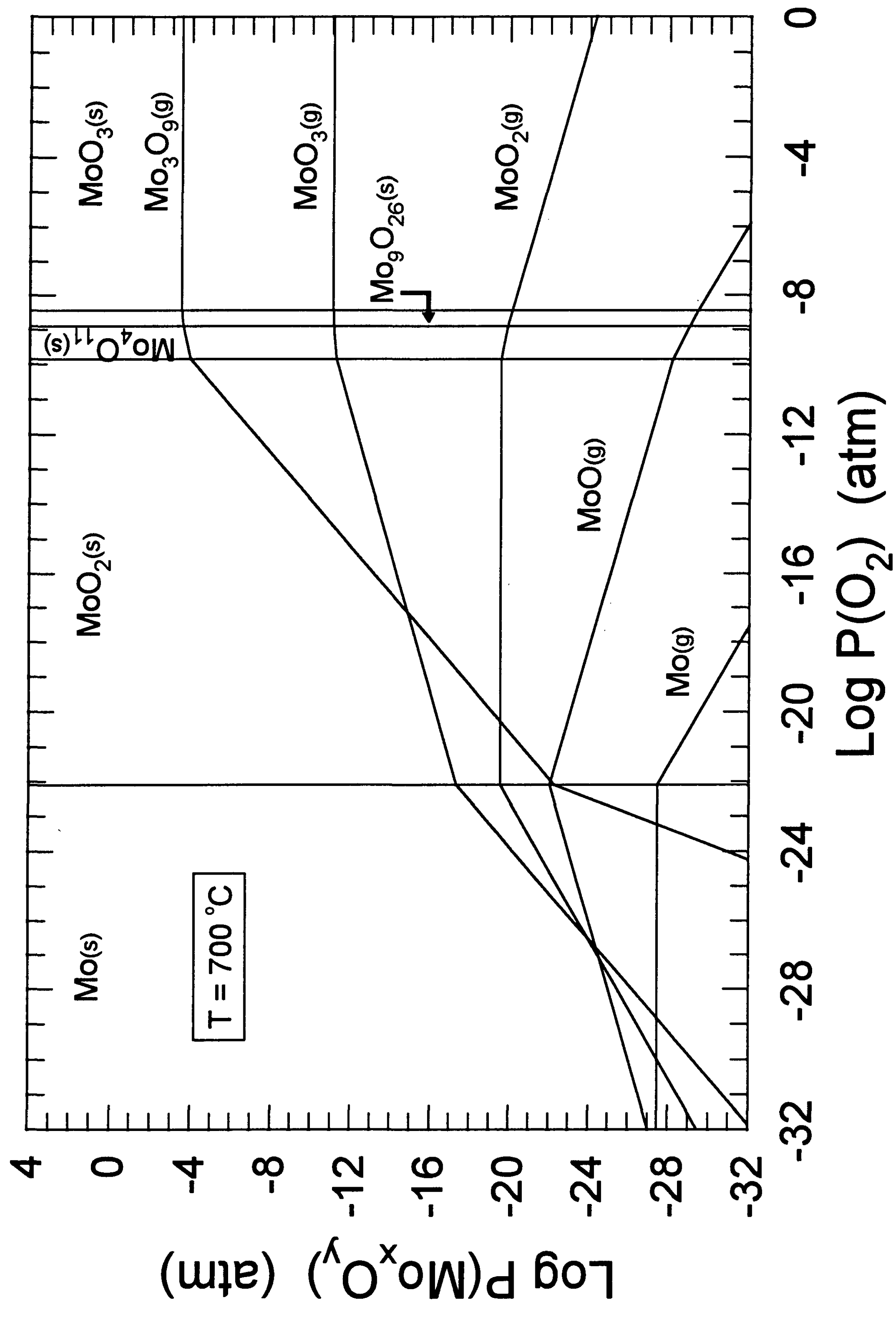

Figure 2.5 Stability diagram for the Mo-O system at 700 °C.

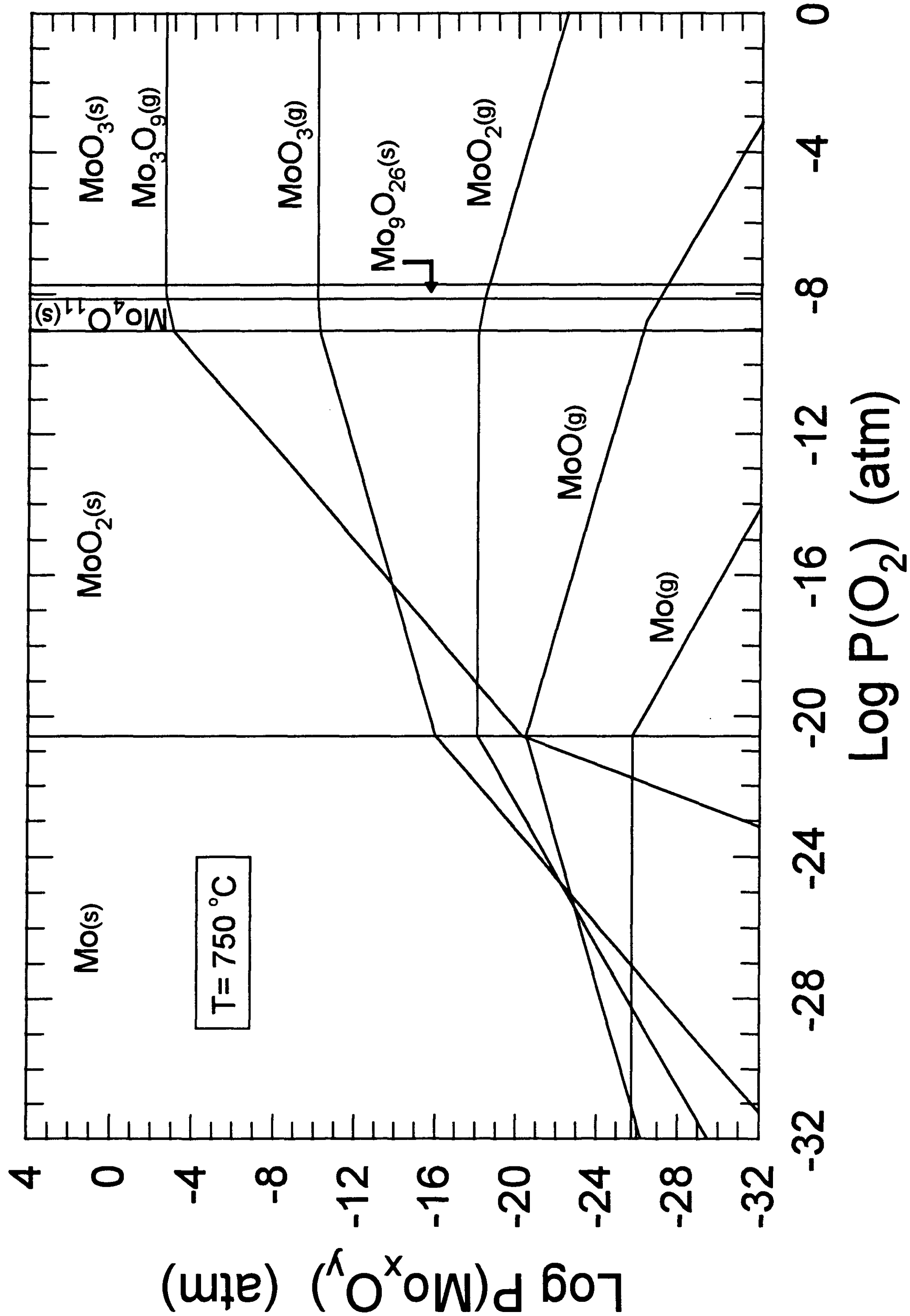

Figure 2.6 Stability diagram for the Mo-O system at 750 °C.

of MoO_3 (1428 °K), he proceeded to estimate the vapor pressure below the boiling point by using the simple relation:

$$\frac{\text{Vapor pressure at T}}{\text{760 mm}} = \frac{\text{Wt. loss/time at T}}{\text{Wt. loss/time at bp}} \tag{2.24}$$

He also attempted to calculate the vapor pressure of $MoO_3(s)$ by comparing its sublimation/time with the vaporization/time of another oxide of known vapor pressure, under his experimental conditions. He assumed that this technique would give him the vapor pressure of $MoO_3(s)$. However, the results obtained by this technique were in serious disagreement with his previous calculated vapor pressures. He concluded that these discrepancies could be explained if the vapor species were in the polymeric form.

The first mass spectrometric studies were conducted by Berkowitz, Inghram, and Chupka[33], who detected the presence of three polymeric species: $(MoO_3)_3$, $(MoO_3)_4$, and $(MoO_3)_5$. From these, $(MoO_3)_3$ was determined to be the predominant species in their studied temperature range of 810 to 1000 °K. They estimated a $\pm$ 4 kcal error in the free energy equation due to temperature variations ($\pm$ 10 °C) and uncontrolled leakages from the cell. Their reported vaporization reactions were:

$$3MoO_3(s) = Mo_3O_9(g) \tag{2.25}$$

$$\Delta G° = 80{,}500 - 65.6\ T \quad \text{(cal/mole of gas)}$$

$$4MoO_3(s) = Mo_4O_{12}(g) \tag{2.26}$$

$$\Delta G^{\circ} = 93{,}600 - 78.1\ T \quad \text{(cal/mole of gas)}$$

Ikeda et al.[34] also conducted experiments using a mass spectrometer in the temperature range of 850 to 940 °K. They detected the presence of the same polymeric species as Berkowitz et al. and also reported Mo_3O_9 as being the predominant species. Their calculated vapor pressures, however, were slightly lower than those of Berkowitz et al.. Ikeda et al., also compared their work with that of Kazenas and Tsuvetkov[35] and Aleshko-Ozhevskaya et al.[36], who also conducted mass spectrometric studies. Ikeda and co-workers concluded that, although they agreed with the polymeric species reported by these investigators, they did not agree with the magnitude of the vapor pressures. They also found some differences in the temperature dependance of the pressure of the polymeric gaseous species. Their reported equations for both the trimer and tetramer species were:

$$3MoO_3(s) = Mo_3O_9(g) \tag{2.27}$$

$$\Delta G^{\circ} = 69{,}556 - 52.81\ T \quad \text{(cal/mole of gas)}$$

$$4MoO_3(s) = Mo_4O_{12}(g) \tag{2.28}$$

$$\Delta G^{\circ} = 80{,}995 - 64.73\ T \quad \text{(cal/mole of gas)}$$

Blackburn et al.[37] measured the volatilization of $MoO_3(s)$ in the temperature range of 808 to 958 °K, using the Knudsen effusion method. Based on the paper by Berkowitz et al.[33], they assumed that the predominant volatile species was $Mo_3O_9(g)$ and calculated their vapor pressures accordingly. Applying the Clausius-Clapeyron equation to their calculated vapor pressures, they obtained an equation for the vapor pressure as a function of temperature. By manipulating this equation, the free energy equation for the sublimation reaction was derived as:

$$3MoO_3(s) = Mo_3O_9(g) \tag{2.29}$$

$$\Delta G^\circ = 79{,}741 - 67.81\ T \quad \text{(cal/mole of gas)}$$

Ueno et al.[38] also measured the vapor pressure of Mo_3O_9 by measuring the weight loss in a Knudsen effusion cell suspended from a quartz fiber balance. As in the case of Blackburn et al., they computed the heat of sublimation from the slope of a Clausius-Clapeyron plot in the temperature range of 908 to 948 °K. They reported the following free energy equation:

$$3MoO_3(s) = Mo_3O_9(g) \tag{2.30}$$

$$\Delta G^\circ = 63{,}700 - 46.5\ T \quad \text{(cal/mole of gas)}$$

Gulbransen et al.[39] also studied the vaporization of $MoO_3(s)$ using the Knudsen effusion method in the temperature range of 873 to 973 °K. Based on the work of Berkowitz et al., they also considered Mo_3O_9 as the main volatile oxide of $MoO_3(s)$ with small contributions to the total vapor pressure from Mo_4O_{12} and Mo_5O_{15}. In order to calculate their vapor pressures, they used an average molecular weight of the gaseous species as calculated by Horbe, Knacke, and Prescher[40]. Horbe et al. based their calculations on the distributions of Berkowitz . Gulbransen et al. extrapolated the data of Selikman et al.[41], who studied the vaporization of liquid MoO_3, to the melting point and used this value in the Clausius-Clapeyron regression of their data. In this way they adjusted their equation to agree with Selikman's equation at the melting point. Their obtained equation was :

$$\bar{n}\,MoO_3(s) = (MoO_3)_{\bar{n}}(g) \tag{2.31}$$

$$\Delta G^\circ = 75{,}400 - 62.3\ T \quad \text{(cal/mole of gas)}$$

Gulbransen et al. also combined their calculated ΔH° of vaporization for the solid phase with the ΔH° of vaporization of the liquid phase of 35.2 kcal/mole calculated by Horbe et al [40], to obtain a ΔH° of fusion of 12.4 kcal/mole. It is important to note that Horbe et al.'s work was conducted with solid MoO_3 using an average molecular weight of the vapor species based on Berkowitz et al.'s mass spectrometric study, and that the calculated ΔH° of vaporization over the liquid phase was based on their review of the works of Feiser[32] and Selikman[41].

Ackermann et al.[42] conducted experiments to measure the vaporization of $MoO_3(s)$ in the temperature range of 980 to 1060 °K using the transpiration technique. Based on the work of Berkowitz, they calculated an average molecular weight of the vapor species and reported the sublimation of MoO_3 as:

$$\bar{n}\,MoO_3(s) = (MoO_3)_{\bar{n}}(g) \tag{2.32}$$

$$\Delta G^\circ = 87{,}800\ (\pm\ 1000)\ -\ 73\ (\pm\ 1)\ T \quad \text{(cal/mole of gas)}$$

In comparing their results with other researches, they argued that the assumption made by some investigators that Mo_3O_9 is the sole predominant species was not satisfactory; and that both $Mo_3O_9(g)$ and $Mo_4O_{12}(g)$ were important. They indicated that, although Berkowitz et al. reported that Mo_3O_9 was approximately three times more abundant than $Mo_4O_{12}(g)$ at 850 °K, if their reported equations were used to estimate abundance ratios at higher temperatures, $Mo_4O_{12}(g)$ became more significant. Consequently, it should be taken into account at higher temperatures calculations.

In an attempt to explain the discrepancies in the literature, they proceeded to recalculate the enthalpies and entropies of sublimation reported by other investigators, assuming average molecular weights based on the relative gaseous distributions of Berkowitz. They concluded, however, that the recalculated enthalpies and entropies of sublimation did not change significantly and thus, the large differences could not be attributed to the assumption that Mo_3O_9 was the sole predominant species.

Ariya et al.[43] conducted their measurements in the temperature range of 941 to 987 °K using the transpiration technique . Assuming that Mo_3O_9 was the main volatile species of $MoO_3(s)$, they obtained the following equation for the sublimation of molybdenum trioxide:

$$3MoO_3(s) = Mo_3O_9(g) \tag{2.33}$$

$$\Delta G^\circ = 68{,}100 - 56.9\ T \quad \text{(cal/mole of gas)}$$

Selikman et al.[41] measured the sublimation of liquid molybdenum trioxides in the temperature range of 1178 to 1373 °K using the transpiration technique. They concluded that Mo_3O_9 was the predominant volatile species and reported the sublimation of $MoO_3(l)$ as:

$$3MoO_3(l) = Mo_3O_9(g) \tag{2.34}$$

$$\Delta G^\circ = 35{,}200 - 24.6\ T \quad \text{(cal/mole of gas)}$$

When Ackermann et al.[42,43] reviewed the work of Selikman, they noted that their measurements yielded an average molecular weight of 3.2 times the monomer whereas the measurements of Berkowitz et al.[33], yielded an extrapolated value of 3.6. It is the writer's opinion that this may be an indication that the tetramer abundance actually decreases with increasing temperature. This observation was consistent with Brewer and Elliot's[44] observations that at 1200 °C the vapor phase average formula was less than $(MoO_3)_{1.5}$; although, as observed by Berkowitz, they might have supersaturated the gas.

Glemser and Haeseler[31], conducted experiments on the sublimation of $MoO_3(s)$ using the transpiration technique. They assumed that $Mo_3O_9(g)$ was the predominant gaseous species in the temperature range of 908 to 1028 °K based on the studies of Berkowitz. They obtained the following free energy equation:

$$3MoO_3(s) = Mo_3O_9(g) \tag{2.35}$$

$$\Delta G^\circ = 83{,}237 - 69.56\ T \quad \text{(cal/mole of gas)}$$

This work was of special importance to the present investigation because Glemser and Haeseler[31] also studied the formation of volatile hydroxides with $MoO_3(s)$. Since with the transportation technique only total apparent pressures can be measured, they had to determine the contribution of the volatile oxides first. Only then, they could study the formation of volatile hydroxides.

A graphical comparison of the work reported by the different investigators is presented in Figure 2.7. In this figure, three sets of data were identified in the solid phase. These were a lower set comprising the work of Gulbransen, Blackburn, and Ariya; a higher set consisting of the work of Berkowitz, Ikeda, Ueno, and Ackermann; and finally, a middle line corresponding to the work of Glemser. In the liquid phase, only the results of the work of Selikman were available.

It was evident, from this literature review, that there were still considerable discrepancies among the reported vapor pressures of the oxides in equilibrium with solid MoO_3. It was also clear that these discrepancies had to be resolved before the study on the formation of volatile hydroxides could be undertaken.

Thus, measurements of the vaporization of $MoO_3(s)$ in the absence of water vapor were incorporated in the present investigation to accurately account for the vapor transport due to the formation of volatile oxides.

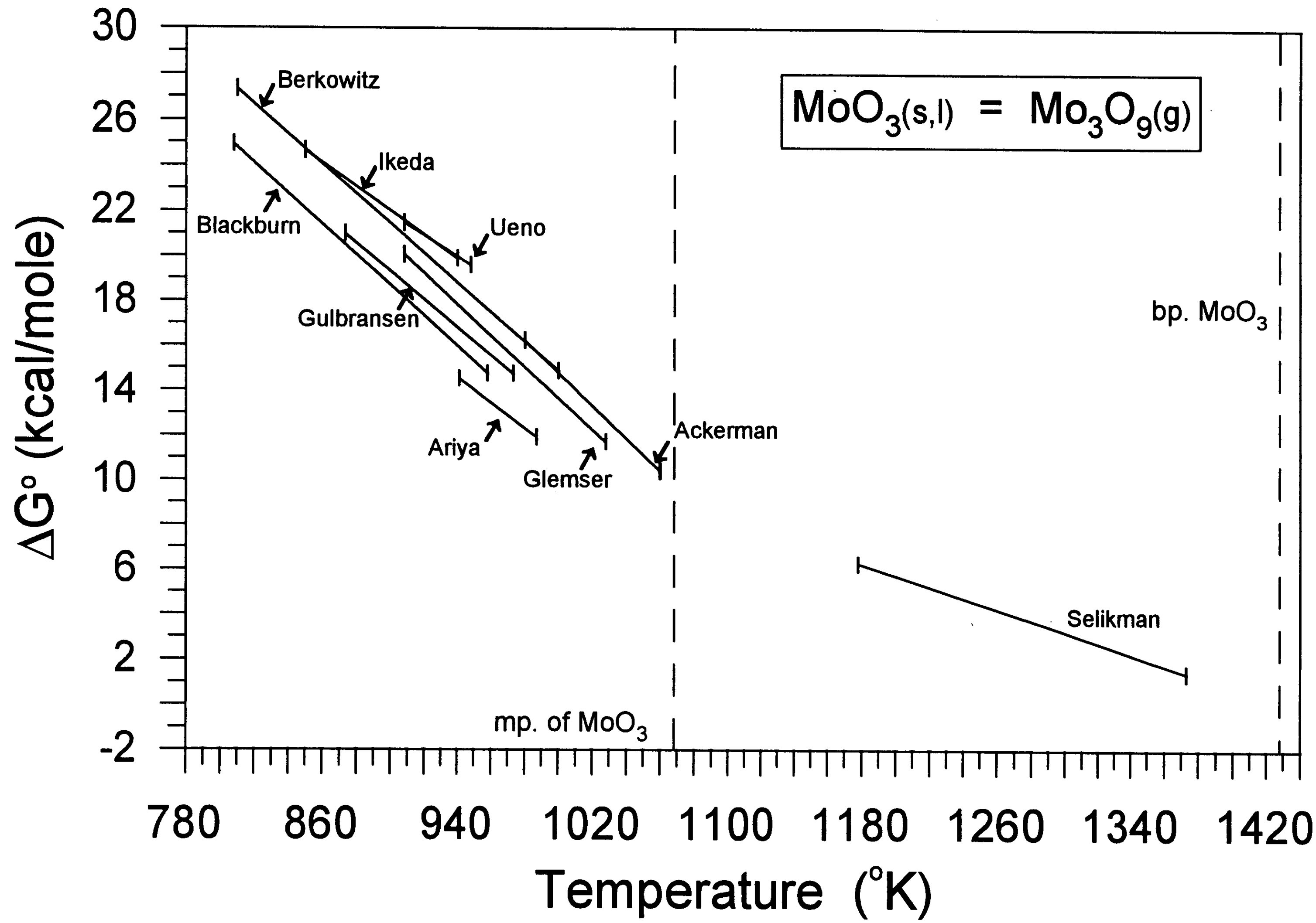

Figure 2.7 Gibbs free energy of sublimation for MoO_3(s,l) as reported by the different investigators.

2.3.2 Enhancement of the Volatility of MoO_3(s,l) in the Presence of Water Vapor

Increased volatility of MoO_3(s) was first observed by Millner and Neugebauer[45] in the temperature range of 600 to 700 °C. Later, Brewer and Elliot[44] conducted experiments in the presence of water vapor at 560 °C. In their experiments, they measured how much MoO_3 was vaporized in a sealed silica tube when exposed to water vapor. They concluded that MoO_3 reacted with water to form $MoO_2(OH)_2$(g) according to:

$$MoO_3(s) + H_2O(g) = MoO_2(OH)_2(g) \tag{2.36}$$

Ten years later, Glemser and Haeseler[31] investigated the formation of volatile hydroxides above MoO_3(s) in the temperature range of 873 to 963 °K. Since they used the transpiration technique, they first had to measure the vapor pressure of the volatile oxides in the absence of water vapor in order to be able to subtract this value from the total measured vapor pressure in the presence of steam. In agreement with Brewer and Elliot, they also reported $MoO_2(OH)_2$(g) as being the predominant gaseous hydroxide formed, according to:

$$MoO_3(s) + H_2O(g) = MoO_2(OH)_2(g) \tag{2.37}$$

$$\Delta G^\circ = 35{,}378 - 24.94\ T \quad \text{(cal/mole)}$$

Wendlant and Glemser[46] studied the formation of volatile hydroxides at elevated pressures and at 500 °C. They concluded, in agreement with previous investigators, that there was a linear dependance of the vapor pressure of the hydroxide to the water pressure.

Belton and Jordan[47] were also interested in the formation of volatile hydroxides of molybdenum. Using the transpiration technique in the temperature range of 1473 to 1773 °K, they studied the enhancement of the volatility of Mo metal in the presence of water vapor. In order to prevent the oxidation of the metal, they used hydrogen-water vapor-argon mixtures at reducing conditions.They cleverly accounted for the contributions of the volatile oxides to the total vapor pressures by fixing the water to hydrogen ratio (oxygen potential) and varying the water potential at a fixed temperature. In this manner, any contribution that was independent of the water potential was attributed to the volatile oxides. Thus, the intercept of a plot of apparent vapor pressure as a function of water pressure should have given them the vapor pressure of the volatile oxides. The results of Belton and Jordan were summarized as:

$$M(s) + 4H_2O(g) = MoO_2(OH)_2(g) + 3H_2(g) \qquad (2.38)$$

$$\Delta G^o = 40{,}410 - 7.10\ T \quad (\pm\ 450\ \text{cal/mole M(s)})$$

They also reported a probable value for the entropy of formation of the hydroxide as 137.9 $\pm$ 0.55 eu at 1600 °K.

A graphical comparison of the available results from the different investigators is shown in Figure 2.8. Since Belton and Jordan worked with molybdenum metal, their reported equation was appropriately combined with the free energies of formation of water and molybdenum trioxide, to facilitate the comparison with the work of Glemser

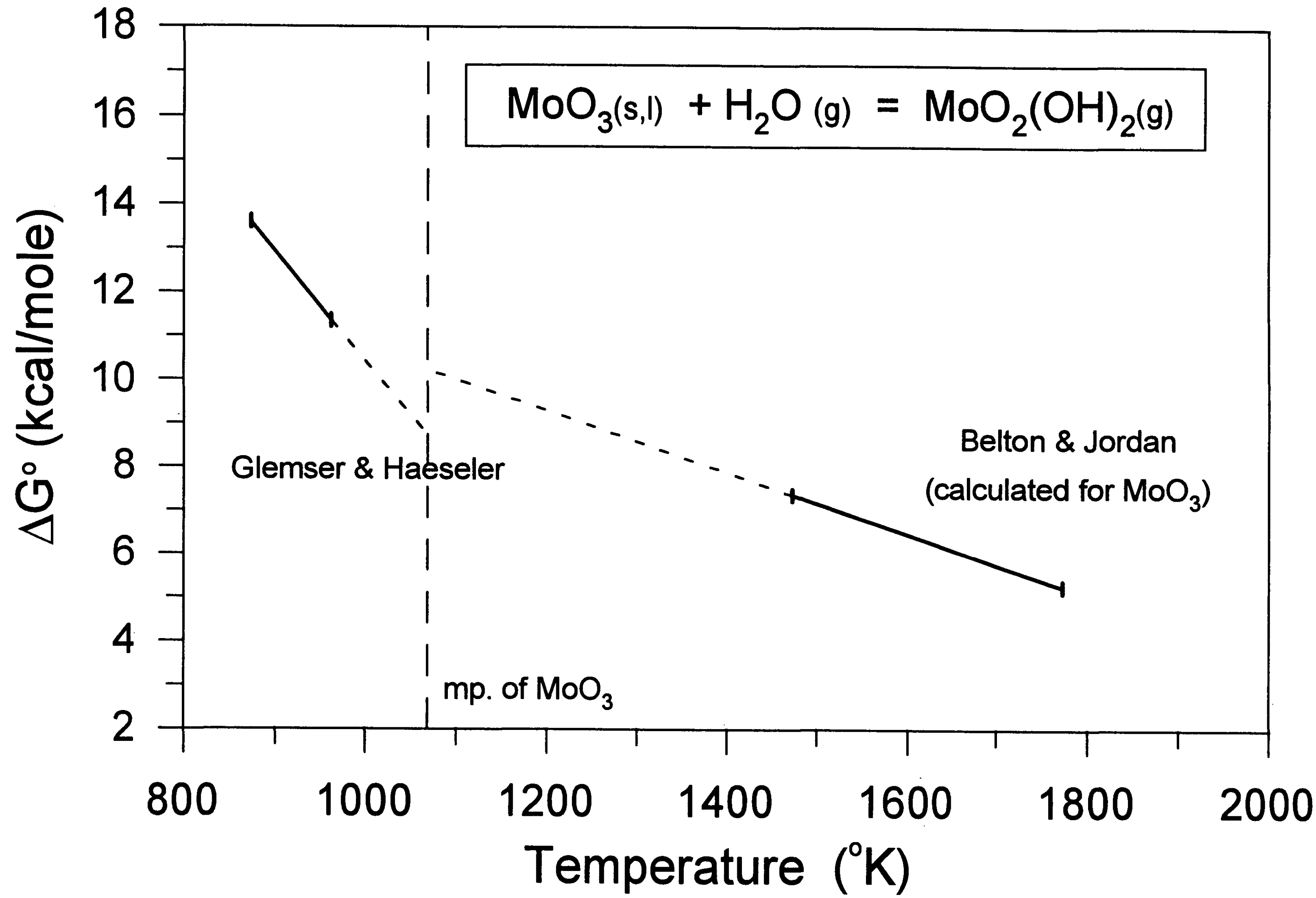

Figure 2.8 Gibbs free energy of reaction as a function of temperature as reported in the literature.

and Haeseler.

It was evident, from this comparison, that although the different investigators agreed in the molecularity of the hydroxide species formed, they disagreed in the magnitude of its vapor pressure. Therefore, it was the objective of the present investigation to conduct experiments to study the formation of volatile hydroxides with $MoO_3(s)$ and definitively resolve the discrepancies found in the literature.

2.4 Tungsten Trioxide

The main oxides of tungsten reported in the literature were $WO_2(s)$ and $WO_3(s)$. Between these oxides three other phases were reported in the JANAF tables[2]: $WO_{2.72}(s)$, $WO_{2.9}(s)$, and $WO_{2.96}(s)$. An attempt to calculate the oxygen pressures for the equilibria between the different phases, using the JANAF tables, was unsuccessful due to the inconsistencies in the data. The oxygen pressure for the equilibrium between $WO_{2.9}$ and $WO_{2.96}$ (10^{-16} atm) at 1100 °K, for example, was lower than that for $WO_{2.72}$ and $WO_{2.90}$ (10^{-13} atm) at the same temperature. The only sequence that was consistent with the oxygen equilibrium pressures, using the available data, was WO_2-$WO_{2.72}$-$WO_{2.96}$-WO_3. The phase diagram reported by Phillips, Chang and Scroger[48], however, does not show the $WO_{2.96}(s)$ phase (see Figure 2.9). Given these inconsistencies, it was clear that the W-O system was not yet properly defined.

For the purposes of the present study, the tungsten rich boundary of stability of $WO_3(s)$ was taken as that of $WO_{2.96}(s)$ and $WO_3(s)$. This boundary provided a higher (and

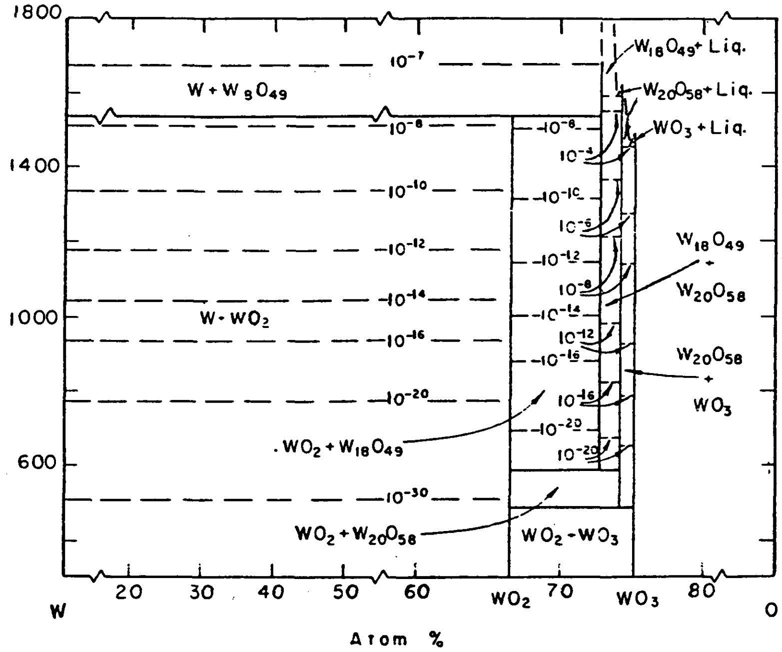

Figure 2.9 Equilibrium phase diagram for the tungsten-oxygen system[48].

therefore safer) theoretical O_2 pressure to maintain the integrity of $WO_3(s)$ than the pressures corresponding to the boundary with any of the other lower oxides. For the temperature range of interest in the present investigation, the oxygen equilibrium pressures for the equilibrium of these phases are shown in Table 2.6

Table 2.6 Equilibrium Oxygen Pressures for the Lower Limit of Stability of $WO_3(s)$

T °K	P_{O2} (atm)	Log P_{O2} (atm)
1000	1.00×10^{-13}	-13.00
1300	1.78×10^{-9}	-8.75

Since these oxygen pressures were several orders of magnitude lower than the working oxygen pressures of 0.10 to 0.82 atm used in this investigation, no problems were encountered in maintaining the integrity of the condensed sample.

2.4.1. Baseline Vapor Chemistry Above $WO_3(s)$

Once the stability ranges of the W-O system had been established, the next step was to determine the contribution of the volatile oxides to the total vapor pressure.

Stability diagrams at three selected temperatures within the temperature range of interest (727 to 1027 °C) were constructed utilizing the stability ranges for the condensed phases obtained in the previous section. To these ranges, lines representing the vapor pressures of the principal volatile oxides were superimposed. The data for the construction of these diagrams was obtained from the JANAF tables[2], (see Figures 2.10 to 2.12).

It was observed that, at all three temperatures, the main volatile oxide above $WO_3(s)$ was $W_3O_9(g)$. I was also observed that the vapor pressure of this gaseous oxide was lower than 1×10^{-7} atm. Since these magnitudes of vapor pressure were below the detection limit of the transpiration technique (2.5×10^{-7} atm.), their contribution to the total measured vapor pressure was practically null.

This conclusion was important since it allowed the direct measurement of the partial pressures of the hydroxides formed above $WO_3(s)$ in the presence of water vapor with no interference of volatile oxides. However, to provide a final check on the contribution of these gaseous species to the measured vapor pressure in the absence of

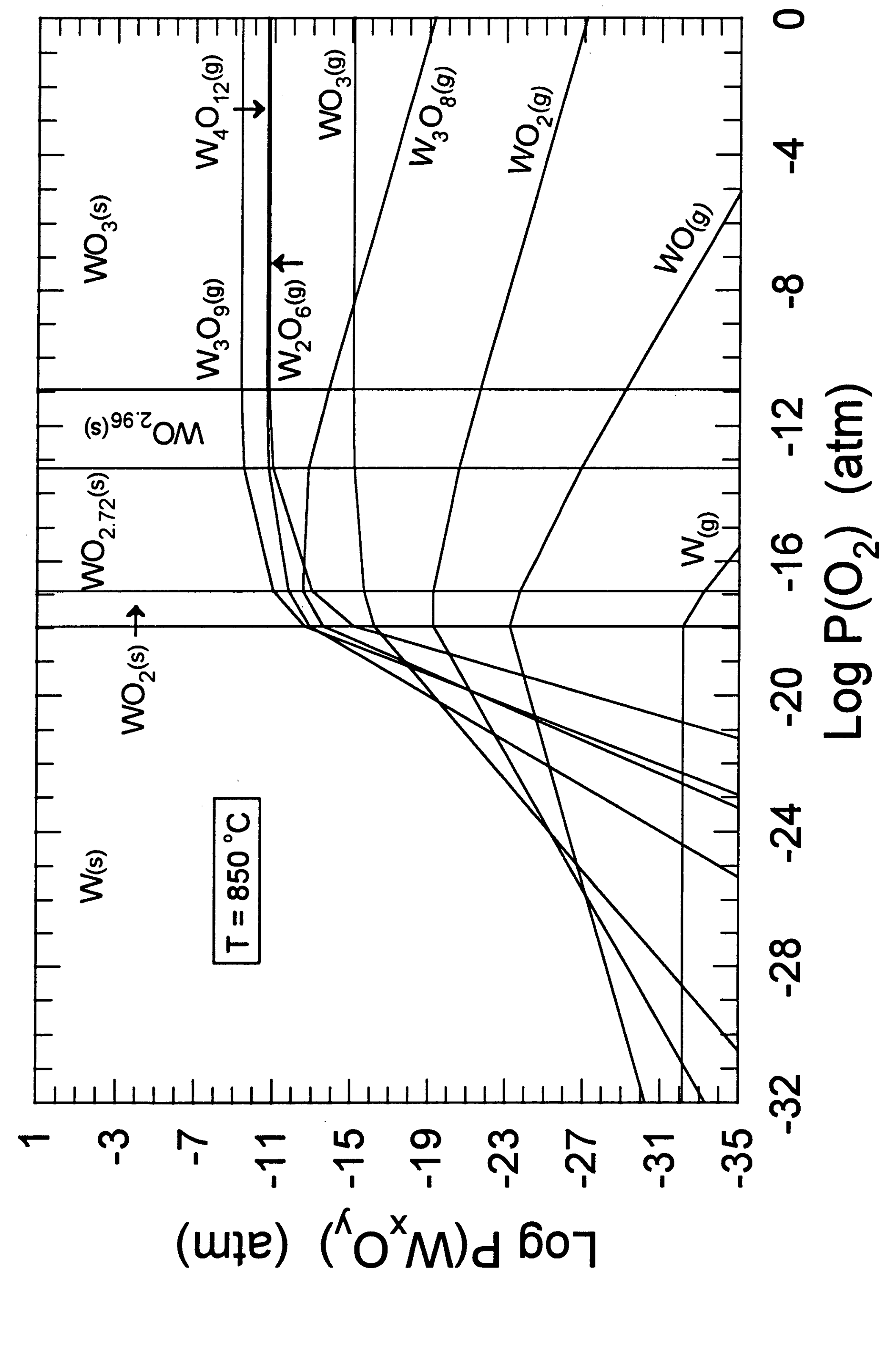

Figure 2.10 Stability diagram for the W-O system at 850 °C.

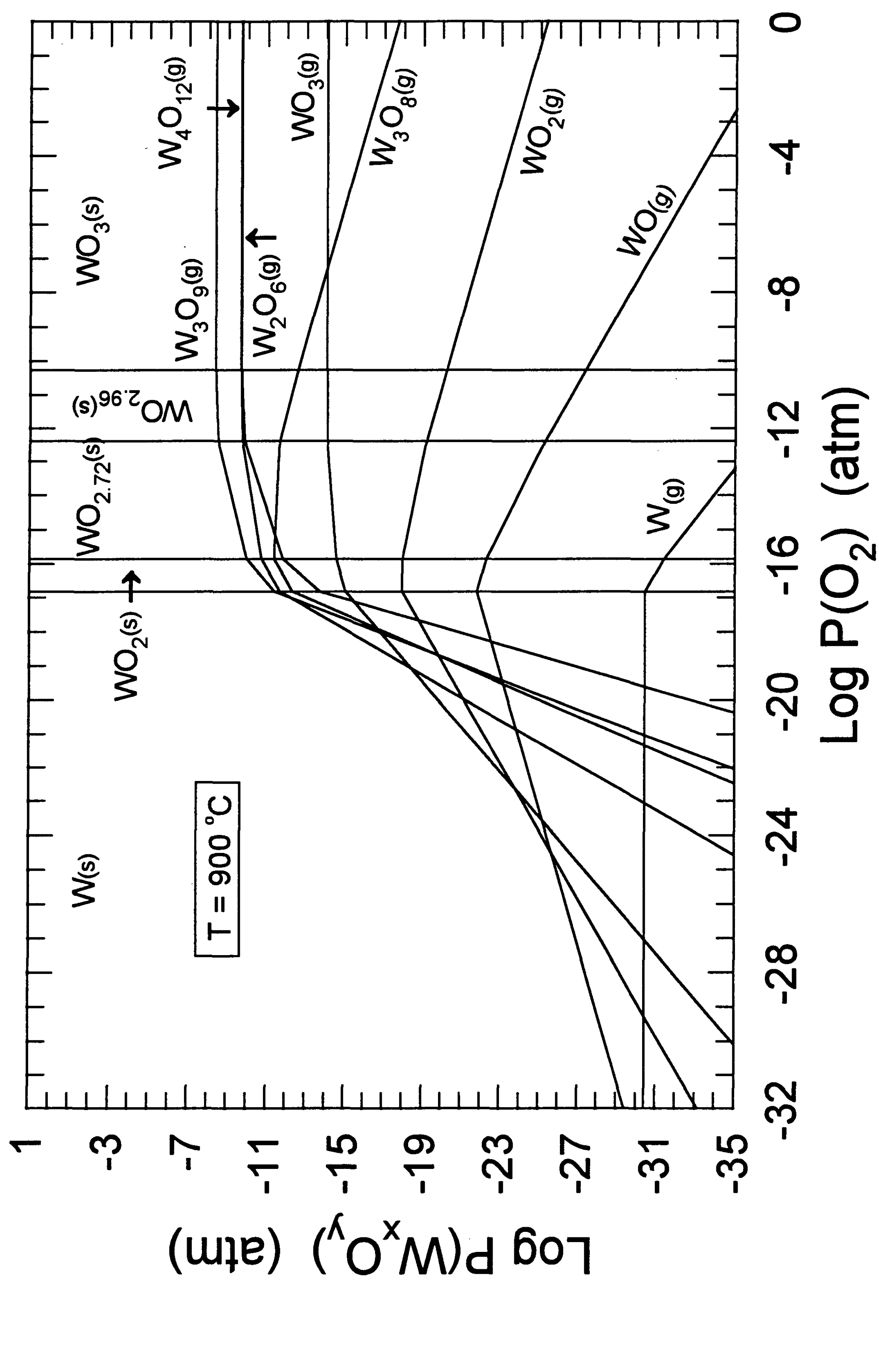

Figure 2.11 Stability diagram for the W-O system at 900 °C.

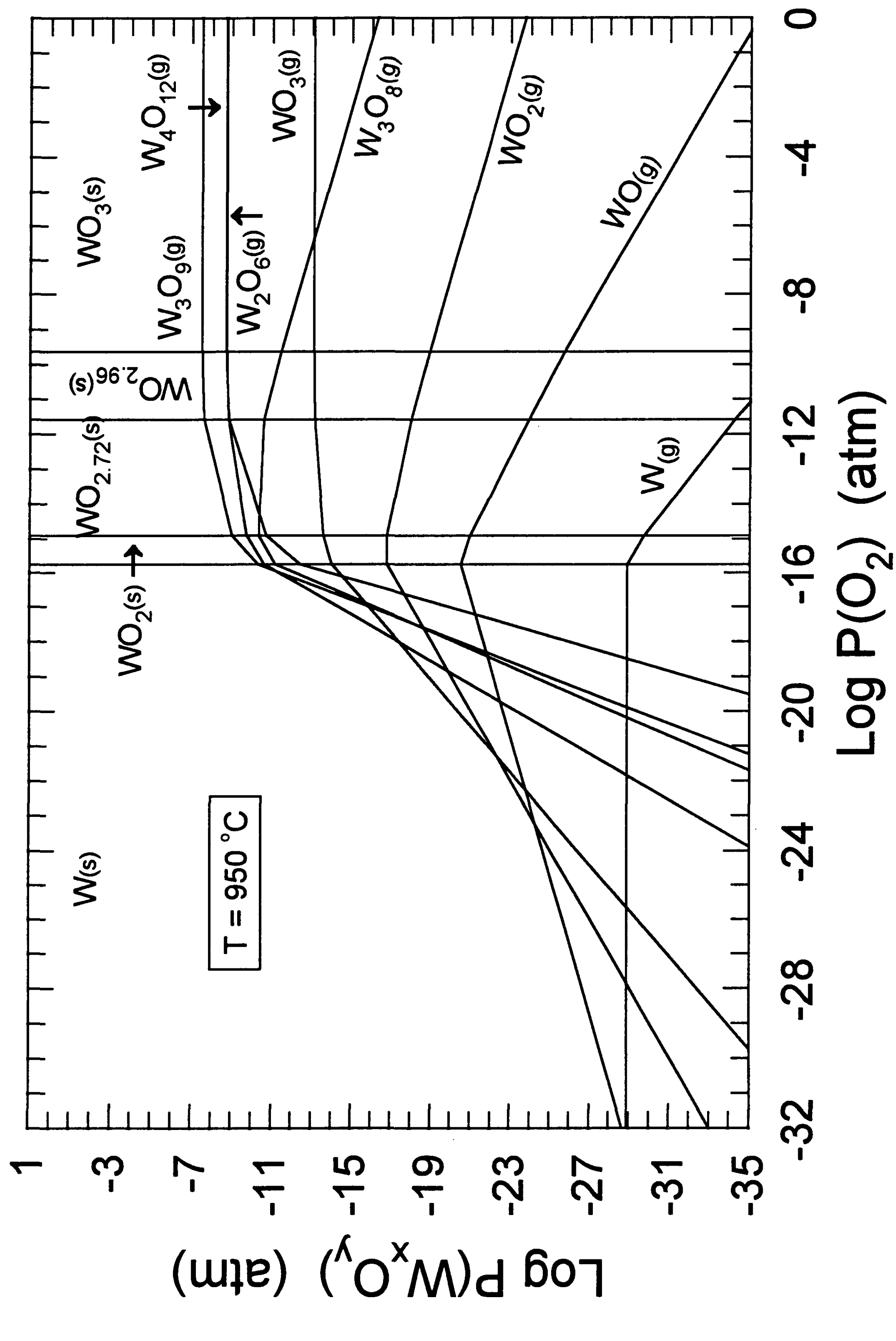

Figure 2.12 Stability diagram for the W-O system at 950 °C.

$H_2O(g)$, baseline vapor pressure measurements were conducted.

2.4.2 Enhancement of the Volatility Above $WO_3(s)$ in the Presence of Water Vapor

Increased volatility above $WO_3(s)$ was first observed by Millner and Neugebauer[45] at 1 atm and 1000 °C. They proposed that water, in the gaseous phase, can form bonds strong enough to remove the oxides from the crystal lattice of $WO_3(s)$.

Although they did not report a possible molecularity for the formed hydroxides, Grossweiner and Seifert[49], using Millner and Neugebauer's data, suggested that $WO_2(OH)_2(g)$ might be the gaseous hydroxide formed.

Glemser and Volz[50] studied the formation of volatile hydroxides using the transpiration technique in the temperature range of 1100 to 1200 °C. Using nitrogen-water mixtures as the carrier gas, they reported the formation of $WO_2(OH)_2(g)$ according to:

$$WO_3(s) + H_2O(g) = WO_2(OH)_2(g) \qquad (2.39)$$

$$\Delta G^\circ = 38{,}100 - 16.7\,T \text{ (cal/mole)}$$

A few years later, Glemser and Haeseler[31] studied the formation of volatile hydroxides in the temperature range of 900 to 1000 °C. Using oxygen-water vapor mixtures as the carrier gas, they reported the same molecularity as Glemser and Volz, but different thermodynamic parameters. Their work was summarized as:

$$WO_3(s) + H_2O(g) = WO_2(OH)_2(g) \qquad (2.40)$$

$$\Delta G^\circ = 39{,}900 - 18.8\,T \text{ (cal/mole)}$$

Meyer et al.[51] also conducted experiments with $WO_3(s)$ to investigate the formation of volatile hydroxides of tungsten. Using the transpiration technique in the temperature range of 1120 to 1250 °C, they reported the formation of $WO_2(OH)_2(g)$ as:

$$WO_3(s) + H_2O(g) = WO_2(OH)_2(g) \tag{2.41}$$

$$\Delta G° = 25{,}800 - 8.4\ T\ \text{(cal/mole)}$$

Belton and McCarron[52] also studied the formation of volatile hydroxides of tungsten. Using the transpiration technique in the temperature range of 1200 to 1500 °C, they investigate the enhancement of the volatility of W metal in the presence of water vapor. In order to prevent the oxidation of the metal they used reducing argon-hydrogen-water vapor mixtures. Their results were summarized as:

$$W(s) + 4H_2O(g) = WO_2(OH)_2(g) + 3H_2(g) \tag{2.42}$$

$$\Delta G° = 26{,}700 - 5.56\ T\ \text{(cal/mole)}$$

Belton and McCarron also combined their results over tungsten metal with the appropriate data from JANAF[2] and NBS[53], to obtain an equation for the enhancement of the volatility of $WO_3(s)$:

$$WO_3(s) + H_2O(g) = WO_2(OH)_2(g) \tag{2.43}$$

$$\Delta G° = 42{,}260 - 21.18\ T\ \text{cal/mole}$$

They also reported a possible value for the entropy of the hydroxides as 136.7 ± 1.05 eu at 1600 °K.

A graphical comparison of the available results from the different investigators is shown in Figure 2.13. It is evident, from this comparison, that although the different investigators agreed in the molecularity of the hydroxide formed, they disagreed in the magnitude of its vapor pressure. Therefore, it was a final objective of the present investigation to conduct experiments to study the formation of volatile hydroxides with $WO_3(s)$ and definitively resolve the discrepancies found in the literature.

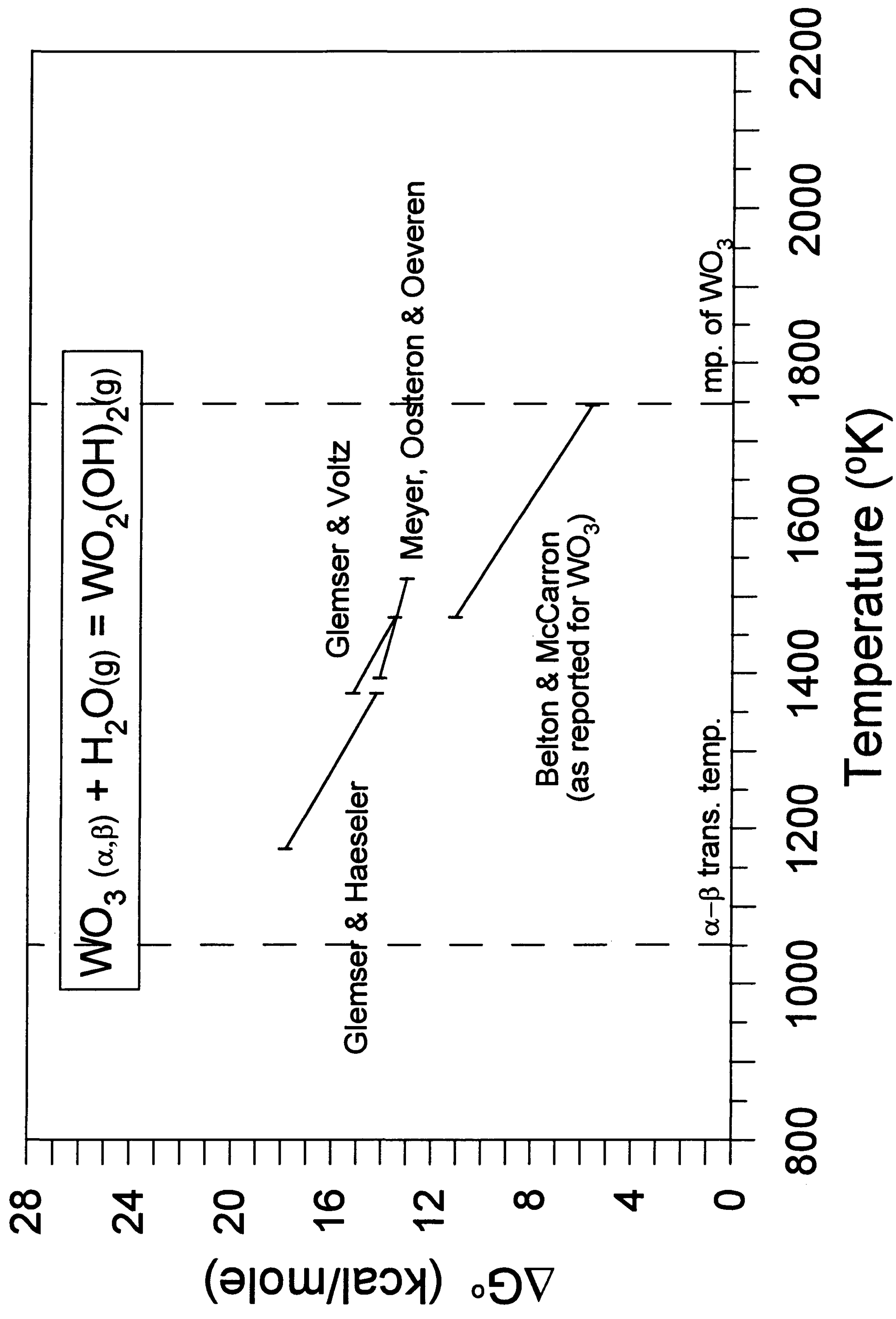

Figure 2.13 Gibbs free energy of reaction as a function of temperature as reported in the literature.

III. EXPERIMENTAL TECHNIQUE

In this chapter, several aspects of the experimental technique used in the present investigation are discussed. The chapter is organized into six sections. The first three and the last two sections are pertinent to the experimental method and its sources of error. Section 3.4, describes the data analysis necessary to obtain the molecularity, the vapor pressures, and the thermodynamic parameters necessary to characterize the formation of volatile hydroxides in equilibrium with their condensed phases.

For each condensed phase (V_2O_5, V_2O_3, MoO_3 and WO_3), the first series of experiments were conducted in the absence of water vapor. The purpose of these experiments was to measure the contribution of the volatile oxide species to the total vapor pressure. In the second series of experiments, water was added to the carrier gas and the formation of volatile hydroxides was investigated.

3.1 Principles of the Transpiration Technique

The transpiration method was selected for this investigation because of the importance of maintaining an adequate oxygen potential throughout the experiments,which assured the integrity of the condensed phases.

In the transpiration method, a condensed phase is equilibrated with a carrier gas under a controlled atmosphere. The carrier gas mixture, which may contain inert or reactive gases at pre-specified ratios, is passed over the condensed sample at a rate sufficient for equilibrium to be established between the gas and the condensed phase. The saturated gas carries the volatile species to the condenser system where they are collected and quantified. The vapor pressures of these volatile species can be calculated either from their weight loss of the condensed sample or from the amount of material transported to the condenser system. For such calculations it is necessary to know the following parameters:

1) moles of material transported
2) carrier gas flowrate
3) duration of the run
4) reaction temperature and pressure
5) ambient temperature and pressure

Moreover, a mole or mass balance of the atomic species involved in the reactions is necessary in order to calculate the number of moles of each species in the equilibrated gas mixture.

A very important consideration for these calculations is the saturation of the carrier gas. This equilibrium saturation depends mainly on the rate of vaporization of the sample, the exposed surface area, the diffusivity of the vaporized molecules, and the flow regime, composition, and volumetric flow rate of the carrier gas. As noted by Alcock and Hooper[54], plug flow is the ideal flow regime for the transpiration technique. The attainment of saturation of the carrier gas is confirmed when, by controlling the flow rate, an equilibrium plateau is obtained when plotting the apparent vapor pressure versus the carrier gas flow rate. A typical curve of the apparent vapor pressure as a function of flow rate is depicted in Figure 3.1.

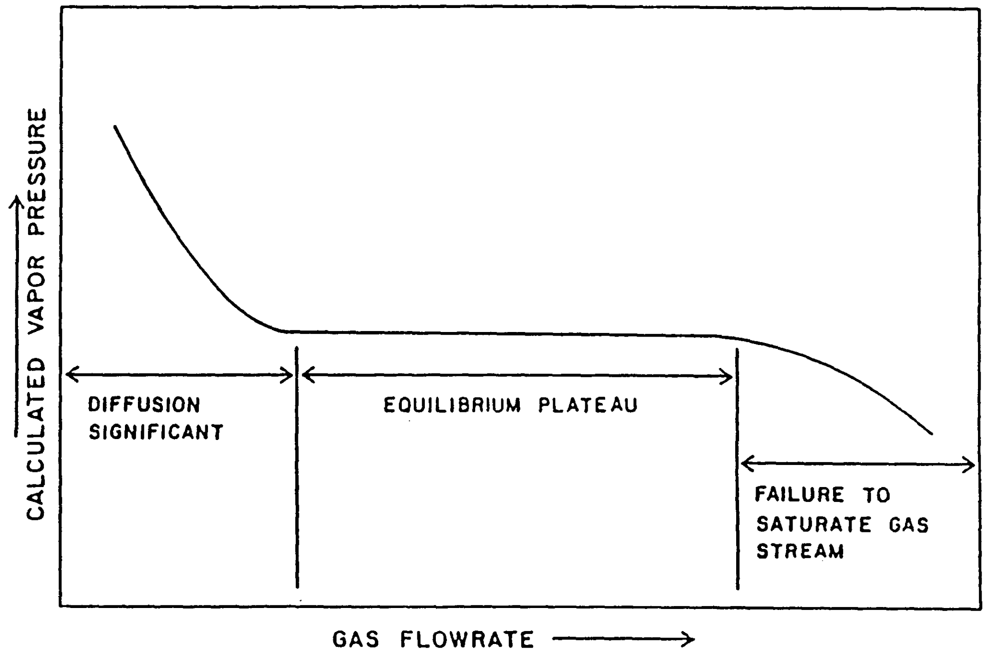

Figure 3.1 Typical curve shape of $P_{Apparent}$ as a function of carrier gas flow rate.

At low flow rates, the apparent vapor pressures are higher than expected from equilibrium saturation because of diffusive flow of the vapor molecules out of the reaction zone. At high flow rates, on the other hand, the apparent vapor pressures tend to be lower because there is not enough time for saturation to be attained. The attainment of equilibrium is thus confirmed, when the measured equilibrium constants are independent of the flowrates used.

The main limitation of the transpiration technique is that one must have *a priori* knowledge or idea of the vapor species present. For this reason a meticulous and comprehensive literature review is necessary to characterize, as best as possible, the vapor chemistry of the substances to be studied.

3.2 Transpiration Apparatus

3.2.1 Reactor System

Two electric furnaces in series were used to supply heat to the reactor. These furnaces had multiple electrical taps to allow for the control of the temperature profile along the length of the reactor. These taps were connected in a parallel configuration to the heating elements, and the current that passed through them was adjusted using variable resistors. In this way, a flat temperature profile was obtained in the reaction zone. An electronic controller was used in the Proportional-Integral-Derivative mode (PID) to control the temperature of each furnace to $\pm$ 1 °C.

A schematic of the transpiration system used for the Me-O-H vapor transport studies is given in Figure 3.2 . The reactor tube and the sample carrier tube were made of quartz. One slot of 16.5 cm was provided in the carrier tube to hold 3 alumina sample boats (5 cm in length each). The annular area between the carrier tube and the reactor tube was minimized to prevent back diffusion of the carrier gas during the run (all calculations were based on the assumption of plug flow of the gases through the reaction chamber). The sample carrier tube was inserted into the reactor by means of

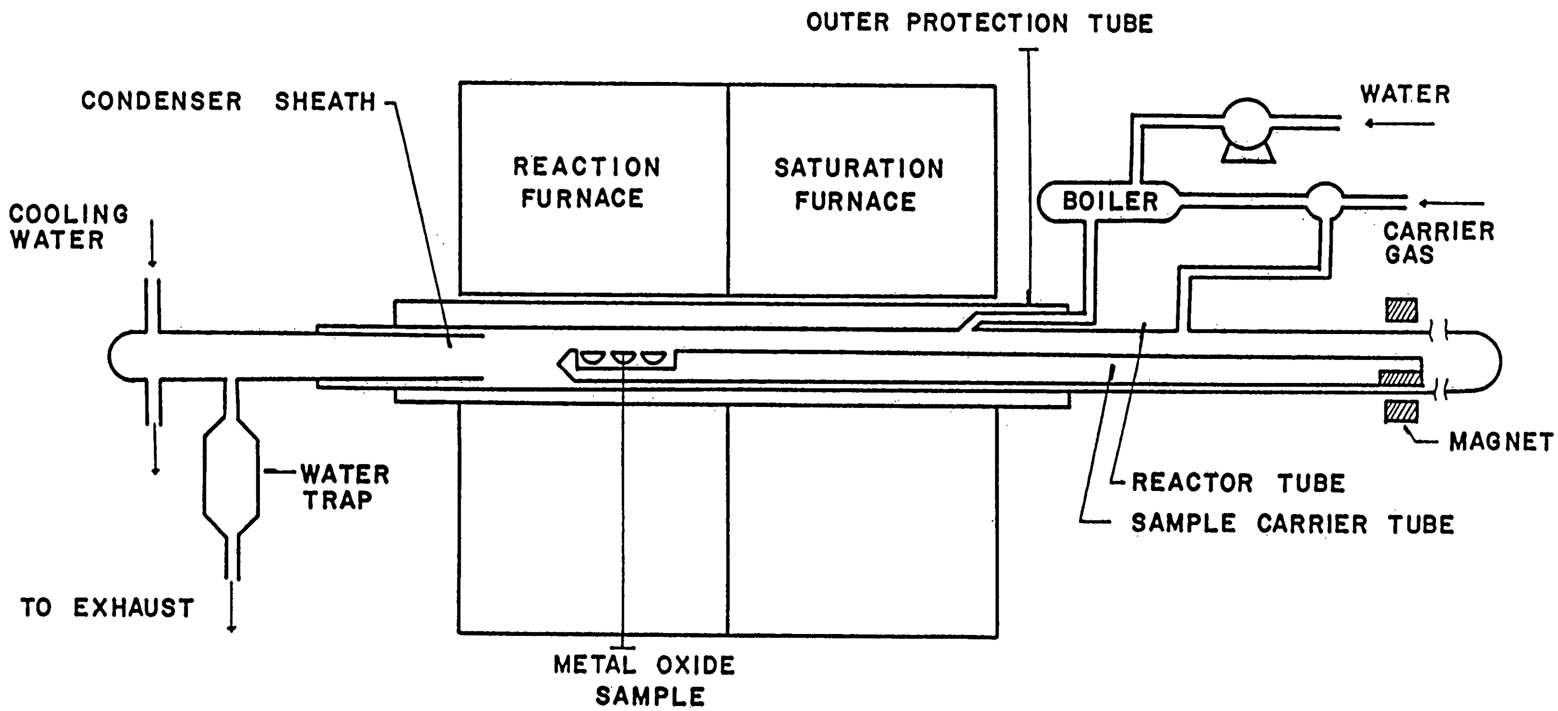

Figure 3.2 Schematic diagram for the transpiration system.

a magnetic coupling device.

The temperature profile along the reactor was determined using a calibrated type "K" thermocouple assembly. The calibration of the thermocouple was measured against the melting point of Al and Ag. Dry deoxidized argon was continuously passed above the melt to provide an inert atmosphere during the calibration. The temperature measuring assembly was inserted into the reactor tube and was allowed to equilibrate for approximately 10 to 12 hrs before the temperature profile was determined.

3.2.2 Gas Train

A schematic diagram of the gas train system used for this investigation is shown in Figure 3.3. High purity gases were used as received from the supplier. Individual flowrates were measured by precision capillary flowmeters located downstream from the gas regulators. Constant head tanks, placed between the flowmeters and the gas regulators, were used to eliminate variations in the flow due to oscillations in the regulator outputs. The delivery pressures, and consequently, the flowrates, were varied by adjusting the depth of the "T's" inside the constant head tanks . The glass "T's" were connected to both the flowmeters and the regulators with polyethylene tubing. The gases were dried, before entering the flowmeters, in drying columns (in series) using a mixture of silica gel and magnesium perchlorate as the desiccant. In the case of argon, deoxidation was achieved by passing the argon through a deoxidation column, packed with Cu strips. The temperature of the column was kept at 450 °C.

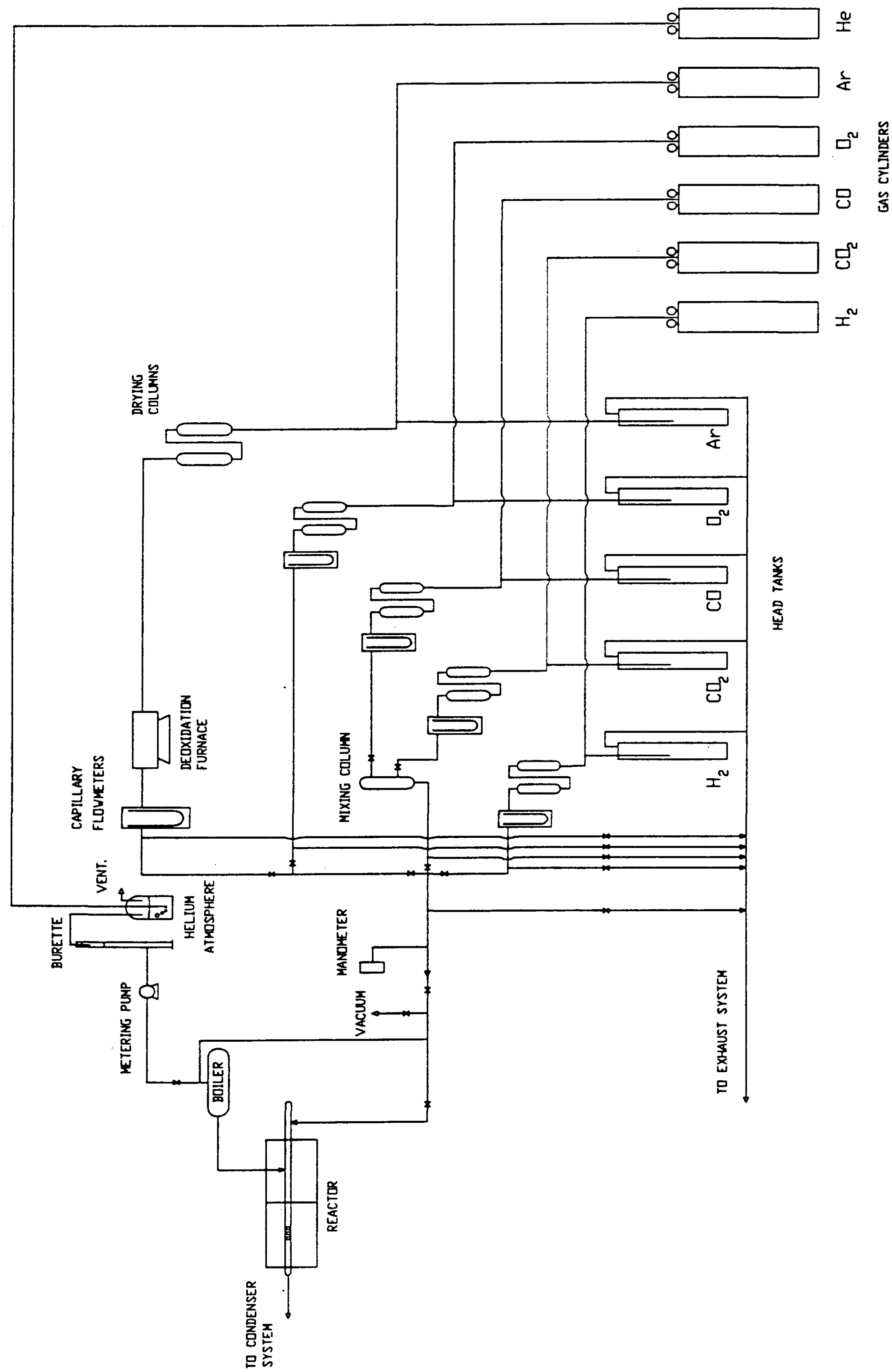

Figure 3.3 Schematic diagram of the gas train.

The gases, when passing through the capillary tubes, caused a displacement in the flowmeter proportional to the flowrate according to Poiseuille's equation:

$$Q = \frac{\pi g \rho_l D^4}{128 \mu_g L} h \tag{3.1}$$

where,

h : displacement of the liquid inside the meter

ρ_l : density of the liquid being displaced

D : diameter of capillary

L : length of capillary

μ_g : viscosity of the gas

Q : flowrate

This equation was used to estimate the size of the capillary tubes required for a desired "h" at a given flowrate. It was desirable to maximize the displacement in order to minimize the reading errors.

The calibration of the flowmeters was performed using the rising bubble method as described by Annamalai[55].

3.2.3 Water Injection System

The water injection system consisted of a 100 ml burette maintained under a helium atmosphere, a peristaltic pump with a ten rollers head, and a specially designed boiler (see Figure 3.3). The water used in all experiments was distilled in one stage, and deaerated by bubbling helium through it for two hours in batches of 200 ml.

The purpose of the distillation and deareation was twofold. First, it was necessary to remove impurities and dissolved gases to minimize the possibility of mineral scale and unwanted side reactions. Chlorine for example, is known to form stable gaseous compounds when in contact with metals at high temperatures. The second purpose was to minimize gas dissolution from the water while it was being pumped; when the roller head of a peristallic pump compresses the tubing, it tends to induce a vacuum which could promote gas dissolution.

In order to prevent reaeration of the water, as well as evaporation, the top of the burette was subjected to an atmosphere of moist helium. No significant loss due to vaporization was observed when the water was left standing under these conditions for 24 hrs

The water was loaded into a 100 ml burette and pumped into the boiler using a Gilson 2 Plus peristaltic pump.

The peristaltic water pump was calibrated by measuring the quantity of water pumped per unit time at a given setting. A calibration curve was constructed and utilized as a means of estimating the water flowrates needed for the various experimental runs. The actual water injected was directly measured from the burette, and compared to the water collected in the condenser assembly.

The boiler was constructed of stainless steel and during operation was maintained at 450 °C with an electric heating element . A schematic diagram of the boiler is shown in Figure 3.4.

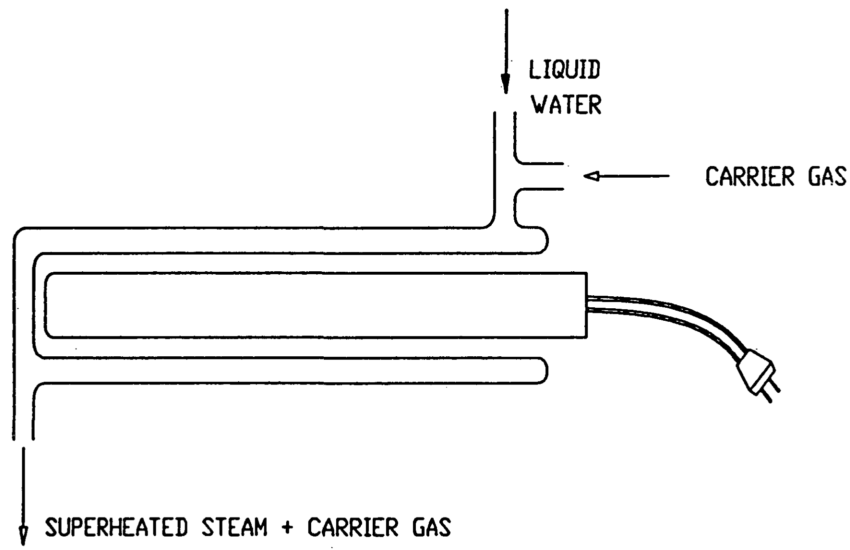

Figure 3.4 Schematic diagram of the boiler assembly.

The liquid water was metered from the burette into the boiler where it was vaporized and mixed with the carrier gas, and then transported into the reacting chamber. All lines downstream of the boiler were heated using heating tape and insulated to prevent water condensation. After the gas stream equilibrated with the solid oxide, it passed through a condenser assembly and water trap where both the transported material and condensed water were collected and quantified. Mass closures for water of up to 97% recovery in the condenser assembly were realized in most of the experiments.

3.3 Experimental Procedure

The experimental procedure followed to investigate the formation of volatile hydroxides of Mo, W, and V is presented in the following paragraphs.

1) The temperature measuring assembly was inserted into the reactor and was allowed to reach thermal equilibrium, for at least 12 hrs, with the atmosphere inside the reactor. This atmosphere consisted of flowing argon at 90 cc/min.

2) The temperature profile was then taken along the length of the reacting zone (13 cm). If the temperature was not flat within $\pm$ 1 °K in the reacting zone, the appropriate rheostats were adjusted, and after 4 hrs, the temperature profile was taken again. This procedure was repeated until a flat temperature profile was obtained.

3) Samples of high purity V_2O_5, V_2O_3, MoO_3, and WO_3 were loaded into high purity alumina boats and weighted on a 5-decimal place analytical balance; the sample purities were 95, 99.995, 99.9995, and 99.9994%, respectively, and that of the alumina boats was 99.8%.

4) The boats were placed into the carrier tube and the system sealed and evacuated for 5 minutes.

5) The desired flowrate and composition of the carrier gas was established : Ar-O_2 mixtures for the baseline experiments with V_2O_5(s), MoO_3(s), and WO_3(s); and CO-CO_2 mixtures for the baseline experiments with V_2O_3(s).

For the experiments in the presence of water vapor , $Ar-O_2-H_2O$ mixtures were used for $V_2O_5(s)$, $MoO_3(s)$, and $WO_3(s)$; and $CO-CO_2$ $-H_2$ $-H_2O$ mixtures for $V_2O_3(s)$.

6) The system was backfilled and flushed with the carrier gas before the sample carrier tube was inserted into the reactor under the flow of the carrier gas. The samples boats were inserted at a rate of 10 cm/min by means of a magnetic coupling device. In the cases where water addition was required, although most of the carrier gas was directed into the boiler and mixed with the water vapor, enough gas was deviated to the entrance of the furnace to prevent possible water back diffusion.

7) During the run, the ambient temperature, the ambient pressure, the reactor pressure, and the flowrates were monitored at regular intervals. Run times varied from 3.5 to 48 hrs depending of the oxide being studied. For all the baseline experiments the run started the moment the insertion of the boats started, and ended, the moment they were completely withdrawn. In the cases where water vapor was added, except for the case of molybdenum, the runs started, with the boats in the reacting zone, the moment the water was turned on. The runs ended the moment the water was turned off (with the boats still in the reacting zone). In the case of molybdenum trioxide, due to its high volatilization even in the absence of water, the run started when the water was turned on (immediately before inserting the boats), and ended

when the water was turned off (immediately after the boats were withdrawn).

8) After a pre-specified equilibration time, the samples were withdrawn at the same rate they were inserted. Once totally withdrawn, the sample boats were allowed to cool down for 20 min under an atmosphere of $Ar-O_2$ mixtures for the case of $V_2O_5(s)$, $MoO_3(s)$, and $WO_3(s)$; and $CO-CO_2$ mixture for the case of $V_2O_3(s)$.

9) The sample boats were then transferred to a desiccator and allow to thermally equilibrate with the room temperature for approximately 2 hrs. Then they were reweighed and the weight recorded.

10) The condenser sheath was removed and chemically stripped with H_2SO_4 1.8 N for $V_2O_5(s)$; NaOH 1N for $MoO_3(s)$; NaOH 1N (hot) for $WO_3(s)$; and HNO_3 conc. for $V_2O_3(s)$. Also, in the cases where water was added, the collected water was quantified in a graduated cylinder.

3.4 Data Analysis

3.4.1 Vanadium Pentoxide

As noted in the literature review, the contribution of volatile oxides of vanadium to the total vapor pressure of $V_2O_5(s)$, in the temperature range of interest (560 to 660 °C), was below the detection limits of the experimental technique. Thus, the vapor pressure of the volatile hydroxides could be determine directly from the total measured vapor pressures.

The proposed reactions for the formation of volatile hydroxides above $V_2O_5(s)$ were:

$$V_2O_5(s) + 3H_2O(g) = 2VO(OH)_3(g) \tag{3.2}$$

$$\text{Log } P_{VO(OH)_3} = \frac{3}{2}\text{Log } P_{H_2O} + \frac{1}{2}\text{Log } K$$

$$V_2O_5(s) + 2H_2O(g) = V_2O_3(OH)_4(g) \tag{3.4}$$

$$\text{Log } P_{V_2O_3(OH)_4} = 2\text{Log } P_{H_2O} + \text{Log } K$$

$$V_2O_5(s) + 2H_2O(g) + \frac{1}{2}O_2(g) = 2VO_2(OH)_2(g) \tag{3.6}$$

$$\text{Log } P_{VO_2(OH)_2} = \text{Log } P_{H_2O} + \frac{1}{4}\text{Log } O_2 + \frac{1}{2}\text{Log} K$$

The above linearization of the equilibrium constant for each reaction was useful in establishing the stoichiometry of the principal volatile hydroxides formed. When the logarithm of the apparent vapor pressure was plotted as a function of the logarithm of either the partial pressure of water or oxygen, a straight line was obtained and its slope determined the major gaseous hydroxide species formed. Table 3.1 summarizes the theoretical slopes for each reaction.

The calculation of the partial pressure of the volatile hydroxide species formed, according to reaction (3.2), was described in the following paragraphs, assuming a carrier gas mixture or Ar, O_2, and H_2O. The equilibrium vapor pressures considering the other two proposed species can be calculated in a similar fashion.

The partial pressure for the volatile hydroxide was expressed as:

$$P_{VO(OH)_3} = \frac{n'_{VO(OH)_3}}{n'_T} P_T \tag{3.8}$$

where,

$n'_{VO(OH)3}$: moles of $VO(OH)_3$ in the equilibrated gas mixture

n'_T : total number of moles in the equilibrated gas mixture

P_T : total pressure in atmospheres

The moles of $VO(OH)_3$ in the equilibrated gas mixture were obtained from a mole balance for atomic vanadium as:

Table 3.1 Slopes for the Linearized Equilibrium Constant Expressions for Reactions (2), (4), and (6)

Species	Slope	
	Log $P(H_2O)$	Log $P(O_2)$
$VO(OH)_3$	1.5	0.00
$V_2O_3(OH)_4$	2.0	0.00
$VO_2(OH)_2$	1.0	0.25

$$n'_{VO(OH)_3} = 2n^{\circ}_{V_2O_5} = 2\,\frac{\text{Wt.loss}}{mw_{V_2O_5}} \tag{3.9}$$

where,

n°_{V2O5} : moles of $V_2O_5(s)$ transported as determined by the weight loss

mw_{V2O5} : molecular weight of $V_2O_5(s)$

On the other hand, if the moles of vanadium collected at the condenser were measured, the moles of $VO(OH)_3$ were also directly calculated as:

$$n'_{VO(OH)_3} = n_V \tag{3.10}$$

where,

n_V : moles of vanadium collected at the condenser

Using the expression:

$$n'_T = \Sigma n'_i = n'_{H_2O} + n'_{O_2} + n'_{Ar} + n'_{VO(OH)_3} \tag{3.11}$$

the total number of moles of the gaseous species in the equilibrated gas mixture was calculated from the obtained value of $n'_{VO(OH)3}$ and the moles of H_2O, O_2, and Ar in the equilibrated gas mixture. The moles of H_2O, O_2, and Ar were obtained from elemental mole balances for H, O, and Ar.

1. Mole balance for atomic H:

$$n'_{H_2O} = n^{o}_{H_2O} - \frac{3}{2}n'_{VO(OH)_3} \tag{3.12}$$

2. Mole balance for atomic O:

$$n'_{O_2} = n^{o}_{O_2} + \frac{5}{2}n^{o}_{V_2O_5} + \frac{1}{2}n^{o}_{H_2O} - \frac{1}{2}n'_{H_2O} - 2n'_{VO(OH)_3} \tag{3.13}$$

3. Mole balance for atomic Ar:

$$n'_{Ar} = n^{o}_{Ar} \tag{3.14}$$

where,

n'_{H2O} : moles of H_2O in the equilibrated gas mixture

n'_{O2} : moles of O_2 in the equilibrated gas mixture

n'_{Ar} : moles of Ar in the equilibrated gas mixture

n^{o}_{H2O} : moles of H_2O introduced into the carrier gas

n^{o}_{O2} : moles of O_2 introduced into the carrier gas

n^{o}_{Ar} : moles of Ar introduced into the carrier gas

Equations (3.9), (3.11), (3.12), (3.13), and (3.14) were arranged to yield:

$$n'_{T} = n^{o}_{O_2} + n^{o}_{Ar} + n^{o}_{H_2O} - \frac{1}{2}n'_{VO(OH)_3} \tag{3.15}$$

Once the above calculations were completed, the partial pressure of $VO(OH)_3$(g) was calculated from equation (3.8).

The partial pressures of the remaining species were calculated using:

$$P_i = \frac{n'_i}{n'_T} P_T \tag{3.16}$$

where,

n'_i : moles of species "i" in the equilibrated gas mixture

P_i : partial pressure of species "i" in the equilibrated gas mixture

After calculating the partial pressures of the species, the equilibrium constants for the reactions were computed. In the case of reaction (3.2) the equilibrium constant was calculated as follows:

$$K = \frac{P_{VO(OH)_3}{}^2}{P_{H_2O}{}^3} \tag{3.17}$$

Once the equilibrium constant was determined, the standard Gibbs free energy change for the reaction was calculated as:

$$\Delta G^\circ = - RT \ln K \tag{3.18}$$

In order to calculate the ΔG° of the reaction with temperature, the Second Law Method (Sigma-Plot method) was used. The application of the Second law method to rigorously correlate ΔG° with temperature is describe in the following paragraphs.

$$\frac{d(\Delta H^\circ)}{dT} = \Delta Cp^\circ \tag{3.19}$$

where,

$\Delta C_p°$ (the heat capacity change of the reaction) is expressed as:

$$\Delta Cp° = \Delta a + \Delta bT + \Delta cT^{-2} \tag{3.20}$$

Substituting equation (3.20) into equation (3.19) and integrating, equation (3.21) is obtained:

$$\Delta H° = \Delta H_o + \Delta aT + \frac{\Delta bT^2}{2} + \Delta cT^1 \tag{3.21}$$

where: ΔH_o is a constant of integration.

The Gibbs-Helmholtz equation is:

$$\frac{d\,(\frac{\Delta G°}{T})}{dT} = \frac{-\Delta H°}{T^2} \tag{3.22}$$

Substituting equation (3.21) into equation (3.22) and integrating, equation (3.23) is obtained

$$\Delta G° = \Delta H_o + IT - \Delta aT\ln T - \frac{\Delta bT^2}{2} - \frac{\Delta cT^{-1}}{2} \tag{3.23}$$

where I = constant of integration.

Expressing $\Delta G°$, in equation (3.23), as -RT Ln K and dividing both sides by T,

$$-R \ln K = \frac{\Delta H_o}{T} + I - \Delta a \ln T - \frac{\Delta bT}{2} - \frac{\Delta cT^{-2}}{2} \tag{3.24}$$

Rearranging equation (3.24) and defining Σ as :

$$\Sigma = -R \ln K + \Delta a \ln T + \frac{\Delta bT}{2} + \frac{\Delta cT^{-2}}{2} \tag{3.25}$$

the following expression for Σ is obtained:

$$\Sigma = \frac{\Delta H_o}{T} + I \tag{3.26}$$

When Σ from equation (3.26) is plotted as a function of the inverse of the temperature, a straight line is generated and the values of the constants $\Delta H°$ ad I are readily obtained. These values, in turn, can be substituted in equation (3.23) to obtain an expression for the $\Delta G°$ of reaction as a function of temperature.

It is evident from equation (3.23) that if $\Delta C_p°$ is equal to zero, then $\Delta H_o = \Delta H°$ and $I = -\Delta S°$. Thus, equation (3.23) may be expressed as:

$$\Delta G° = \Delta H° - T\Delta S° \tag{3.27}$$

The results obtained by the Second Law method could be further checked using the Third Law method of analysis, which utilizes the free energy functions (fef') of both the reactants and products.

$$\text{fef}' = \frac{(G^\circ_T - H^\circ_{298})}{T} \tag{3.28}$$

Since the fef' functions of each individual substance are related to the ΔG° of reaction, then the following expression is obtained:

$$\Delta\ \text{fef}' = \frac{(\Delta G^\circ_T - \Delta H^\circ_{298})}{T} \tag{3.29}$$

From equation (3.29), an expression for ΔH°_{298} can be derived from the measured equilibrium constant at any temperature:

$$\Delta H^\circ_{298} = T\ (-R\ \ln K\ \Delta \text{fef}') \tag{3.30}$$

The usefulness of this method is that it allows for an independent check of each measurement and, consequently, for the reliability of the obtained data. Both the Second and Third Law methods of analysis are usually conducted for these purposes.

3.4.2 Vanadium Trioxide

Baseline experiments were conducted in the absence of water vapor to corroborate the null contribution of volatile oxide species to the total vapor pressure suggested in the literature in the temperature range of 600 to 900 °C. The same experimental system and technique as in the case of V_2O_5(s) was used. In this experiments, however, the oxygen potential was controlled by using a mixture of CO and CO_2 gas.

Once the baseline experiments were completed, $H_2(g)$ and $H_2O(g)$ were added to the carrier gas to provide for controlled $P_{CO2} : P_{CO}$ and $P_{H2O} : P_{H2}$ ratios. The carrier gas composition was pre-adjusted taking into account the gas shift reaction:

$$CO(g) + H_2O(g) = CO_2(g) + H_2(g) \tag{3.31}$$

in order to assure the desired composition in the reaction chamber. The purpose of these experiments was to identify and quantify the volatile hydroxide of vanadium in equilibrium with $V_2O_3(s)$. However, no evidence was found of the formation of volatile hydroxides with $V_2O_3(s)$.

3.4.3 Molybdenum Trioxide

It was evident from the literature review, that the contribution of volatile oxides to the total vapor pressure of $MoO_3(s)$ was significant. Thus, baseline experiments with $MoO_3(s)$ were conducted.

The experimental procedure used was the same as for the case of $V_2O_5(s)$. The data analysis, however was different because of the mentioned contribution of volatile oxides of molybdenum to the total vapor pressure.

3.4.3.1 Baseline Data Analysis. It was found, from the literature review, that the main volatile oxide above $MoO_3(s)$, at temperatures around 850 °K, could be assumed to be $Mo_3O_9(g)$. Actually, it was based on this assumption, that most of the investigators interpreted their results on the sublimation of $MoO_3(s)$. However, it was also found that some authors disagreed with this assumption and argued that, if the mass-spectrometric results were extrapolated to higher temperatures, the contribution of $Mo_4O_{12}(g)$ became more significant. Thus a more rigorous interpretation at temperatures above 850 °K would have to include both species. In order to do this, however, the exact gas distribution of Mo_3O_9 and Mo_4O_{12} would have to be known. Since these investigators did not know these distributions, they assumed that the relative proportions given by Berkowitz et al.[33] were correct, and, accordingly, calculated an average molecular weight for the gaseous species. In this way, the sublimation of $MoO_3(s)$ was proposed as:

$$\bar{n}MoO_3(s) = (MoO_3)_{\bar{n}}(g) \tag{3.32}$$

The average stoichiometric coefficient ($\bar{n}$) was calculated as follows.

Let A be equal to the relative proportion of $P(Mo_3O_9)$ to $P(Mo_4O_{12})$, derived from the mass-spectrometric studies, based on the following reactions:

$$3MoO_3(s) = (MoO_3)_3(g) \tag{3.33}$$

$$4MoO_3(s) = (MoO_3)_4(g) \tag{3.34}$$

thus,

$$A = \frac{e^{\frac{-\Delta G^\circ(3.33)}{RT}}}{e^{\frac{-\Delta G^\circ(3.34)}{RT}}} = \frac{P(MoO_3)_3}{P(MoO_3)_4} \qquad (3.35)$$

The total apparent vapor pressure above MoO_3(s) is:

$$P_{(MoO_3)_3} + P_{(MoO_3)_4} = P_{Apparent} \qquad (3.36)$$

Simultaneously solving equations (3.35) and (3.36):

$$P_{(MoO_3)_4} = \frac{P_{Apparent}}{A + 1} \qquad (3.37)$$

$$P_{(MoO_3)_3} = \frac{A}{A + 1} P_{Apparent} \qquad (3.38)$$

The average molecular weight (mw) was calculated as:

$$\overline{mw} = \frac{P_{(MoO_3)_4}}{P_{Apparent}} mw_{(MoO_3)_4} + \frac{P_{(MoO_3)_3}}{P_{Apparent}} mw_{(MoO_3)_3} \qquad (3.39)$$

Substituting eq. (3.37) and (3.38) into (3.39) and simplifying:

$$\overline{mw} = \frac{1}{A + 1} [mw_{(MoO_3)_4} + A\ mw_{(MoO_3)_3}] \qquad (3.40)$$

Dividing eq. (3.40) by the molecular weight of MoO_3:

$$\bar{n} = \frac{1}{143.94(A + 1)} [mw_{(MoO_3)_4} + A\ mw_{(MoO_3)_5}] \tag{3.41}$$

The pressure of $(MoO_3)_{\bar{n}}$, according to reaction (3.32) is:

$$P_{(MoO_3)\bar{n}} = \frac{n'_{(MoO_3)_{\bar{n}}}}{n'_T} P_T = K \tag{3.42}$$

where,

$n'_{(MoO3)\bar{n}}$: moles of $(MoO_3)_{\bar{n}}$ in the equilibrated gas

n'_T : total number of moles in the equilibrated gas mixture

P_T : total pressure in atmospheres

A mole balance for atomic molybdenum yields:

$$n'_{(MoO_3)_{\bar{n}}} = \frac{n^{o}_{MoO_3(s)}}{\bar{n}} = \frac{1}{\bar{n}} \left(\frac{wt.loss}{mw_{MoO_3}}\right) \tag{3.43}$$

where,

n^{o}_{MoO3} : moles of $MoO_3(s)$ transported as determined by the weight loss

mw_{MoO3} : molecular weight of $MoO_3(s)$

The total number of moles in the equilibrated gas mixture is given by:

$$n'_T = n'_{(MoO_3)_{\bar{n}}} + n'_{Ar} + n'_{O_2} \tag{3.44}$$

where,

n'_{Ar} : moles of Ar in the equilibrated gas mixture

n'_{O2} : moles of O_2 in the equilibrated gas mixture

Since, according to reaction (3.32), Ar and O_2 do not participate in the reaction, n'_{Ar} and n'_{O2} are equal to n^o_{Ar} and n^o_{O2}, respectively. n^o_{Ar} and n^o_{O2} are the initial number of moles for these species.

Thus, equation (3.44) can be written as:

$$n'_T = n'_{(MoO_3)_{\bar{n}}} + n^o_{Ar} + n^o_{O_2} \tag{3.45}$$

Substituting eq. (3.45) and (3.43) into (3.42), the vapor pressure of $(MoO_3)_{\bar{n}}$ and the equilibrium constant for reaction (3.32) was calculated at each experimental temperature.

Subsequently, the standard Gibbs free energy change for the reaction is:

$$\Delta G^o = - RT \ln K$$

It is important to note that if $Mo_3O_9(g)$ were assumed to be the sole predominant species, then $\bar{n}$ would be directly substituted by a "3" in the above calculation.

<u>3.4.3.2 Data Analysis in the Presence of Water Vapor.</u> It was found in the literature review, that $MoO_2(OH)_2(g)$ was the predominant hydroxide species in equilibrium with $MoO_3(s)$ according to:

$$MoO_3(s) + H_2O(g) = MoO_2(OH)_2(g) \tag{3.46}$$

$$\text{Log } P_{MoO_2(OH)_2} = \text{Log } P_{H_2O} + \text{Log } K \tag{3.47}$$

It can be appreciated that if the above reactions apply, then the slope of a plot of Log $P_{MoO2(OH)2}$ versus Log P_{H2O} should be 1.

Assuming the molecularity proposed in reaction (3.32), and taking into consideration the contribution of the volatile oxides, the vapor pressure of the hydroxide was calculated as follows; using argon-oxygen-water mixtures as carrier gas:

$$\bar{n}MoO_3(s) = (MoO_3)_{\bar{n}}(g) \tag{3.48}$$

$$MoO_3(s) + H_2O = MoO_2(OH)_2(g) \tag{3.49}$$

$$P_{MoO_2(OH)_2} = \frac{n'_{MoO_2(OH)_2}}{n'_T} P_T \tag{3.50}$$

where,

$n'_{MoO2(OH)2}$: moles of $MoO_2(OH)_2$ in the equilibrated gas mixture

n'_T : total number of moles in the equilibrated gas mixture

A mole balance on atomic Molybdenum yields:

$$n'_{MoO_2(OH)_2} = n^o_{MoO_3} - \bar{n}\, n'_{(MoO_3)_{\bar{n}}} \tag{3.51}$$

$$n'_{MoO_2(OH)_2} = n^o_{MoO_3} - \bar{n}\, n'_{(MoO_3)_{\bar{n}}} \tag{3.52}$$

where,

$\bar{n}$: is calculated as shown in section (3.4.3.1)

A mole balance on molecular H_2 yields:

$$n'_{H_2O} = n^o_{H_2O} - n'_{MoO_2(OH)_2} \tag{3.53}$$

The total number of moles in the equilibrated gas mixture is

$$n'_T = n'_{(MoO_3)_n} + n'_{MoO_2(OH)_2} + n'_{H_2O} + n'_{Ar} + n'_{O_2} \tag{3.54}$$

where,

n'_i : denotes the number of moles of each species in the equilibrated gas mixture.

The number of moles of the oxide was calculated by:

$$n'_{(MoO_3)_n} = \frac{K_{oxide}\, n'_T}{P_T} \tag{3.55}$$

where K_{oxide} is the equilibrium constant for the sublimation of $MoO_3(s)$. This equilibrium constant was calculated as described in section (3.4.3.1)

Since Ar and O_2 do not participate in the reaction, n'Ar and $n'O_2$ are equal to the number of initial moles of Ar and O_2. Thus, substituting equation (3.53) in (3.54),

$$n'_T = n'_{(MoO_3)_n} + n^o_{H_2O} + n^o_{Ar} + n^o_{O_2} \tag{3.56}$$

The vapor pressure of the hydroxide was calculated by substituting equation (3.56) and (3.52) into equation (3.50).

Also, the partial pressure of water was calculated by:

$$P_{H_2O} = \frac{n'_{H_2O}}{n'_T} P_T \tag{3.57}$$

Combining equation (3.50) and (3.57), the equilibrium constant for reaction (3.49) at the experimental temperature was calculated as:

$$K = \frac{P_{MoO(OH)_2}}{P_{H_2O}} \tag{3.58}$$

Subsequently, the standard Gibbs free energy change for the reaction (3.49) was calculated as:

$$\Delta G^\circ = - RT \ln K \tag{3.59}$$

Furthermore, ΔG° of the reaction was correlated with temperature by applying the Second Law (Sigma-Plot method) as described in section (3.4.1).

It is important to note that if Mo_3O_9(g) were considered as the sole predominant gaseous oxide above MoO_3(s), then $\bar{n}$ would be directly substituted by a "3" in the above calculations.

3.4.4 Tungsten Trioxide.

As noted in the literature review, the contribution of volatile oxides of tungsten to the total vapor pressure of $WO_3(s)$, in the temperature range of interest (1000 to 1300 °K), was below the detection limits of the experimental technique. Thus, the vapor pressure of the volatile hydroxides were determine directly from the total measured vapor pressures.

The proposed reaction for the formation of volatile hydroxides above $WO_3(s)$ was:

$$WO_3(s) + H_2O(g) = WO_2(OH)_2(g) \tag{3.60}$$

$$\text{Log } P_{(WO_2(OH)_2)} = \text{Log } P_{(H_2O)} + \text{Log } K \tag{3.61}$$

The above linearization of the equilibrium constant was useful in corroborating the stoichiometry of the proposed hydroxide. When the logarithm of the apparent vapor pressure is plotted as a function of the logarithm of the water vapor, a straight line, with a slope of 1 should be obtained. A slope significantly different than 1 would indicate that different or additional species are responsible for the measured vapor pressure.

Assuming that reaction (3.60) describes the formation of volatile hydroxides above $WO_3(s)$, one can determine the vapor pressure of the gaseous species as follows:

$$P_{WO_2(OH)_2} = \frac{n'_{WO_2(OH)_2}}{n'_T} P_T \tag{3.62}$$

where,

$n'_{WO2(OH)2}$: moles of $WO_2(OH)_2$ in the equilibrated gas mixture

n'_T : total number of moles in the equilibrated gas mixture

P_T : total pressure in atmospheres

A mole balance for atomic tungsten yields:

$$n'_{WO_2(OH)_2} = n^{o}_{WO_3} = \frac{wt.loss}{mw_{WO_3}} \tag{3.63}$$

where,

n^{o}_{WO3} : moles of $WO_3(s)$ transported as determine by the weight loss

mw_{WO3} : molecular weight of $WO_3(s)$

A mole balance on molecular H_2 yields:

$$n'_{H_2O} = n^{o}_{H_2O} - n'_{WO_2(OH)_2} \tag{3.64}$$

where,

n'_{H2O} : moles of water in the equilibrated gas mixture

n^{o}_{H2O} : initial moles of water

Finally, assuming that the carrier gas mixture is composed of argon, oxygen and water, the total number of moles in the equilibrated gas mixture was calculated as:

$$n'_T = n'_{H_2O} + n'_{WO_2(OH)_2} + n'_{Ar} + n'_{O_2} \tag{3.65}$$

where,

n'_{Ar} : moles of Ar in the equilibrated gas mixture

n'_{O2} : moles of O_2 in the equilibrated gas mixture

Since Ar and O_2 do not participate in the reaction n'_{Ar} and n'_{O2} are equal to the initial moles of Ar and O_2, respectively.

Thus, substituting equations (3.64) in (3.65), and simplifying:

$$n'_T = n^{o}_{H_2O} + n^{o}_{Ar} + n^{o}_{O_2} \tag{3.66}$$

Substituting equation (3.66) and (3.63) in equation (3.62), the vapor pressure of $WO_2(OH)_2$ was calculated.

In a similar fashion, the partial pressure of water can be calculated by:

$$P_{(H_2O)} = \frac{n'_{H_2O}}{n'_T} P_T \tag{3.67}$$

Combining equations (3.67) and (3.62), the equilibrium constant for reaction (3.60) was calculated as:

$$K = \frac{P_{WO_2(OH)_2}}{P_{H_2O}} \tag{3.68}$$

Subsequently, the standard Gibbs free energy for the reaction was calculated as:

$$\Delta G^\circ = -RT \ln K \tag{3.69}$$

Furthermore, ΔG° was correlated with temperature by applying the Second Law method as described in section (3.4.1).

3.5 Pertinent Statistical Analysis

In section 3.4, a systematic method was described to delineate the molecularity of the hydroxide species based on the linearization of the equilibrium constants of the proposed reactions. It was mentioned that, by plotting the logarithm of the apparent vapor pressure as a function of the logarithm of the water or the oxygen pressures, a straight line is obtained and its slope used to determine the molecularity of the gaseous hydroxide formed. However, due to the small differences among the values of the slopes of the three equations proposed for V_2O_5(s) (see Table 3.1.1 on page 68), a statistical analysis was desirable to determine the 95% confidence interval for the slopes obtained. Moreover, it was important to statistically compare the experimentally obtained slopes with the theoretical slopes of the different equations to determine whether or not they were statistically different .

The confidence interval for a slope obtained using linear regression of the type:

$$y = a + bx$$

is given by:

$$\text{Confidence Interval} = b \pm t_{\alpha/2}\, s(b)$$

where,

b : slope obtained through linear regression

$s(b)$: standard error of the slope

$t_{\alpha/2}$: t - test statistical parameters evaluated at the significance level α, divided by 2 (obtained from statistical tables)

$$s(b) = \frac{\sqrt{\dfrac{(y_i - \hat{y}_i)^2}{n - 2}}}{\sqrt{\Sigma x_i^2 - \dfrac{(\Sigma x_i)^2}{n}}} \tag{3.70}$$

where,

y_i : actual measured value of the dependent variable

$\hat{y}$: predicted value of the dependent variable

x_i : value of the independent variable

n : number of observations

In order to determine if one slope is statistically different from another, the calculated "t" parameter has to be compared with the tabulated t at the significance level of interest. If the calculated t value at the required significance level is greater than the tabulated "t" value, at the required α, then the alternative hypothesis that the slopes are statistically different, is accepted. The t - test parameters for a null hypothesis that the two slopes are equal is calculated as:

$$t = \frac{B - b}{s(b)} \tag{3.71}$$

where B is the slope against which the obtained slope is to be compared.

In order to calculate the confidence range of the regression for any estimated value of the dependent variable the following expression was used:

$$\text{Confidence range} = \hat{Y}_i \pm t_{\alpha/2}\, S(\hat{Y}_i)$$

where,

$$S(\hat{Y}_i) = [S^2(\hat{y})\ (1 + \frac{1}{n} + \frac{(\bar{x} - x_i)^2}{\Sigma' x_2})]^{1/2}$$

$$S^2(\hat{y}) = \Sigma\ \frac{(y_i - \hat{y}_i)}{n-2}$$

$$\Sigma' x^2 = \Sigma x^2 - \frac{(\Sigma x)^2}{n}$$

It is clear that the confidence range for any estimated value of the regression depends on the value of the independent variable. Thus, it should be expressed as a function of the independent variable, rather than as single interval. In the present investigation however, the confidence ranges for the regressions of ΔG° as a function of temperature, were expressed as the maximum variation of ΔG° in the temperature ranges studied. The purpose of expressing the confidence ranges in this manner was to facilitate the comparison with similar correlations reported by other investigators, who only reported a single value for the variation of the estimated free energies.

3.6 Sources of Error

Several variables were measured during the course of the transpiration runs. In the following paragraphs, the errors involved in measuring these variables is discussed. Moreover, the effects of these errors are estimated for the Gibbs free energies of the following reactions:

$$V_2O_5(s) + 3H_2O(g) = VO(OH)_3(g) \tag{3.75}$$

$$3MoO_3(s) = Mo_3O_9(g) \tag{3.76}$$

$$MoO_3(s) + H_2O(g) = MoO_2(OH)_2(g) \tag{3.77}$$

$$WO_3(s) + H_2O(g) = WO_2(OH)_2(g) \tag{3.78}$$

3.6.1 Reactor Temperature

The temperature of the reaction zone was measured with a calibrated type "K" thermocouple. The calibration was conducted against the melting point of Al (660.1 °C)[56] and Ag (960.8 °C)[56] under an atmosphere of deoxidized argon. In both cases the temperature was increased 40 °C above the melting point. The temperature was then slowly decreased and plots of measured temperature versus time were constructed. The temperature decreased steadily until the melting point was reached. At the melting point the measured temperature remained constant for 10 to 12 minutes before it decreased again. This temperature plateau was taken to be the melting point as determined from the thermocouple being calibrated. The agreement between the measured melting point and the established melting point of the metals was within $\pm$ 1 °K.

The reactor's electronic controller was able to maintain the temperature of the reaction zone to within $\pm$ 1 °K of the set temperature during each run.

The temperature profile along the length of the reacting zone (13 cm) had a $\pm$ 1 °K variation.

The results of the above observations indicated that the temperature measurements were accurate to within $\pm$ 3 °K. A variation of this magnitude resulted in the following uncertainties in the Gibbs free energies:

Reaction (3.75)	$\pm$ 164 cal/mol
Reaction (3.76)	$\pm$ 67 cal/mol
Reaction (3.77)	$\pm$ 49 cal/mol
Reaction (3.78)	$\pm$ 47 cal/mol

3.6.2 Weight Loss Determination

The balance used in this investigation was a Mettler H-20 with a five decimal place analog read out. It was placed on top of a marble table in an isolated area to minimize disturbances due to air currents and drastic temperatures changes. It was calibrated yearly by a professional technician from the Mettler Co. By weighing a variety of standards weights several times, the precision of the balance was determined as ± .05 mg for the weight ranges used in this investigation. A weighing error of this magnitude resulted in the following uncertainties in the Gibbs free energies:

Reaction (3.75)	± 450 cal/mol
Reaction (3.76)	± 14 cal/mol
Reaction (3.77)	± 0 cal/mol
Reaction (3.78)	± 2 cal/mol

3.6.3 Carrier Gas Flowrates

The capillary flowmeters were calibrated using the rising bubble method. Plots of flowrate as a function of liquid displacement in the flowmeter were constructed for all the gases (O_2, H_2, Ar, CO and CO_2).

Straight lines were obtained in all cases. Linear regression analysis, constraining the "y" intercept through zero, were performed for all the calibration lines. The standard errors for both, the "y" estimate and the "x" coefficient of each regression are presented in Table 3.2.

The flowmeter displacement was read to 0.1 cm. The displacement varied during the run by ± 2 mm. Based on these variations, the estimated error for a given gas mixture was determined by estimating the error for each gas and adding the contributions of the different gases (see Table 3.3). The error for each gas was calculated by multiplying 2 mm times the slope for the corresponding calibration lines, and adding this product to the standard error of the estimate. Sample calculations showed that the uncertainty in measuring the flowrates results in the following error in the Gibbs free

Table 3.2 Standard Error for the Slope and "y" Estimate of the Flowrate Calibration Curves

Gases	Standard error "y" estimate	Standard error of the slope	Range (mil/min)	Slope
H_2O	0.63 (ml/min)	0.013	8 - 85	2.49
O_2	0.42 (ml/min)	0.004	13 - 65	1.09
Ar (1)	0.16 (ml/min)	0.001	10 - 50	0.67
Ar (2)	0.64	0.009	50 - 80	0.68
CO	0.32 (ml/min)	0.004	3 - 94	1.47
CO_2	0.57 (ml/min)	0.005	5 - 75	1.24

energies:

Reaction (3.75)	± 5 cal/mol
Reaction (3.76)	± 9 cal/mol
Reaction (3.77)	± 1 cal/mol
Reaction (3.78)	± 0 cal/mol

Table 3.3 Estimated Errors in the Measurement of the Carrier Gas Flowrate, Depending on the Specified Gas Mixture

Gas Mixture	Error (ml / mm)
H_2 - CO - CO_2	2.56
O_2 - Ar (1)	0.92
O_2 - Ar (2)	1.41
CO - CO_2	1.43

3.6.4 Water Injection

The total amount of water that was injected in the system was directly read from the burette. The burette was read to an accuracy of ± 0.5 ml. An error of this magnitude resulted in the following uncertainties of the Gibbs free energies:

Reaction (3.75)	± 23 cal/mol
Reaction (3.76)	no water injected
Reaction (3.77)	± 68 cal/mol
Reaction (3.78)	± 64 cal/mol

3.6.5 Run Duration

For the baseline experiments, the runs started the moment the boats were inserted, and ended, the moment they were completely withdrawn. It was rationalized that if the boats were inserted and withdrawn at the same rate, the time that the boats were not at the reaction temperature during insertion, was compensated by the time it took for them to cool down while withdrawing.

In the case where water was added, except for the experiments on molybdenum, the runs started (with the boats placed in the reacting zone) the moment the water was turned on. The runs ended the moment the water was turned off (with the boats still in the reacting zone). In the experiments with molybdenum trioxide in the presence of water vapor, the same procedure was used as in the baseline experiments. In this case, however, the run started when the water was turned on (immediately before inserting the boats), and ended when the water was turned off (immediately after the boats were withdrawn).

The time it took to either insert the boats or to withdraw them was approximately 8 minutes. If 8 minutes were taken as the uncertainty in the time of the run, the resulting uncertainties of the Gibbs free energies are:

Reaction (3.75)	$\pm$ 18 cal/mol
Reaction (3.76)	$\pm$ 14 cal/mol
Reaction (3.77)	$\pm$ 43 cal/mol
Reaction (3.78)	$\pm$ 2 cal/mol

3.6.6 Ambient Pressure

In order to convert the volumetric flowrate to molar flowrate, the pressure at which the gases were measured was needed. The pressure was measured with a mercury barometer. The expected error in reading the barometer was $\pm$ 0.5 mm of Hg. Errors of this magnitude did not affect the Gibbs free energies of the reactions more than $\pm$ 1 cal/mol.

3.6.7 Ambient Temperature

A standard mercury thermometer was used to measured the ambient temperature, which could be read to $\pm$ 0.5 °K. Errors of this magnitude did not affect the Gibbs free energies of the reactions more than $\pm$ 1 cal/mol.

3.6.8 Summary of the Error Analysis

The errors calculated in the previous paragraphs represent estimated errors in "worst case" scenarios in the experimental conditions. Consequently, they reflect the maximum errors that would be incurred due to the uncertainty in the measurements by the instruments utilized.

In general, with the exception of the experiments with V_2O_5(s), it is apparent that the determination of the Gibbs free energies for the established reactions is dependent on two variables: temperature and water flowrate. In addition, for the case of V_2O_5(s), it is also sensitive to the variability of the weighing instrument. This is mainly due to the small weight losses associated with the low vapor pressure of $VO(OH)_3$. Because of this sensitivity of the Gibbs free energy of reaction (3.75) on page 89) to errors in the weight loss measurements, the duration of the runs for these experiments was from 12 to 48 hrs, depending on the temperature under investigation. Also, higher flowrates were utilized (160 cc/min as opposed to 90 cc/min) to increase the weight loss during an experiment. In this way, the effects of the variability of the balance on the measured Gibbs free energy was minimized.

An estimate of the maximum total error, attributed to the measuring instruments, for the measured Gibbs free energies for the established reactions was obtained by adding the estimated error for the individual terms discussed in the previous paragraphs:

Reaction (3.75)	$\pm$ 662 cal/mol
Reaction (3.76)	$\pm$ 106 cal/mol
Reaction (3.77)	$\pm$ 163 cal/mol
Reaction (3.78)	$\pm$ 117 cal/mol

It was evident from this analysis that the magnitude of the error is similar for the last three reactions. For the first reaction, however, the error is approximately six times greater. This is due, as explained earlier, to the higher sensitivity of the Gibbs free energy for this reaction to the weight loss measurement, particularly at low temperatures, where the vapor pressure of $VO(OH)_3$ is very small.

IV. RESULTS AND DISCUSSION

The results obtained in the present investigation for $V_2O_5(s)$, $V_2O_3(s)$, $MoO_3(s)$, and $WO_3(s)$ are described in this section. For each of the compounds the baseline results from the experiments without water are presented first; followed by the results for the enhancement of the volatility in the presence of water. Finally, process conditions for extraction of these metals from feedstocks and wastes are discussed.

In most of these experiments, the samples used were reutilized from previous experiments. However, when fresh samples were used, these were conditioned in the absence of water vapor before the actual experiments were conducted. The purpose of this conditioning was to eliminate any volatile impurities in the sample. For the condensed phases above which no significant vaporization was expected ($V_2O_5(s)$, $V_2O_3(s)$, and $WO_3(s)$), samples were conditioned several times until no weight change was observed. In the case of $MoO_3(s)$, where significant volatilization was expected, consecutive runs under the same conditions were conducted, until no significant difference in the measured vapor pressure was observed.

4.1 Vanadium Pentoxide

4.1.1 Baseline Vapor Pressures for $V_2O_5(s)$

No volatilization was detected in the experiments conducted in the absence of water vapor. A summary of the experimental conditions, after conditioning the sample, is presented in Table 4.1.

Table 4.1 Experimental Conditions for the Baseline Experiment Above $V_2O_5(s)$

Condensed Phase	Amb. P (atm)	Amb T °C	T °C	P_{O2} (atm)	P_{Ar} (atm)	Run Time (hrs)	Wt.Loss (gr)
$V_2O_5(s)$	0.82	21	646	0.17	0.85	24	0.00000

As appreciated from the results of this experiment, the fact that no weight loss was realized after 24 hrs of equilibration, corroborates the data reported in the literature that the contribution of volatile oxides to the total vapor pressure was practically null. As mentioned earlier, this was an important consideration because it allowed the direct determination of the vapor pressure of the volatile hydroxides from the total measured vapor pressures.

4.1.2 Measurements on $V_2O_5(s)$ in the Presence of Vapor

In order to determine the molecularity of the gaseous hydroxide species formed above $V_2O_5(s)$, a systematic series of experiments were conducted based on the proposed species found in the literature.

Reactions (4.1) to (4.6) suggest that the vapor pressure of two of the possible volatile hydroxide species reported, depended only on water vapor, while the third, depended on both the water and oxygen potentials.

$$V_2O_5(s) + 3H_2O(g) = 2VO(OH)_3(g) \tag{4.1}$$

$$\text{Log}\,P_{VO(OH)3} = \frac{3}{2}\text{Log}\ P_{H_2O} + \frac{1}{2}\text{Log}\ K \tag{4.2}$$

$$V_2O_5(s) + 2H_2O(g) = V_2O_3(OH)_4(g) \tag{4.3}$$

$$\text{Log}\,P_{V_2O_3(OH)_4} = 2\,\text{Log}\ P_{H_2O} + \text{Log}\ K \tag{4.4}$$

$$V_2O_5(s) + 2H_2O(g) + \frac{1}{2}O_2(g) = 2VO_2(OH)_2(g) \tag{4.5}$$

$$\text{Log}\,P_{VO_2(OH)_2} = \text{Log}\ P_{H_2O} + \frac{1}{4}\text{Log}\ P_{O_2} + \frac{1}{2}\text{Log}\,K \tag{4.6}$$

The first series of experiments were focused on determining the dependance of the apparent vapor pressure on the oxygen potential according to reaction 4.5). Thus, the water potential was fixed and the oxygen potential was varied. The vapor pressure was calculated considering the $VO_2(OH)_2(g)$ as the main volatile species. The results of these experiments are presented in Figure 4.1. Since no oxygen dependance was observed, the species $VO_2(OH)_2(g)$ was eliminated as the principal volatile hydroxide above $V_2O_5(s)$.

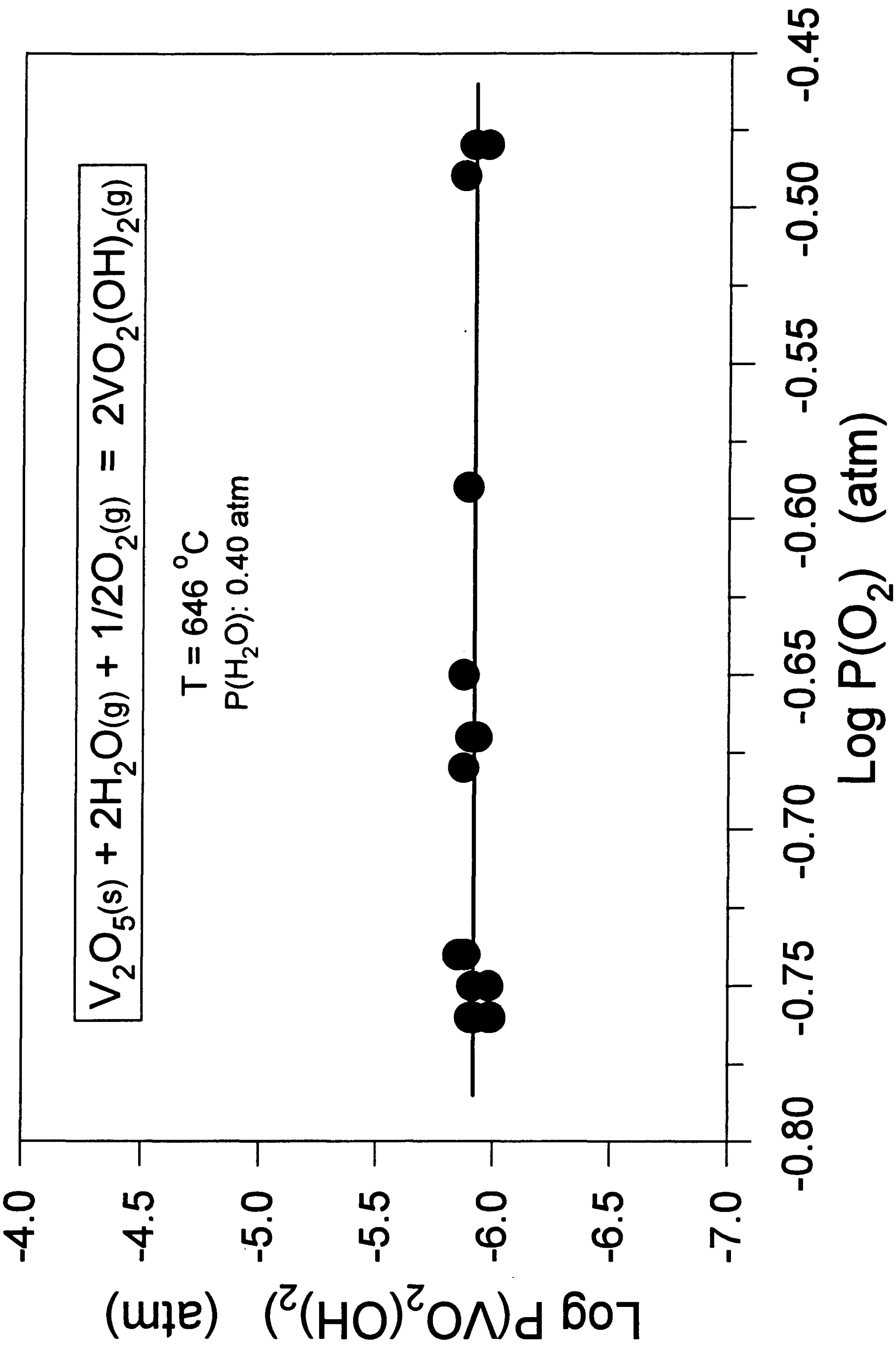

Figure 4.1 Vapor pressure of $VO_2(OH)_2(g)$ as a function of oxygen potential.

The two remaining reactions, (4.1) and (4.3), generated species for which the vapor pressures were solely dependent on the water potential at constant temperature. Experiments were therefore carried out at constant temperature, but varying the water vapor pressure.

The species $V_2O_3(OH)_4(g)$, from reaction (4.3), was the next hydroxide selected for the study. The results of this analysis are presented in Figure 4.2. Given that the obtained experimental slope of 1.48 differed from the expected theoretical slope of 2, the hypothesis that $V_2O_3(OH)_4$ was the main gaseous hydroxide above $V_2O_5(s)$ was also eliminated.

Finally, the species $VO(OH)_3(g)$ was considered, and the partial pressures recalculated on that basis. As shown in Figure 4.3, the experimental slope of 1.49 is in good agreement with the theoretical slope of 1.5, thus suggesting that $VO(OH)_3$ is the principal volatile hydroxide above $V_2O_5(s)$. It is worth noting that varying the oxygen potential had no effect on the results and confirmed the oxygen independence of the vapor pressure of $VO(OH)_3$.

Once the molecularity of the volatile hydroxide formed above solid vanadium pentoxide at 646 °C was established, it was necessary to determined if it prevailed over the temperature range of interest in the experimental plan. Thus, experiments were conducted at two additional temperatures.

As shown in Figure 4.4, the fact that the slopes at all three temperatures were very close to the theoretical slope of 1.5, indicated that the stoichiometry $VO(OH)_3$ is maintained throughout the working temperature range.

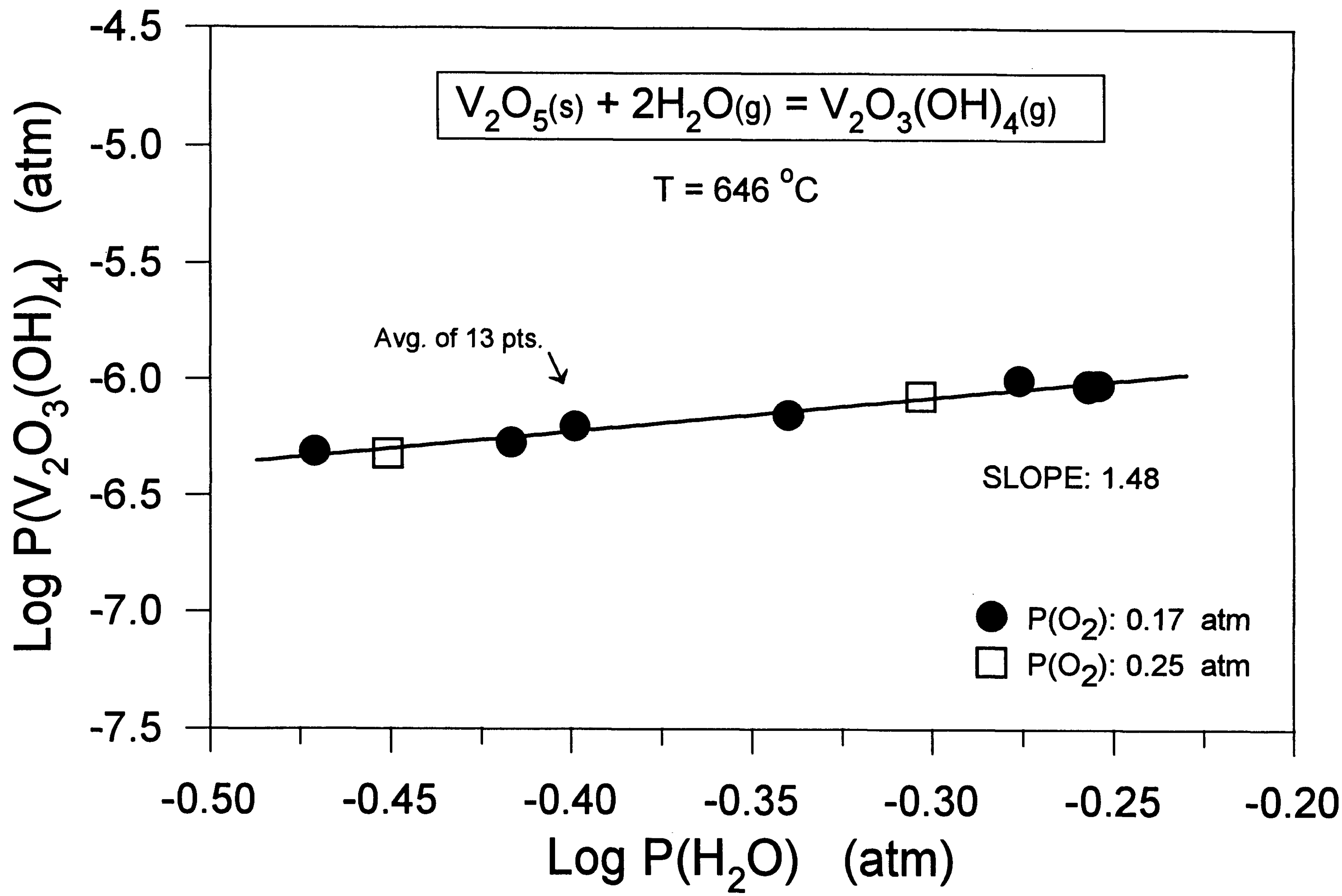

Figure 4.2 Vapor pressure of $V_2O_3(OH)_4(g)$ as a function of water potential.

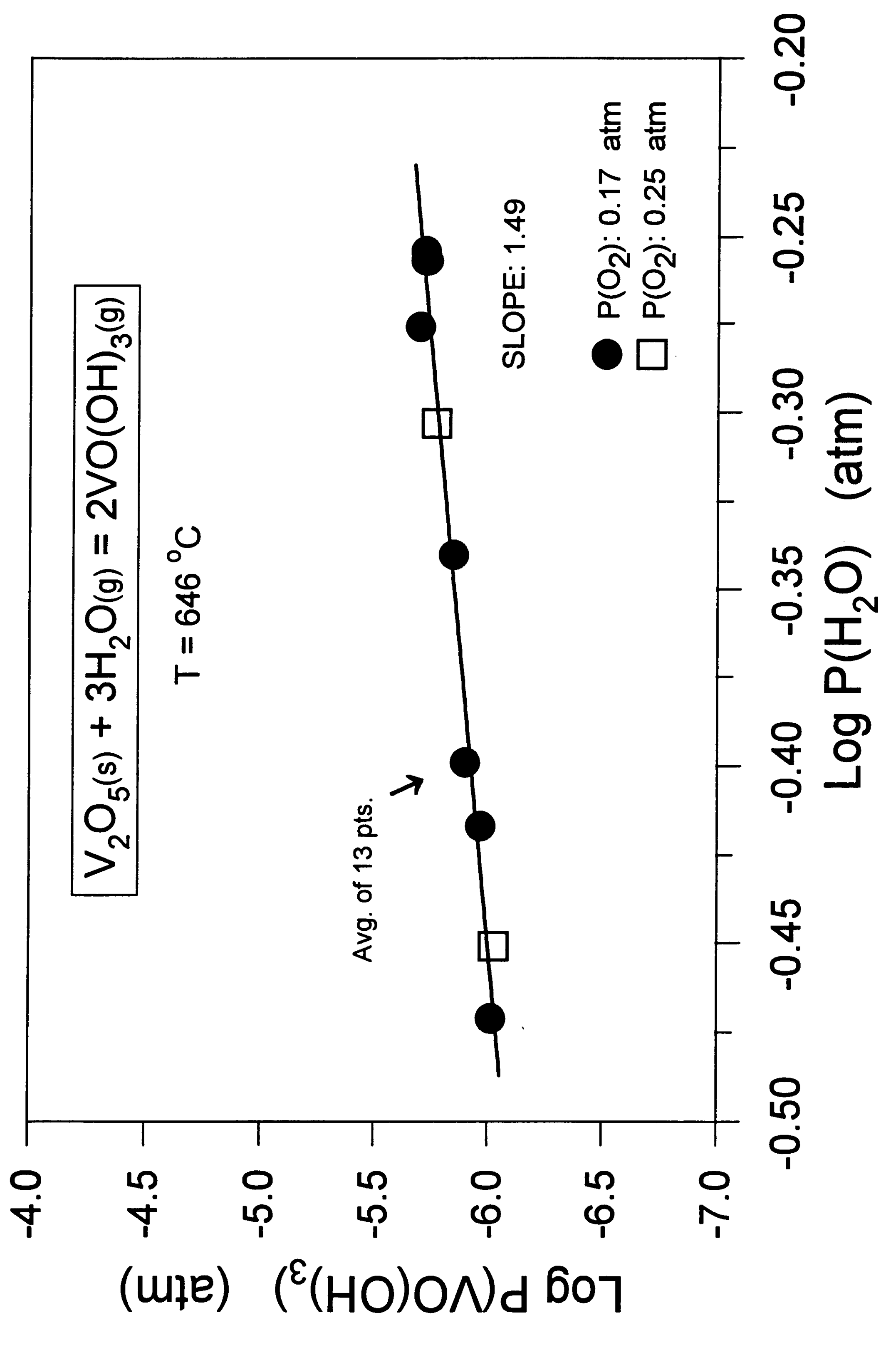

Figure 4.3 Vapor pressure of $VO(OH)_3(g)$ as a function of water potential.

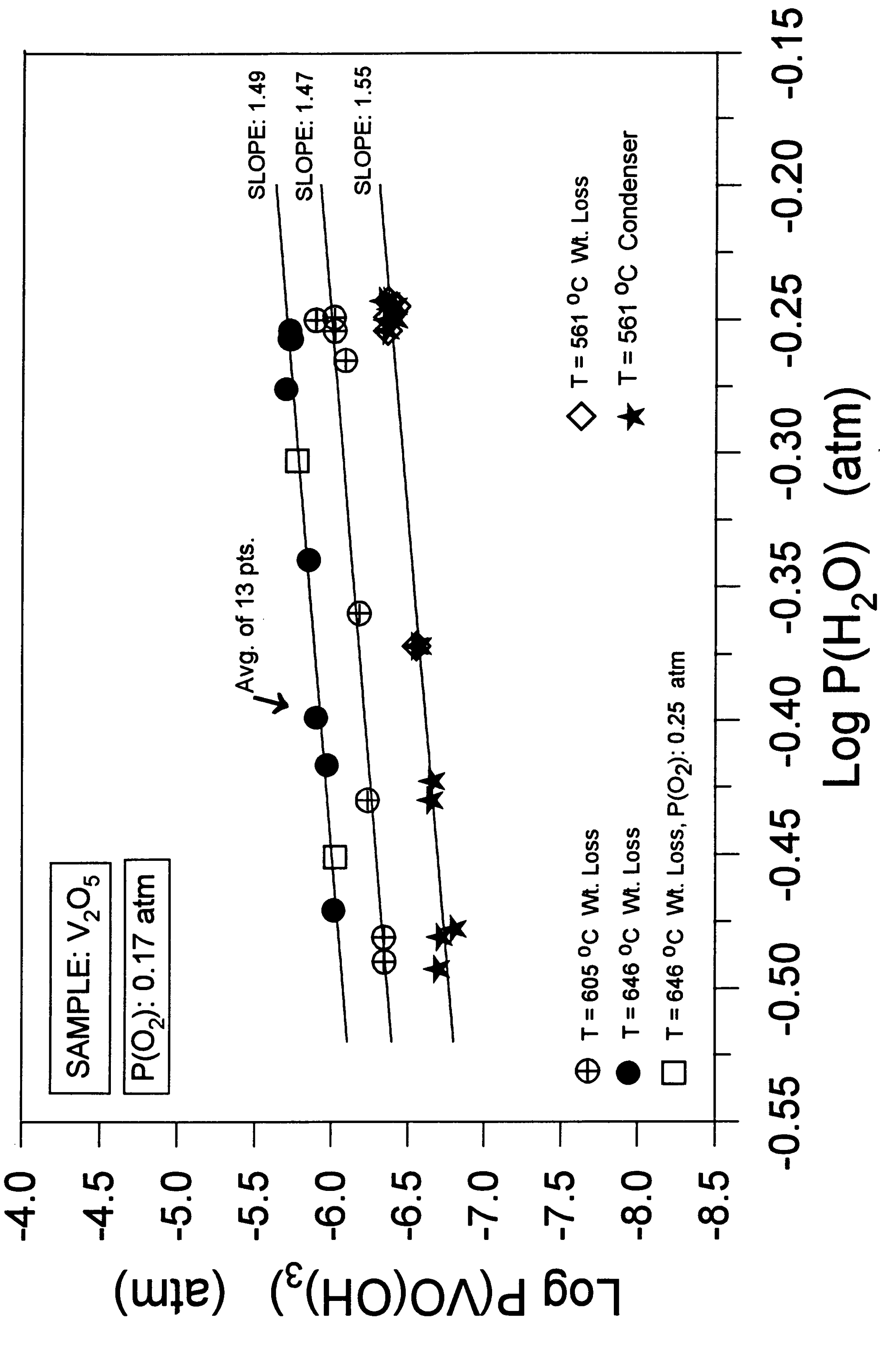

Figure 4.4 Vapor pressure of $VO(OH)_3(g)$ as a function of water potential and temperature.

It is important to note the good agreement between the vapor pressures calculated on the basis of the moles transported by the weight loss measurements and the moles obtained from the condenser analysis. This verification of mass closure not only validated the results of these experiments, but was essential in the interpretation of the results obtained at the lowest working temperature. At this temperature, the weight loss measurements at the lower water vapor pressures became unreliable due to their proximity to the sensitivity limits of the gravimetric method. The condensed material, on the other hand, was chemically analyzed by inductively coupled plasma atomic emission spectrometry (ICP-AES) with a detection limit of 0.01 mg/l, thus providing for the reliable measurement of the vapor pressures at very low levels.

In order to unbiasedly check if the experimental slopes were indeed equal to 1.5 and significantly different from 1 or 2, statistical comparisons were conducted. Table 4.2 and 4.3 summarize the results of this comparison at a significance level (α) of 0.05.

It was clear from Table 4.3, that the experimental slopes obtained were indeed statistically equal to 1.5 and significantly different from 1 and 2. Thus corroborating that $VO(OH)_3$ was the predominant volatile hydroxide in equilibrium with $V_2O_5(s)$.

As mentioned earlier, when conducting transpiration experiments, it is always necessary to demonstrate that equilibrium has been attained. In this study, the logarithm of the equilibrium constants were plotted as a function of both the total flowrate and the water vapor pressure. The choice of using the equilibrium constant, instead of the usual vapor pressure, was based on the fact that its calculation includes the possible experimental errors incurred when measuring the flowrates of each individual species in

Table 4.2 Calculated 95% Confidence Intervals for the Slopes Obtained in Figures 4.2, 4.3, and 4.4

Species	# of Observ.	Degrees of Freedom	Slope	Std. Error of Slope	$t_{\alpha/2}$	Confidence Interval
$V_2O_3(OH)_4$ at 646 °C	10	8	1.476	0.091	2.306	± 0.210
$VO(OH)_3$ at 646 °C	10	8	1.486	0.093	2.306	± 0.215
$VO(OH)_3$ at 605 °C	8	6	1.475	0.187	2.447	± 0.458
$VO(OH)_3$ at 561 °C	14	12	1.550	0.096	2.179	± 0.209

the carrier gas. Since the equilibrium constant is dependent only on temperature, the resulting graphs should reflect its independence from the flowrate and the water potential. Figures 4.5 and 4.6 demonstrate that equilibrium was attained throughout the series of transpiration experiments.

Figures 4.5 and 4.6 not only confirmed that equilibrium was established, but were also useful in obtaining an average value of the equilibrium constant at each temperature for the subsequent calculation of the Gibbs free energy change for the transport reaction.

As mentioned in the section on data analysis (section 3.4), the ΔG° can be correlated with temperature by applying the Second Law method of data analysis to the measured equilibrium constants at the different working temperatures. Unfortunately, since an expression for the C_p° for the volatile hydroxide formed was not available, a rigorous correlation using ΔC_p° for the transport reaction is not possible. However, by allowing ΔC_p° to be equal to zero (a reasonable assumption given that the temperature

Table 4.3 Statistical Comparison between the Slopes Obtained in Figures 4.2, 4.3, and 4.4

Species	Slope	t (α/2)	Null Hypothesis	t calc.	Accept/Reject Null Hypothesis
$V_2O_3(OH)_4$ at 646 °C	1.476	$\pm$ 2.306	slope = 1	-5.23	rejected
			slope = 1.5	0.22	accepted
			slope = 2	5.71	rejected
$VO(OH)_3$ at 646 °C	1.486	$\pm$ 2.306	slope = 1	-5.22	rejected
			slope = 1.5	0.11	accepted
			slope = 2	5.48	rejected
$VO(OH)_3$ at 605 °C	1.475	$\pm$ 2.447	slope = 1	-2.54	rejected
			slope = 1.5	0.16	accepted
			slope = 2	2.83	rejected
$VO(OH)_3$ at 561 °C	1.55	$\pm$ 2.179	slope = 1	-5.74	rejected
			slope = 1.5	0.52	accepted
			slope = 2	4.69	rejected

differences were less than 90 °C), the Second Law method, assuming ΔH° and ΔS° to be constant, was used for the correlation. Thus, the calculated values of ΔG° as a function of temperature have been plotted in Figure 4.7. The Gibbs free energy for the formation of volatile hydroxides above V_2O_5 (s) was:

$$V_2O_5(s) + 3H_2O(g) = 2VO(OH)_3(g) \tag{4.7}$$

$$\Delta G^\circ = 57{,}938 - 14.46\ T \quad (\pm\ 240\ \text{cal/mole})$$

$$\Delta G^\circ = 242{,}413 - 60.50\ T \quad (\pm\ 1004\ \text{J/mole})$$

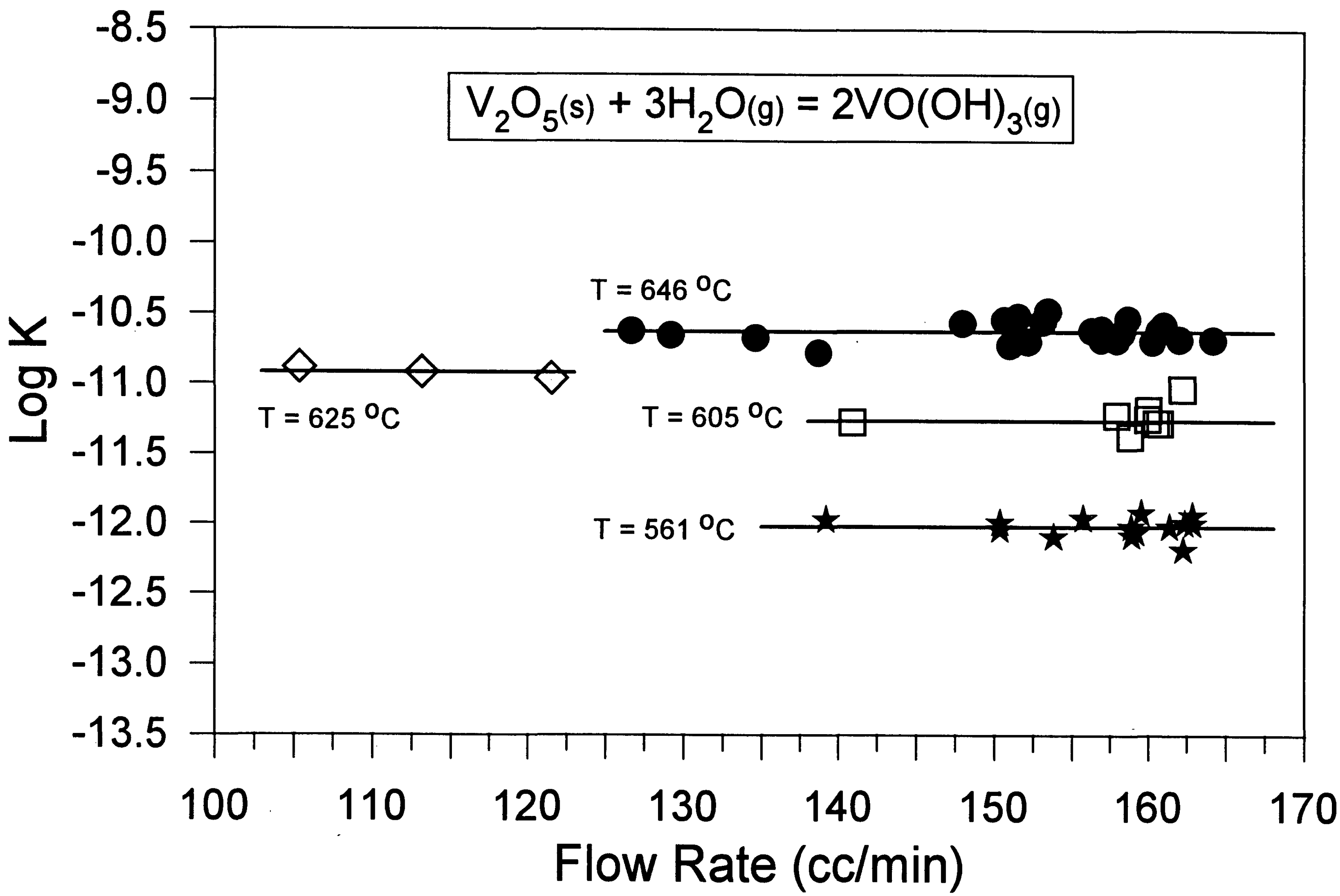

Figure 4.5 Equilibrium constant for the reaction $V_2O_5(s) + 3H_2O(g) = 2VO(OH)_3(g)$ for different temperatures as a function of flow rate.

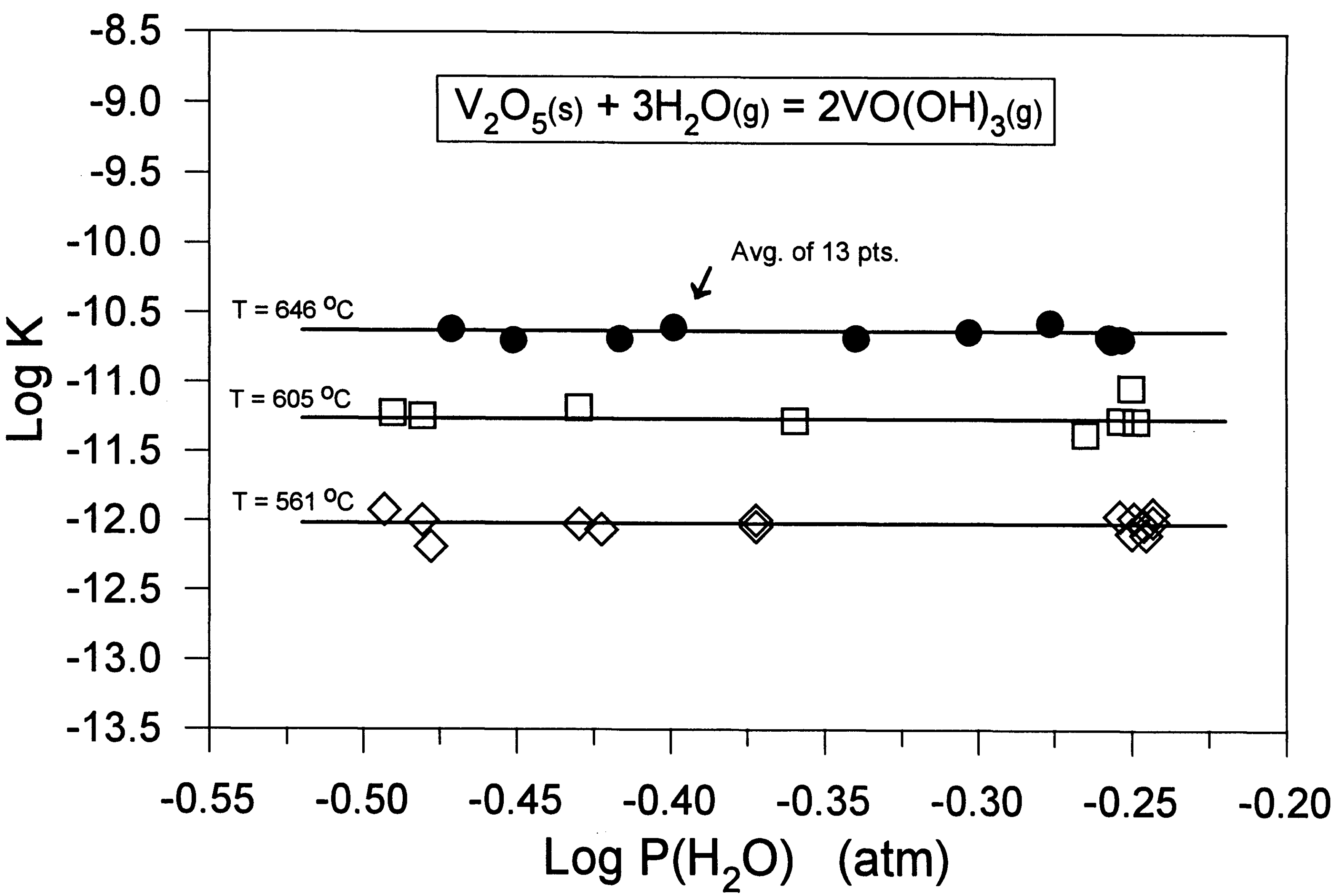

Figure 4.6 Equilibrium constant for the reaction $V_2O_5(s) + 3H_2O(g) = 2VO(OH)_3(g)$ for three different temperatures as a function of water potential.

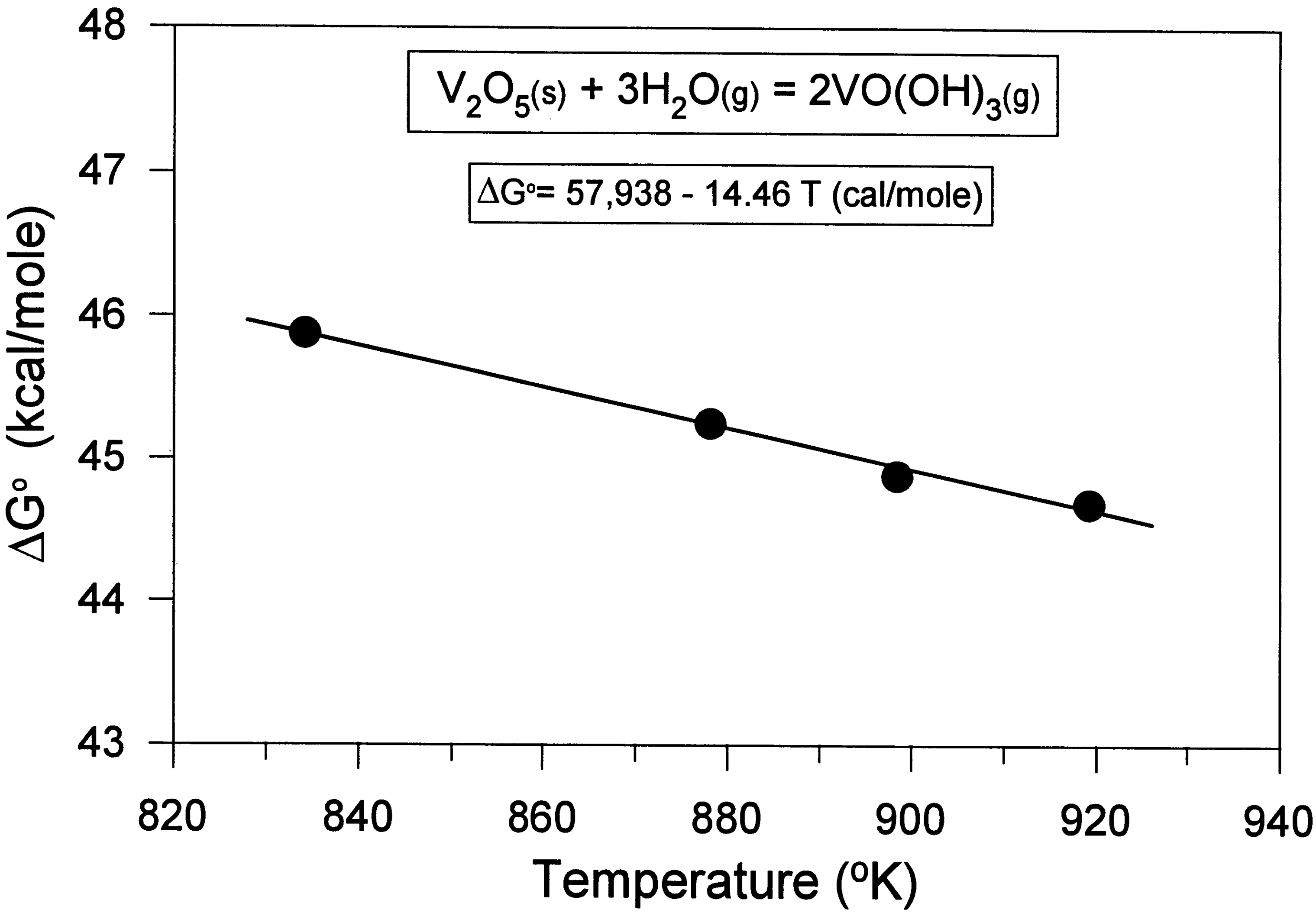

Figure 4.7 Gibbs free energy change for the reaction $V_2O_5(s) + 3H_2)(g) = 2VO(OH)_3(g)$ as a function of temperature.

where the stated error is the 95% confidence range of the regression evaluated at the temperature where the error was the largest within the temperature range studied.

The obtained results seemed reasonable considering the positive signs for both ΔH° and ΔS°. Since $V_2O_5(s)$ was being sublimed into a complex hydroxide species, a heat input and an increase in entropy would be expected.

Combining the equation for the free energy of fusion reported in USBM bulletin # 672[1] with equation (4.7), the following equation was derived:

$$V_2O_5(l) + 3H_2O(g) = 2VO(OH)_3(g) \tag{4.8}$$

$$\Delta G^\circ = 48{,}482 + 11.435\ T\ Ln\ T - 0.004844\ T^2 + 286{,}850/T - 78.625\ T\ \text{(cal/mole)}$$

Moreover, equation (4.7) was combined with the Gibbs free energies of formation for both $H_2O(g)$ and $V_2O_5(s)$, as reported in USBM bulletin #672[1] to obtain the Gibbs free energy of formation of $VO(OH)_3(g)$:

$$V(s) + \frac{3}{2}H_2(g) + 2O_2(g) = VO(OH)_3(g) \tag{4.9}$$

$$\Delta G^\circ_f = -243{,}464.45 + 1.88\ T\ Ln\ T - 0.001838\ T^2 + 100{,}450/T + 50.911\ T\ \text{(cal/mole)}$$

$$\Delta G^\circ_f = -1{,}018{,}655.2 + 7.87\ T\ Ln\ T - 0.007790\ T^2 + 420{,}283/T + 213.011\ T\ \text{(J/mole)}$$

4.1.3 Discussion of Results

A graphical comparison of the results obtained in the present study and the work of the other investigators is presented in Figure 4.8. The reported equations for the Gibbs free energy of the reactions (see reactions (4.1), (4.3), and (4.5), for the suggested

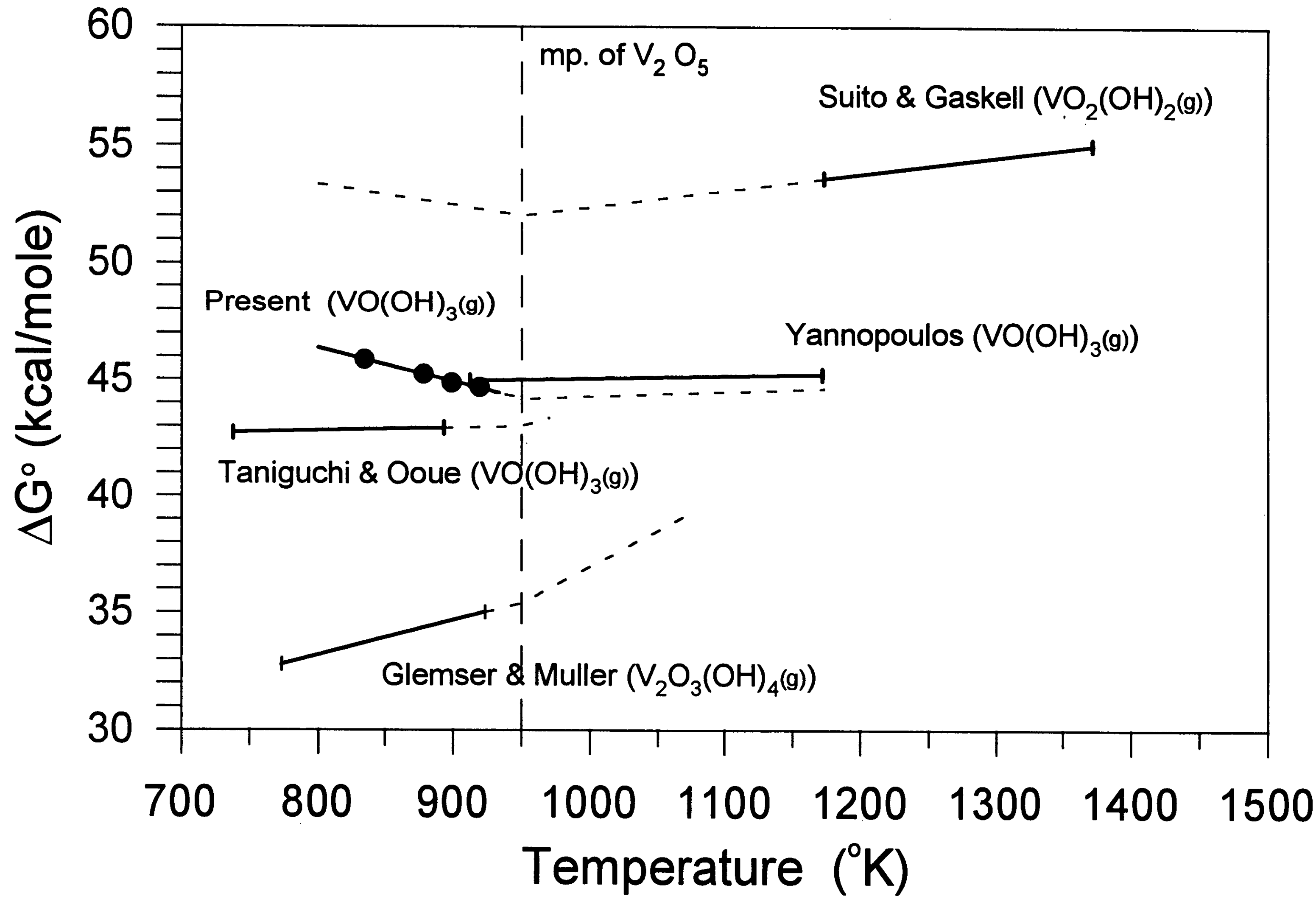

Figure 4.8 Gibbs free energy of reaction as a function of temperature according to reactions (4.2), (4.3), (4.5).

species, were plotted as a function of temperature within the working temperature range of each investigator (solid lines). Moreover, these curves were extrapolated using the ΔG^o of fusion reported by the USBM bulletin # 672[1] to facilitate the comparison (dashed lines).

The most striking observation was the discrepancy in the sign of the slopes (entropy change) of the curves when the volatile hydroxides formed above solid V_2O_5.

The work of Glemser and Muller[15], which shows the most negative entropy change, has been widely criticized[12,14] for not having demonstrated the attainment of equilibrium. Moreover, their chosen stoichiometry was not consistent with the findings of the present investigation.

Although Yannopoulos' measurements were made mainly above V_2O_5(l), he conducted several experiments above V_2O_5(s) (at a single temperature of 639 °C) and concluded that the formation of $VO(OH)_3$(g) from either solid or liquid V_2O_5 could be described by the same equation. This conclusion, however, was based on a single temperature below the melting point and thus, cannot reflect, with any degree of confidence, the trends above the solid phase. Nonetheless, it is worth noting that his experimental values above V_2O_5(s) are in very close agreement with the values obtained in the present investigation. Also, his experimental results above the liquid phase are in good proximity with the extrapolated values of the present work (less than 500 cal/g-mole difference). This difference might be attributed to Yannopoulos' probable experimental difficulty in maintaining unit activity V_2O_5(s) of in the liquid phase. This possibility was pointed out by Suito and Gaskell[14] who argued that oxygen dissolves in the melt and the activity of V_2O_5 decreases. In order for the above argument to be consistent with both theoretical hypothesis and experimental evidence, the following analysis was pertinent. If the activity of V_2O_5(l) in Yannopoulos' experiments were indeed less than one, the expected partial pressure of the volatile hydroxide would have been smaller than that predicted considering unit activity of the liquid phase. If one compares the extrapolated curve from the present work with that of Yannopoulos, one can ascertain, given the higher ΔG° from the work of Yannopoulos, that, indeed, the partial pressures obtained by the latter author were smaller than the predicted values obtained from the results of the present investigation; thus suggesting that the activity of V_2O_5(l) in Yannopoulos' experiments might have been less than one.

Even though Yannopoulos only reports one equation for both solid and liquid V_2O_5, it is interesting to note that if his equation is combined with the ΔG° of fusion, the entropy of the reaction (not shown in the graph) changes from negative to positive above the solid phase. This change in slope was consistent with the results of the present work.

Taniguchi and Ooue[16] reported the formation of the same volatile hydroxide above V_2O_5(s) as in the present work. However, the reported vapor pressures are considerably higher than the ones obtained in both this investigation and the work of Yannopoulos. Moveover, the negative entropy change reported by Taniguchi and Ooue for reaction (4.1) was inconsistent with the results reported in this study and that of Yannopoulos.

Suito and Gaskell[14] made all of their measurements above V_2O_5(l). They considered the oxygen solubility in the liquid melt and proposed the formation of two volatile hydroxides above the system VO_2-$VO_{2.5}$(l) according to:

$$VO_2(s) + H_2O(g) = VO(OH)_2(g) \tag{4.10}$$

$$VO_{2.5}(l) + H_2O(g) + \frac{1}{4}O_2(g) = VO_2(OH)_2(g) \tag{4.11}$$

where reaction (4.11) was the main reaction contributing to the apparent vapor pressure. Using this equation and combining it with the ΔG° of fusion, an extrapolation into the solid phase was made. It is interesting to note that the slope changes and a positive entropy change was obtained. This species, however, depends on the oxygen potential and in the present study (Figure 4.1), there was no evidence of this dependance above $V_2O_5(s)$.

Although it was difficult to predict the change in entropy for the sublimation of a condensed phase into a complex gaseous species, it was reasonable to infer, given the above analysis, that the change in entropy for the formation of the volatile hydroxide species in this case was positive when considering the solid phase; and negative when considering the liquid phase.

In the literature review, the patent by Chambers[17] was mentioned. Although the mechanisms for the formation of a volatile hydroxide in the presence of water vapor were not clear, he reported unusually high recoveries of vanadium (56 wt.% in 2 hrs at 745 °C) from a slag containing 0.57 wt.% V_2O_5. He also mentioned an optimum temperature range (700 to 900 °C) and that extractions were improved under pressurized conditions. The limitation on the temperature was due to the volatilization of other metals besides vanadium at higher temperatures. Chamber's suggested high vapor pressures, however, were not realized in the present study, nor in the work of other investigators.

Given the above discussion, it was concluded that with the results of the present study, the discrepancies in the vapor chemistry of vanadium pentoxide in the presence of water vapor, have finally been resolved.

4.1.4 Industrial Applications of the Generated Knowledge

The results of this investigation can be used to determine process conditions for the extraction of vanadium from vanadium bearing feedstocks and wastes. Table 4.4 shows the calculated vapor pressures of $VO(OH)_3$ under different processing conditions above $V_2O_5(l)$.

Table 4.4 Calculated Vapor Pressures of $VO(OH)_3$ Above $V_2O_5(l)$ Under Different Processing Conditions

Temperature (°C)	900		1100		1300	
P_{H2O} (atm)	1	10	1	10	1	10
$P_{VO(OH)3}$ (Torr)	0.05	1.64	0.19	6.07	0.51	16.24

As shown in the table above, the vapor pressures of $VO(OH)_3$, under a water pressure of 1 atm, are smaller than 1 Torr at the three proposed temperatures. However, when the water vapor pressure is increased to 10 atm, the resulting vapor pressures of the volatile hydroxide become greater than 1 Torr in all three cases; going as high as

16.24 Torr at 1300 °C. Thus, in order to achieve high vapor pressures of $VO(OH)_3$ for industrial applications, it is recommended to operate at temperatures at least at 1250 °C with a water vapor pressure of at least 5 atm.

Finally, an interesting observation in this study was the fact that volatile vanadium hydroxides significantly attack quartz, and, to a lesser extent, alumina. This finding, may be of considerable interest to the industry, if its processes involve, for example, the use of silica or alumina supported catalysts in the presence of V_2O_5(s) and water vapor. The source of vanadium may be from the catalyst itself or from impurities in the raw materials. When this vanadium containing catalysts are exposed to water vapor, not only will the vanadium react with water to form $VO(OH)_3$(g), but also, the formed hydroxide will attack the silica, diminishing the service life of the catalysts. Since alumina is attacked to a lesser extent than silica, alumina substrates are recommended when the presence of V_2O_5(s) and water vapor is expected in the process.

4.2 Vanadium Trioxide

4.2.1 Baseline Vapor Pressures for V_2O_3(s)

No volatilization was detected in the experiments conducted in the absence of water vapor. A summary of the experimental conditions, after having conditioned the sample, is presented in Table 4.5. As appreciated from the results of these experiments, no appreciable weight loss was realized. Moreover, no evidence of vapor transport of vanadium was found in the condenser system. The weight changes reported are attributed

Table 4.5 Experimental Conditions for the Baseline Experiments Above $V_2O_3(s)$

Condensed Phase	Amb. Press. (atm)	Amb. Temp (°C)	Boats Temp (°C)	P_{CO2}/P_{CO}	Run Time (hrs)	Wt. Change (gm)
$V_2O_3(s)$	0.82	21	603	0.32	6.6	-0.00003
$V_2O_3(s)$	0.82	23	603	2	7.0	+0.00005
$V_2O_3(s)$	0.82	22	743	0.32	7.5	+0.00000
$V_2O_3(s)$	0.82	26	900	1	6.0	+0.00004
$V_2O_3(s)$	0.82	24	900	1	17.6	-0.00009

to the variability of the balance at the fifth decimal place. These results, corroborated the data obtained from the literature that the contribution of volatile oxides to the total vapor pressure was practically null.

4.2.2 Measurements on $V_2O_3(s)$ in the Presence of H_2O

Several experiments were conducted to investigate the formation of volatile hydroxides with $V_2O_3(s)$. The experimental conditions are summarized in Table 4.6

It can be appreciated, that in the cases presented, the sample tended to gain some weight. This weight gain, especially in the case of the first and the third experiments shown in Table 4.6, could not be attributed solely to weighing errors. Given that the weight gains were approximately the same at run times of 17.9 and 4 hrs, it was believed that some oxygen pick up occurred while withdrawing and cooling the sample. It was also probable that the gas mixture did not fully equilibrate in the sections near the entrance of the reactor where the temperature was below 300 °C. The same sample used in the first experiment was used in the second experiment. In the latter case, the boats were withdrawn considerably faster to allow for faster cooling. The sample lost approximately the same amount that it gained in the previous experiment; thus supporting the hypothesis of oxygen pick up during cooling. This rapid quenching, however, caused some practical problems. The heat dissipated by the hot sample boats and carrier tube

Table 4.6 Experimental Conditions for the Experiments Above $V_2O_3(s)$ in the Presence of Water Vapor

Condensed Phase	Amb. P (atm)	Amb. Temp (°C)	Boats Temp (°C)	P_{CO2}/P_{CO}	P_{H2O}/P_{H2}	Run Time (hrs)	Wt. Change (gm)
$V_2O_3(s)$	0.81	21	910	1	1.3	4.0	+0.00082
$V_2O_3(s)$	0.82	25	910	1	1.3	5.1	-0.00083
$V_2O_3(s)$	0.83	26	900	1	1.2	17.9	+0.00090
$V_2O_3(s)$	0.82	25	778	1	0.8	20.8	+0.00051
$V_2O_3(s)$	0.82	25	970	1	1.5	16.4	+0.00006

partially burned the rubber stoppers and other hardware used to center the reactor tube and hold the carrier tube sheath. Thus, the withdrawing rate was reduced to a more acceptable level. Furthermore, no evidence of vanadium transport was evident in the condenser system.

Since no weight loss was observed in these experiments, it was concluded that $V_2O_3(s)$ does not form volatile hydroxides detectable with the transpiration technique in the temperature range studied.

4.3 Molybdenum Trioxide

4.3.1 Baseline Vapor Pressures for $MoO_3(s)$

4.3.1.1 Results. It was found, in the literature review, that the contribution of the volatile oxides to the total vapor pressure was sufficiently high to be detected in the transpiration technique. There was some controversy, however, as to how this sublimation should be interpreted. Some authors[33,31,43,37,38] assumed, based on the results of Berkowitz that Mo_3O_9 was the predominant species at 577 °C, that $Mo_3O_9(g)$ was the sole predominant gaseous species in the temperature range of 580 to 800 °C, and that the sublimation process could be described as:

$$3MoO_3(s) = Mo_3O_9(g) \qquad (4.12)$$

Other investigators[42, 43,34,39], however, argued that this assumption was not satisfactory because, if the results of Berkowitz were extrapolated to higher temperatures, the contribution of Mo_4O_{12} became significant. Thus, both $Mo_3O_9(g)$ and $Mo_4O_{12}(g)$ should be considered. However, in order to consider these two species, their relative contributions to the total vapor pressure have to be known. Since the only information available was the mass spectrometric study of Berkowitz et al., they extrapolated the proposed relative proportions and calculate an average molecular weight as a function of temperature. In this way, they were able to express the sublimation process as:

$$\bar{n}MoO_3(s) = (MoO_3)_{\bar{n}}(g) \tag{4.13}$$

Although this approach was more rigorous than the one described by equation (4.12), a considerable uncertainty was introduced when calculating the vapor pressures of $(MoO_3)_{\bar{n}}$ based on extrapolated gas relative proportions of the gases. This is due to the extreme difficulty in calculating accurate vapor pressures using the mass spectrometric technique. This difficulty arises from the number of assumptions that have to be made to back calculate the vapor pressure from ionic intensities. This uncertainty increases considerably when estimations are done through extrapolation. The recent work of Ikeda et al.[34], serves as an illustration of the errors involved in calculating the relative proportions of the gaseous species through mass spectrometry. The abundance ratio of Mo_3O_9 to Mo_4O_9 based Ikeda's work was approximately a factor of 2 lower than the ratio calculated based on Berkowitz's work.

In the present investigation, the experimental results were interpreted first using equation (4.12). Then for comparative purposes, they were interpreted according to equation (4.13), using the relative distributions for gaseous species reported in the literature. The results of the comparison are shown in Table 4.7.

It was appreciated that there was no significant difference between the obtained free energies using equation (4.12) and (4.13) at the temperature range of interest.

Table 4.7 Comparison of Results Interpreted According to Reaction (4.12) and (4.13)

T (° K)	$\Delta G°$(cal/mole)		
	Mo_3O_9	$(MoO_3)\bar{n}$ (1)	$(MoO_3)\bar{n}$ (2)
921	20,997	21,177	21,250
947	19,222	19,403	19,478
975	17,167	17,400	17,477
1012	14,837	15,124	15,184
1068 (3)	10,985	11,294	11,370

(1) Calculated Mo_3O_9 / Mo_4O_{12} ratios based on Berkowitz's[33] work.
(2) Calculated Mo_3O_9 / Mo_4O_{12} ratios based on Ikeda's[34] work.
(3) Extrapolation to the melting point.

Based on the above comparison, the author preferred to account for the vapor transport of molybdenum solely as Mo_3O_9(g), rather than introducing additional uncertainties to the measurements by using questionable abundance distributions of Mo_3O_9 and Mo_4O_{12}. By so doing, the author acknowledge that some uncertainty in the measurements was introduce but believed, based on the above discussion, that this uncertainty was not significant.

It is important to note that as long as all the moles of molybdenum transported were accounted for, no error would be introduced when calculating the vapor pressures of the volatile hydroxides. This would be true whether reaction (4.12) or (4.13) were used to describe the sublimation of MoO_3(s).

The first series of experiments on the sublimation of MoO_3(s) was aimed at establishing a working range of flowrates where equilibrium would be assured. Thus, experiments were conducted at different flowrates and the vapor pressures calculated

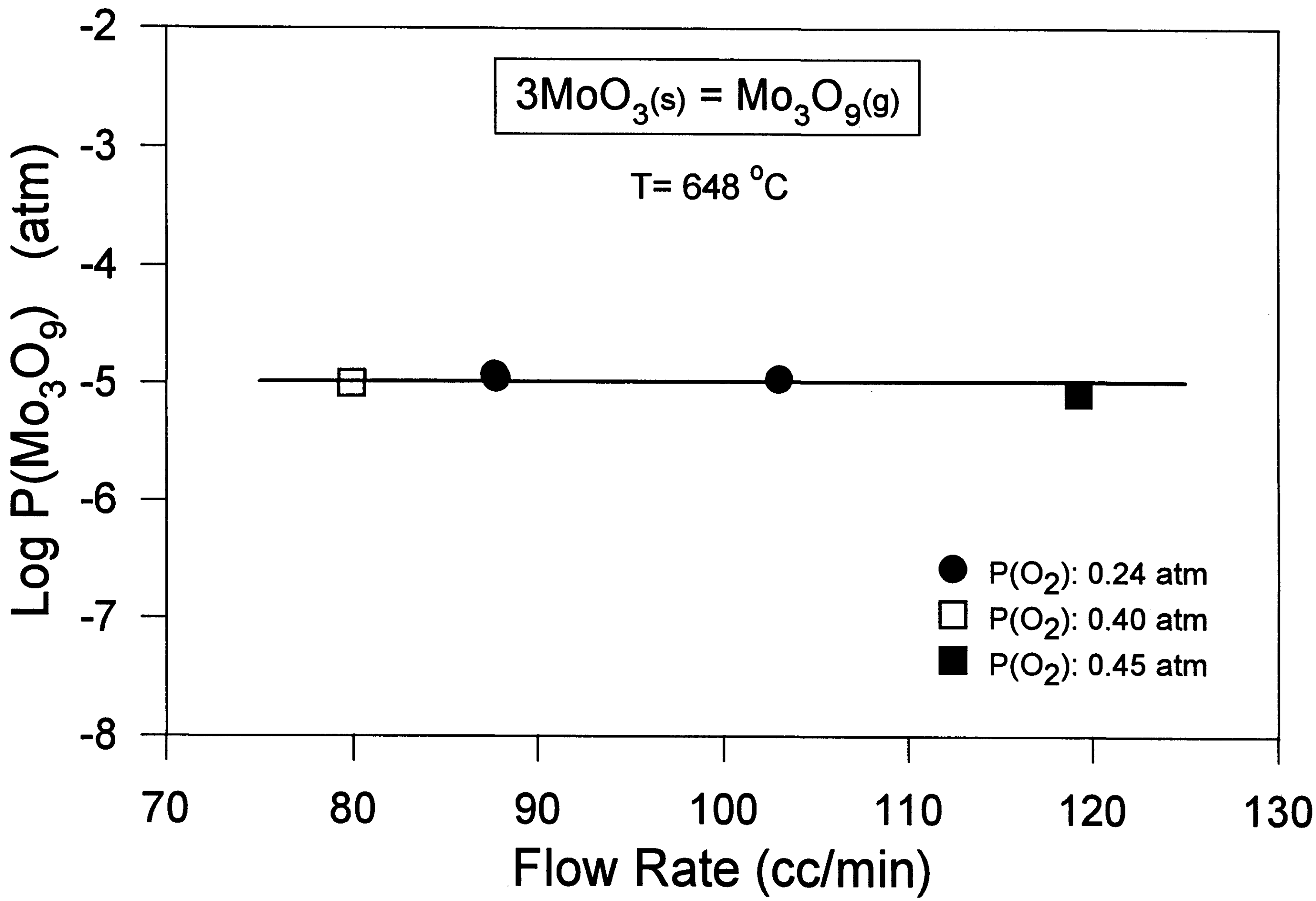

Figure 4.9 Pressure of $Mo_3O_9(g)$ as a function of the flowrate at three different oxygen potentials.

based on reaction (4.12). The results of these experiments are presented in Figure 4.9.

It was appreciated, from Figure 4.9 , that the vapor pressure was independent from the flowrate in the range of 80 to 120 ml/min. Moreover, it was observed that, as expected from reaction (4.12), the pressure of $Mo_3O_9(g)$ was independent of the oxygen potential.

Once the working flowrate range had been established, the next step was to conduct experiments at different temperatures with the objective of correlating the Gibbs free energy for the reaction with the temperature. A summary of the results obtained is presented in Figure 4.10.

The free energy equation obtained, using the Second Law method as the basis for the regression was:

$$\Delta G^\circ = 83{,}684 - 68.07\ T \quad (\pm\ 506\ \text{cal/mol}) \tag{4.14}$$

$$\Delta G^\circ = 350{,}134 - 284.80\ T \quad (\pm\ 2117\ \text{J/mole})$$

where the stated error is the 95% confidence range of the regression evaluated at the temperature where the error was the largest within the temperature range studied.

For the above regression ΔC_p° was considered to be equal to zero because C_p° values for $Mo_3O_9(g)$ were not available. This assumption was considered reasonable, given that the temperature differences were less than 150 °K.

In order to obtain an equation for the ΔG° of sublimation of liquid MoO_3, the equations for $C_p^\circ(T)$ for solid and liquid molybdenum trioxide, reported by Cosgrove and Snyder[57], were used. The enthalpy and entropy of fusion as a function of temperature

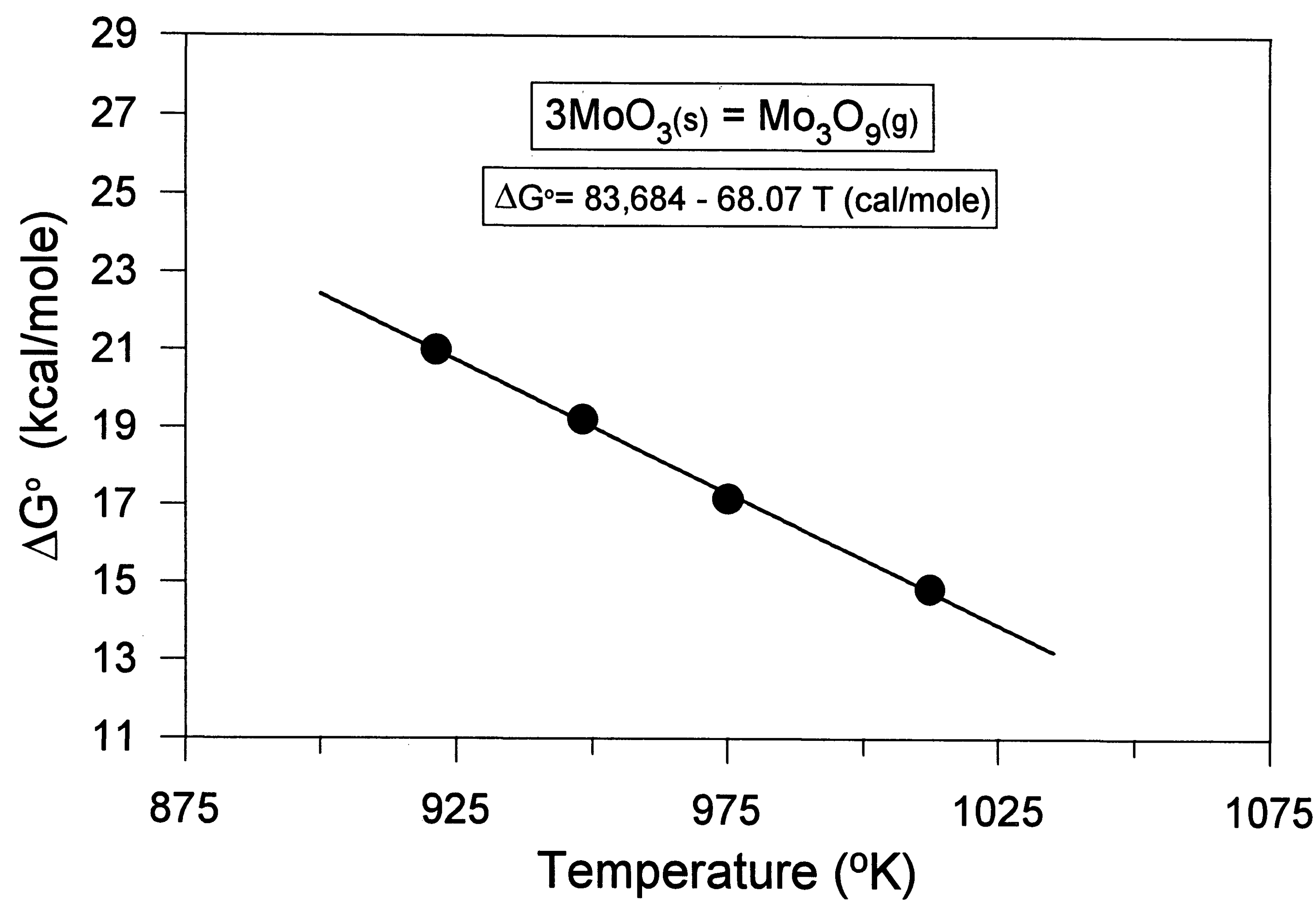

Figure 4.10 Gibbs free energy for reaction (4.12) as a function of temperature.

were obtained by integrating the following equations:

$$MoO_3(s) = MoO_3(l) \tag{4.15}$$

$$\Delta H^{o}_{s-l} = \int \Delta Cp_{s-l} dt + \Delta H_o \tag{4.16}$$

$$\Delta S^{o}_{s-l} = \int \frac{\Delta Cp_{s-l}}{T} dt + I \tag{4.17}$$

The integration constants were evaluated using values of ΔH^{o} fusion and ΔS^{o} fusion at the melting point of MoO_3 (1068.36 °C) reported by Cosgrove and Snyder. The obtained integrated equations were:

$$\Delta S^{o}_{s-l} = -239.784 \ln T + 0.28968T - 3.5x10^{-5}T^{2} \tag{4.18}$$

$$3.68 \text{ x } 10^{5} / 2 \ T^{-2} + 1414.27 \ \text{(cal/mole-°K)}$$

$$\Delta H^{o}_{s-l} = -240.414T + 0.14484T^{2} - \frac{7x10^{-5}}{3}T^{3} \tag{4.19}$$

$$- 3.68 \text{ x } 10^{5} / T + 132{,}867.28 \ \text{(cal/mole)}$$

From equation (4.18) and (4.19), the ΔG^{o} of fusion as a function of temperature was derived as:

$$MoO_3(s) = MoO_3(l)$$

$$\Delta G^{o}_{s-l} = 132{,}867.28T - 1654.684T - 0.14484T^{2} \tag{4.20}$$

$$+ 1.16667 \text{ x } 10^{-5} T^{3} - 5.52 \text{ x } 10^{5} / T + 239.784 \ T \ln T \ \text{(cal/mole)}$$

Combining equation (4.20) with equation (4.14), the equation of the Gibbs free energy of sublimation of liquid MoO_3 was obtained as:

$$3MoO_3(l) = Mo_3O_9(g)$$

$$\Delta G^\circ = -49183.28T + 1586.61T + 0.14484T^2 - 1.16667\times10^{-5}T^3 \quad (4.21)$$
$$+ 5.52 \times 10^5 / T - 239.784 \, T \ln T \quad \text{(cal/mole)}$$

The ΔG°_f of $MoO_3(s)$, calculated based on Cosgrove and Snyder's[57] C_p° function for $MoO_3(s)$ as well as the $\Delta H^\circ_{f(298\,K)}$ for $MoO_3(s)$, S°_{298} for O_2, and S°_{298} for Mo(s) reported in the USBM # 672[1] , was:

$$Mo(s) + 3/2 \, O_2(g) = MoO_3(s)$$

$$\Delta G^\circ_f = -180{,}820.69 - 4.848 \, T \ln T - 1.011\times10^{-3}T^2 \quad (4.22)$$
$$+ 1.7970 \times 10^5 / T + 96.873 \, T \quad \text{(cal/mole)}$$

Finally, combining equation (4.22) with equation (4.14), the free energy of formation of $Mo_3O_9(g)$ was derived as:

$$3Mo(s) + 9/2 \, O_2(g) = Mo_3O_9(g)$$

$$\Delta G^\circ_f = -488{,}778.07 + 14.544 \, T \ln T - 3.033\times10^{-3}T^2 \quad (4.23)$$
$$+ 5.391 \times 10^5 / T + 222.549 \, T \quad \text{(cal/mole)}$$

$$\Delta G^\circ_f = -2{,}045{,}047.4 + 60.852 \, T \operatorname{Ln} T - 12.690 \times 10^{-3} \, T^2$$
$$+ 22.556 \times 10^5 / T + 931.145 \, T \quad \text{(J/mole)}$$

4.3.1.2 Discussion of Results. A graphical comparison of the results of this work with those other investigators is presented in Figure 4.11. As mentioned in the literature review, three different sets of data for the sublimation of MoO_3(s) were identified in this comparison. A lower set consisting of the data reported by Blackburn[37], Gulbransen[39], and Ariya[43]; a higher set comprising the work of Berkowitz[33], Ikeda[34], Ueno[38], and Ackermann[42, 43]; and finally, a middle set corresponding to the work of Glemser[31]. The results of the present study fall in the higher set.

It was appreciated, from Figure 4.11 , that the free energy values obtained in the present work were in good agreement with those reported by Ueno and Ikeda at the lower limit of the temperature range studied. Moreover, it was observed that the line representing the present investigation was in fairly good agreement with the work reported by Berkowitz and Ackermann within their quoted experimental errors; $\pm$ 4 kcal and $\pm$ 2 kcal, respectively. Also, the magnitude of the slope of the line was in fair agreement with the slopes reported by most of the other investigators.

An interesting observation above the lower set of data, was that, except for the work of Ariya, the studies were conducted using a Knudsen effusion cell. In these studies, the MoO_3(s) sample was heated under vacuum and the vapor pressures calculated based on weight loss. The reported experimental pressure was in the order of 10^{-6} mm Hg (1.32 x 10^{-9} atm). However, the stability diagrams for MoO_3(s) above 650 °C indicated that, at these pressures, MoO_3(s) tended to be reduced to Mo_9O_{26}(s), (see Figures 2.4 to 2.6 on pages 30 through 32 . So, there was a high probability that some of the measured weight loss was attributed to oxygen losses, rather than evaporation of

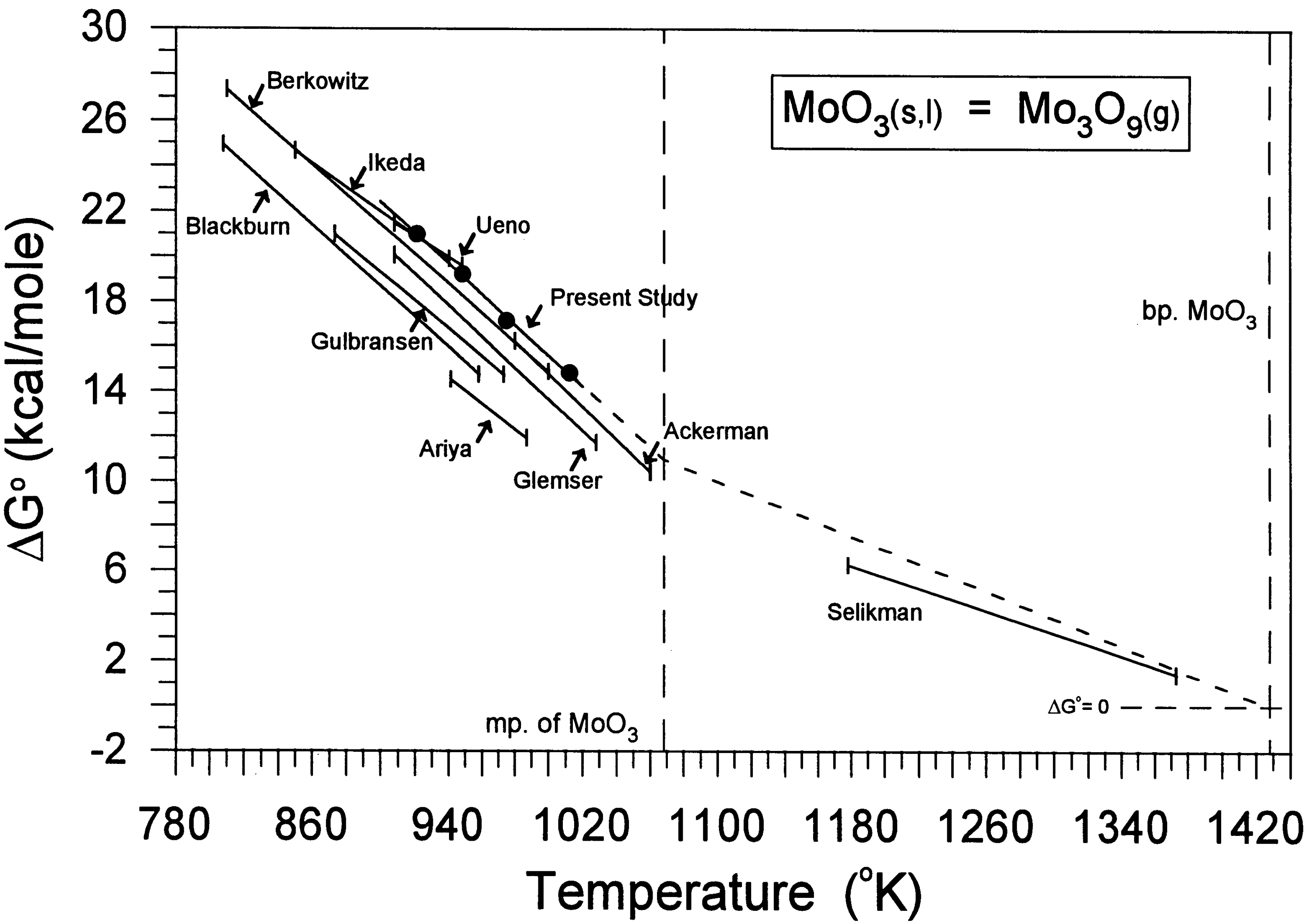

Figure 4.11 Gibbs free energy as a function of sublimation as reported by the different investigators.

the condensed sample. If this were the case, the calculated vapor pressures would be higher than the actual vapor pressures in equilibrium with $MoO_3(s)$. This may explain the higher vapor pressures obtained by Blackburn and Gulbransen.

The differences between the present work and that from Ariya[43] and Glemser et al[31]., could not be explained.

The work of Glemser et al., however, was of the special interest to the present investigation because they also studied the formation of volatile hydroxides above $MoO_3(s)$. Therefore, the difference in the measured vapor pressure of $Mo_3O_9(g)$ between their work and the results obtained in the present study, were reflected in the vapor pressure measurements in the presence of water vapor, as will be discussed.

When the results of the present study were extended into the liquid phase using equation (4.20), and evaluated at the boiling point of $MoO_3(s)$ (1428 °K), the obtained $\Delta G°$ was very close to the expected value of zero. The calculated value using equation (4.20) was -37 cal/mole. This was an excellent agreement given the uncertainties involved in making such a large extrapolation. Also, it was appreciated that there was a very good agreement with the work of Selikman, especially at the higher end of his studied temperature range.

4.3.2 Measurements on $MoO_3(s)$ in the Presence of Water Vapor

4.3.2.1 Results. It was found in the literature, that $MoO_3(s)$ reacts with water according to the reaction:

$$MoO_3(s) + H_2O(g) = MoO_2(OH)_2(g)$$

It was also found that, although the different investigators agreed on the molecularity of the species formed, they did not agree on the vapor pressures of the volatile hydroxides. Therefore, an study on the enhancement of the volatility of $MoO_3(s)$ in the presence of water vapor was undertaken to resolve these discrepancies.

If the equilibrium constant for the above reaction were linearized, the Log $P_{MoO2(OH)2}$ would be a function only of Log P_{H2O} with a slope of 1. A plot of Log $P_{MoO2(OH)2}$ vs. Log P_{H2O} was constructed at two different O_2 potentials (see Figure 4.12). From this Figure, it was determined that the experimental slope of 1.09 agreed very well with the theoretical slope of 1; thus corroborating the molecularity reported in the literature. Moreover, it was appreciated that, as expected from the proposed reaction, the pressure of the volatile hydroxide was not affected by the O_2 pressure.

In Figures 4.13 and 4.14, the attainment of equilibrium was demonstrated by showing the independence of the equilibrium constant from the water potential and the flowrate, respectively. These type of graphs not only confirmed that equilibrium was being reached, but were also useful in obtaining an average value of the equilibrium constant (1.97×10^{-3}) at the shown temperature (702 °C).

Another way of analyzing the data and checking its consistency, was to plot

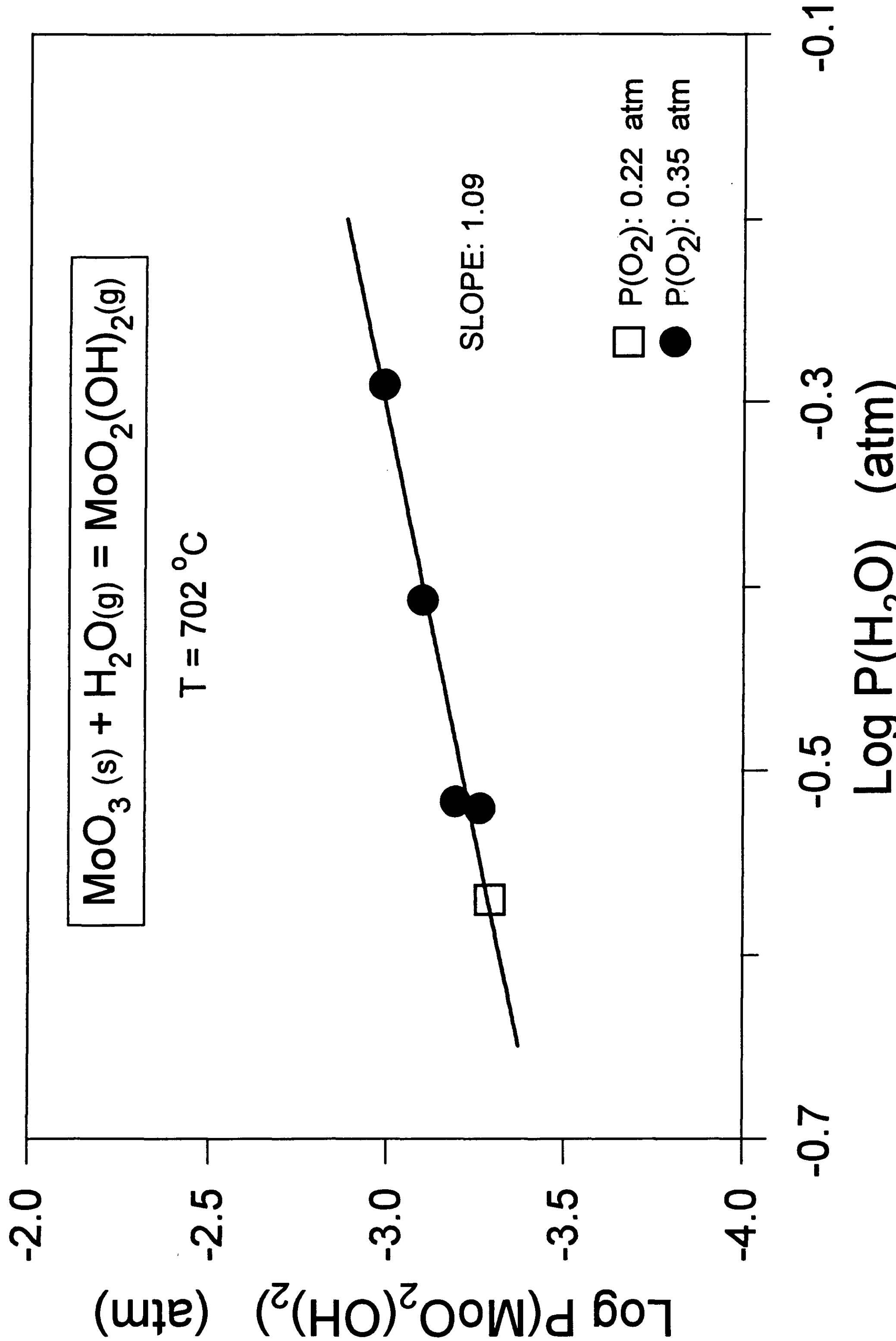

Figure 4.12 Vapor pressure of $MoO_2(OH)_2$ as a function of water potential.

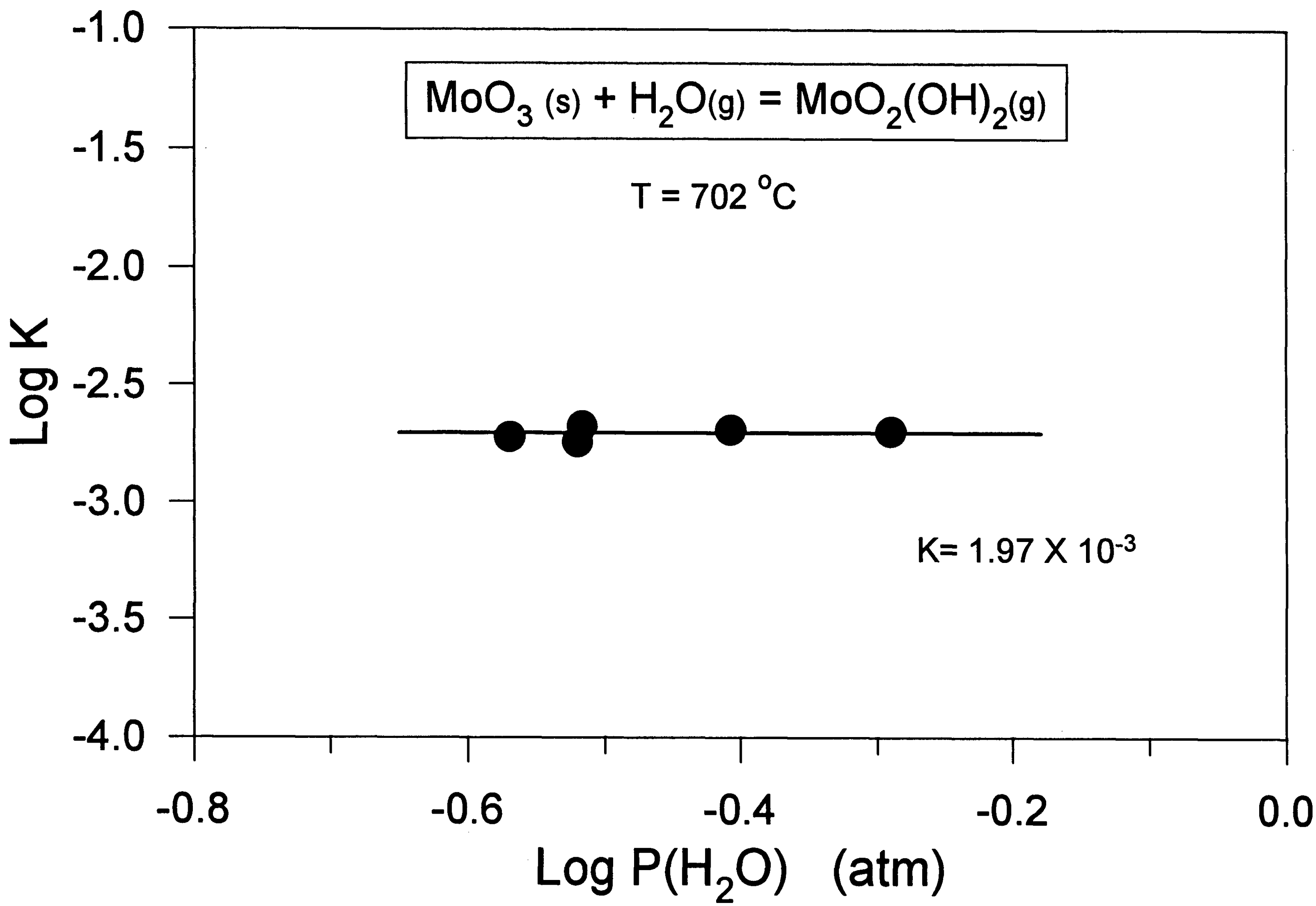

Figure 4.13 Equilibrium constant for the reaction (4.24) as a function of water potential.

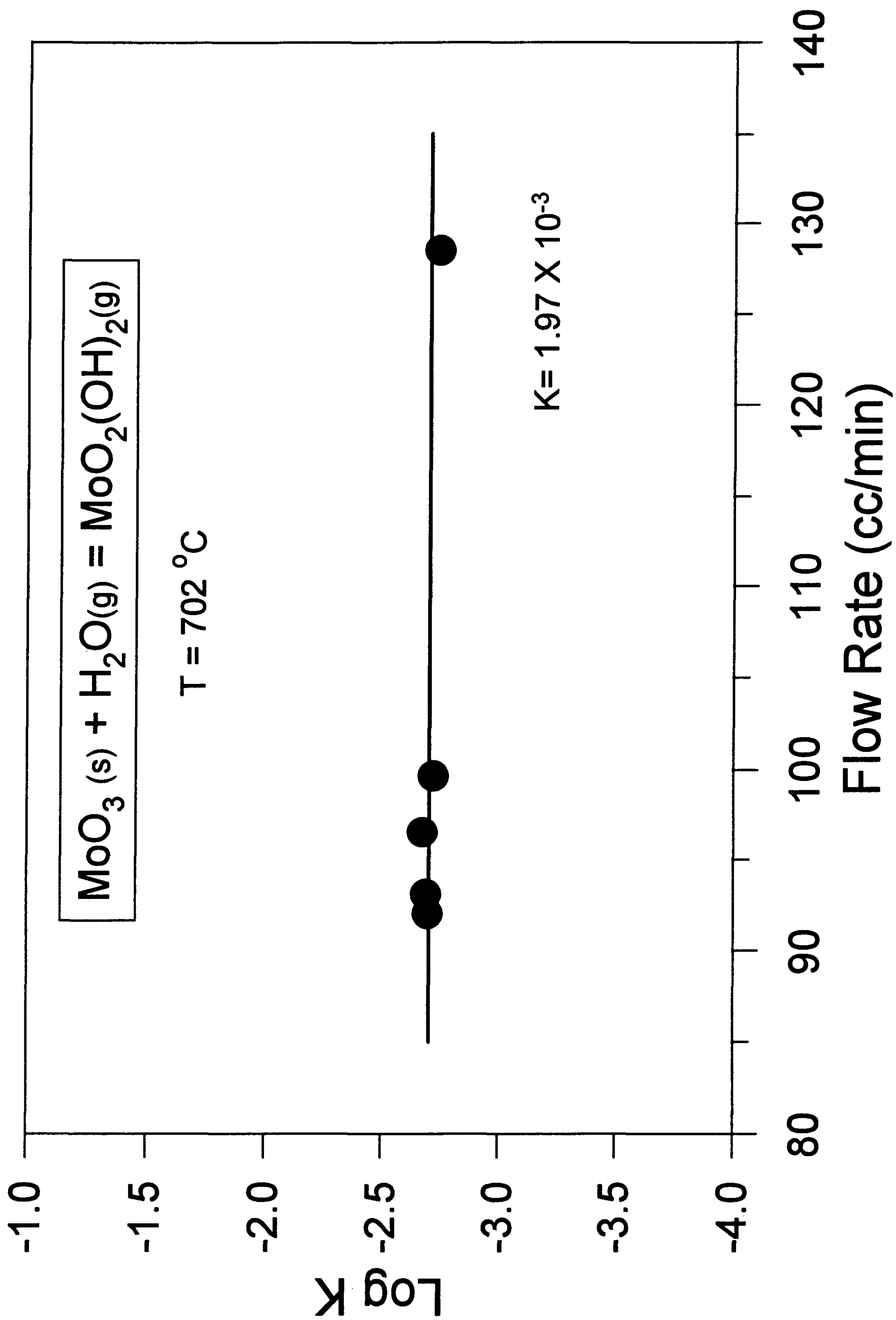

Figure 4.14 Equilibrium constant for the reaction (4.24) as a function of flow rate.

$P_{MO2(OH)2}$ vs. P_{H2O} and force the regression line through zero. Given the dependence of $P_{MoO2(OH)2}$ to the water pressure to the first power, the slope of this line should directly give the equilibrium constant for the reaction. This analysis is represented in Figure 4.15. The slope obtained of 1.99 X 10^{-3} was in excellent agreement with the average value of 1.94 X 10^{-3} previously obtained in Figure 4.12.

Once the molecularity of the volatile hydroxide had been established, measurements at additional temperatures were conducted. A summary of the experimental results is presented in Figure 4.16. The free energy equation obtained, using the Second Law method as the basis for the regression, was:

$$MoO_3(s) + H_2O(g) = MoO_2(OH)_2(g) \qquad (4.24)$$

$$\Delta G^o = 31{,}143 - 19.57\ T \quad (\pm 40\ \text{cal/mole})$$

$$\Delta G^o = 130{,}302 - 81.88\ T \quad (\pm 167\ \text{J/mole})$$

where the stated error is the 95% confidence range of the regression, evaluated at the temperature where the error is the largest within the temperature range studied.

For the above regression ΔC_p^o was considered equal to zero because C_p^o values for $MoO_2(OH)_2(g)$ were not available. Again, this assumption was considered reasonable, given that the temperatures ranges were less than 170 °K.

Equation (4.24) was combined with the Gibbs free energy of fusion to obtain an expression for the formation of volatile hydroxides above liquid MoO_3 according to :

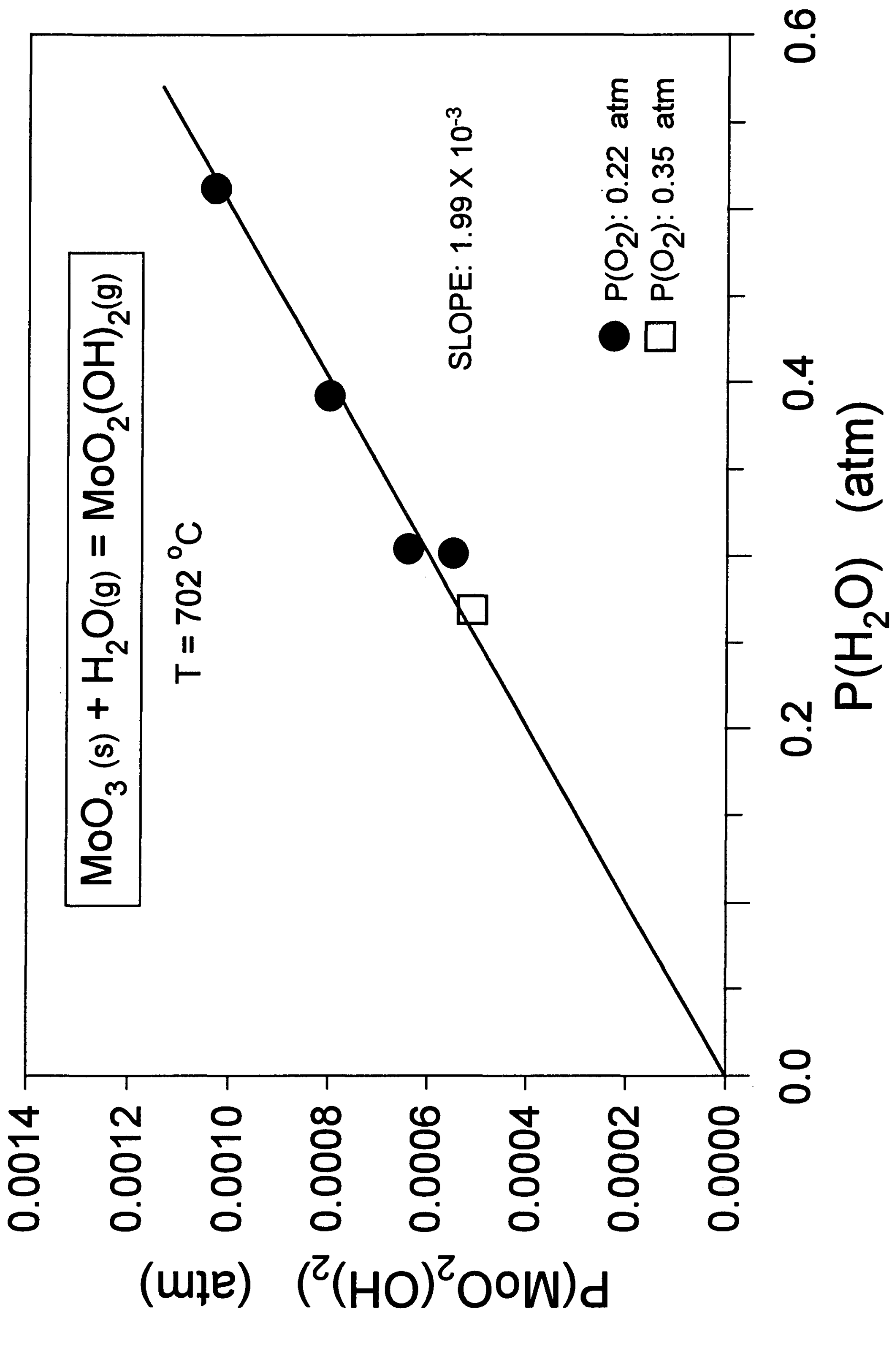

Figure 4.15 Partial pressure of $MoO_2(OH)_2$ as a function of water potential.

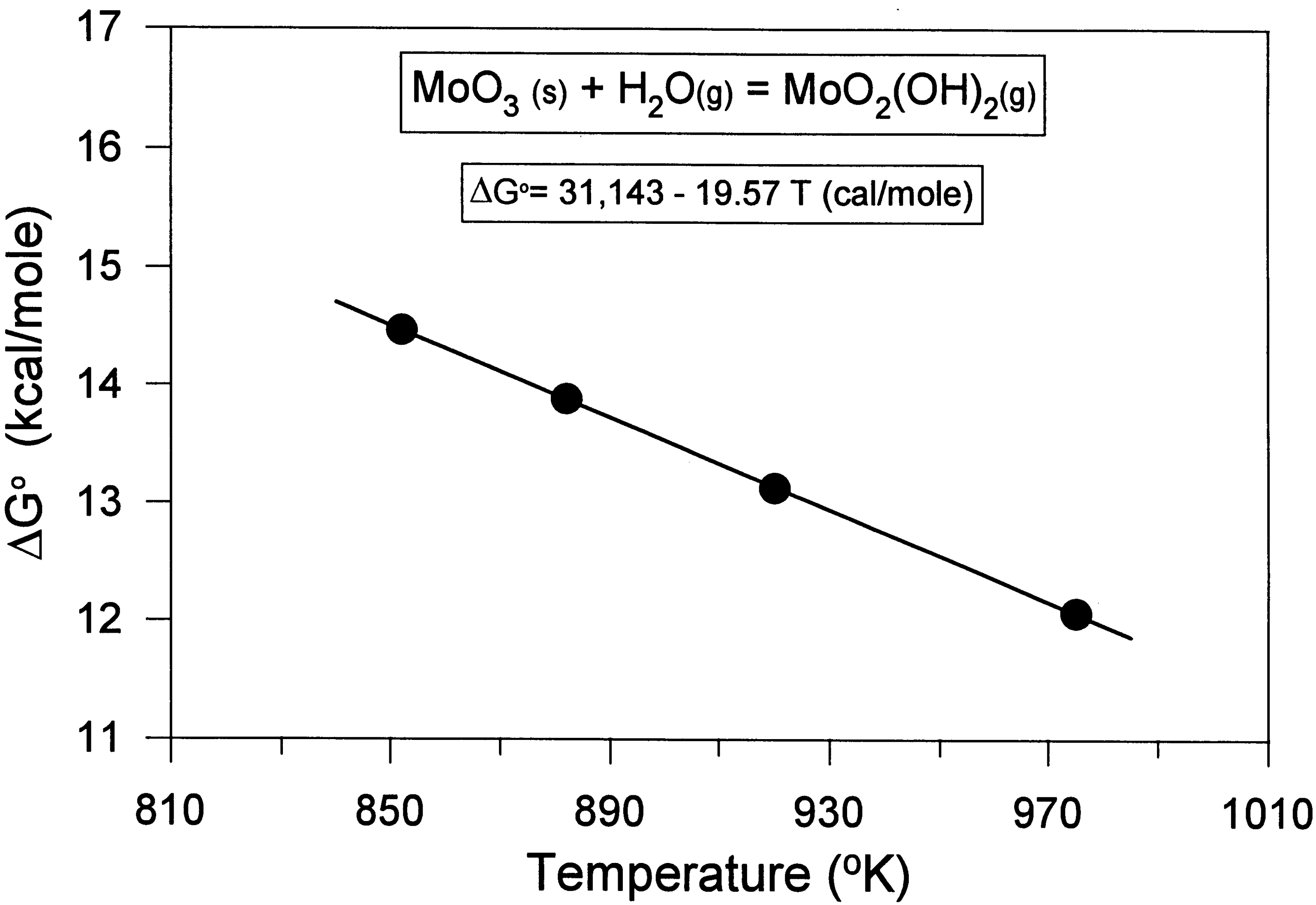

Figure 4.16 Gibbs free energy change for the reaction (4.24) as a function of temperature.

$$MoO_3(l) + H_2O(g) = MoO_2(OH)_2(g) \qquad (4.25)$$

$$\Delta G^\circ_{s-l} = -101{,}724.28 + 1635.11T + 0.14484T^2 \qquad (4.26)$$
$$- 1.16667 \times 10^{-5}\, T^3 + 5.52 \times 10^5 / T - 239.784\, T \ln T \text{ (cal/mole)}$$

Equation (4.24) was also combined with the Gibbs free energy of formation for $MoO_3(s)$ (see equation (4.22)) and the Gibbs free energy of formation of water vapor (as reported in USBM # 672[1]), to obtain the Gibbs free energy of formation for $MoO_2(OH)_2(g)$:

$$Mo(s) + 2O_2(g) + H_2(g) = MoO_2(OH)_2(g) \qquad (4.27)$$

$$\Delta G^\circ_f = -206{,}493.69 - 1.6720\, T \,\mathrm{Ln}\, T - 1.782 \times 10^{-3}\, T^2$$
$$+ 1.6465 \times 10^5 / T + 66.925\, T \quad \text{(cal/mole)}$$

$$\Delta G^\circ_f = -863{,}969.59 - 6.9956\, T \,\mathrm{Ln}\, T - 7.456 \times 10^{-3}\, T^2$$
$$+ 6.8890 \times 10^5 / T + 280.014\, T \quad \text{(J/mole)}$$

4.3.2.2 Discussion of Results. A comparison of the results of the present investigation with the work of other researchers is presented in Figure 4.17. For the construction of this figure, the work of Belton and Jordan, who conducted their experiments with Mo metal, was recalculated (using USBM data) to $MoO_3(l)$ to facilitate the comparison. When the work of the present investigation was extrapolated, using equation (4.26), to the temperature range of Belton and Jordan, an excellent agreement between the two works was obtained. The work of Glemser and Haeseler, on the other hand, followed a lower path with a different slope. The differences of the present work with that of Glemser and Haeseler were attributed, in part, to the differences in the measured vapor pressure of $Mo_3O_9(g)$.

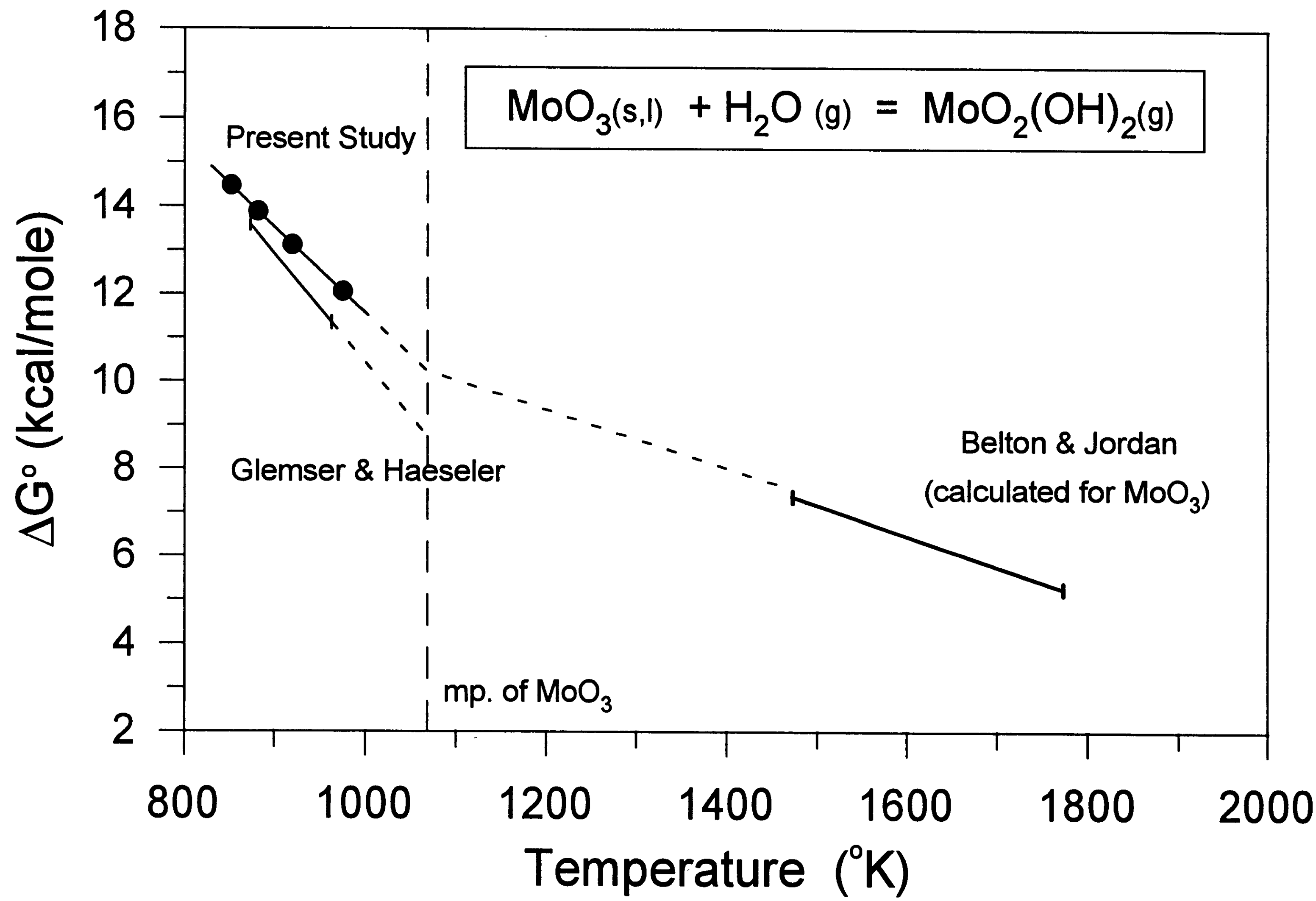

Figure 4.17 Comparison of the Gibbs free energy for reaction obtained in the present study with these others investigators.

It is worth noting, that the agreement between Belton and Jordan's work and the present work, further corroborates the accuracy of the sublimation measurements conducted in the present investigation.

Given the above discussion, it was believed that with the results of the present study, the discrepancies in the vapor chemistry of $MoO_3(s)$ in the absence and presence of water vapor, have been finally resolved .

4.3.3 Industrial Applications of the Generated Knowledge

The results of the present investigation can be used to determine process conditions for the extraction of molybdenum, from molybdenum containing waste. Table 4.8 shows the calculated vapor pressures of both Mo_3O_9 and $MoO_2(OH)_2$ under different process conditions.

It is clear, from Table 4.8, that the vapor pressures at temperatures below 700 °C, are not significant from an industrial stand point, even at high water pressures. At temperatures close to the melting point (795 °C), however, and with water vapor pressures of 1 atm, the total apparent vapor pressure (7.4 Torr) becomes more attractive for industrial application. Moreover, this pressure can be increased by augmenting the pressure of the water vapor. As shown in Table 4.8, for the case of P_{H2O} = 5 atm, the apparent vapor pressures increases to 24.76 Torrs.

In the case of the process conditions above liquid MoO_3, it can be appreciated that the calculated vapor pressures at 900 °C, are significantly higher than those at temperatures just slightly below the melting point. Furthermore, it is important to note

Table 4.8 Calculated Vapor Pressures of Mo_3O_9 and $Mo_2(OH)_2$ Above $MoO_3(s,l)$ Under Different Process Conditions

Temp (°C)	P_{H2O} (atm)	P_{Mo3O9} (Torr)	$P_{MoO2(OH)2}$ (Torr)	$P_{apparent}$ (Torr)
600	0.5	6.5×10^{-4}	0.12	0.12
	1.0	6.5×10^{-4}	0.23	0.23
	5.0	6.5×10^{-4}	1.15	1.15
700	0.5	0.09	0.73	0.82
	1.0	0.09	1.46	1.55
	5.0	0.09	7.29	7.38
780	0.5	2.46	2.48	4.94
	1.0	2.46	4.95	7.41
	5.0	2.46	24.76	27.23
900	0.5	87.80	6.84	94.64
	1.0	87.80	13.68	101.48
	5.0	87.80	68.40	156.20

that at these high temperatures most of the vapor transport is attributed to $Mo_3O_9(g)$. This suggests that, above the melting point, the formation of volatile hydroxides plays a minor role in the extraction of MoO_3, unless water vapor pressures higher than 1 atmosphere are employed.

An economic evaluation would have to be conducted to determine the cost benefit of operating above or below the melting point of MoO_3. From a practical stand point, in the view of the author, it is probably preferable to work with the solid phase at water pressures of 1 atm. At these conditions, not only would the energy requirements be reduced but the handling of the materials greatly simplified. Moreover, in the liquid phase, the effects of other liquid impurities on the activity of MoO_3 would have to be considered to accurately predict the volatilization behavior.

Thus the conditions recommended for the extraction of molybdenum from feestocks and wastes are:

$$T = 780\ ^\circ C$$

$$P_{H2O} = 1\ atm$$

The temperature of 780 °C is 15 °C below the melting point. This value was selected in order to prevent the melting of the condensed phase due to the temperature variations in the reaction chamber. The pressure of 1 atm was chosen because it would not require a special pressurized reactor and thus facilitate the design of a continuous process. Again, thorough economic evaluation would be required to assess the economical feasibility of operating at higher pressures.

It is important to note that the results of this investigation not only suggest the technical feasibility of a recovery process for waste materials. But also suggests that if molybdenum trioxide based materials, such as catalysts, were used in the presence of water vapor, losses to the vapor phase would occur. The magnitude of these losses would depend on the temperature and water pressures inside the reactor. In order to minimize these losses, it is recommended that the working temperature not exceed 500 °C. At this temperature and with a water vapor pressure of 1 atm, the volatilization of MoO_3 is 0.02 Torr.

4.4 Tungsten Trioxide

4.4.1 Baseline Vapor Pressures of $WO_3(s)$

No volatilization was detected in the experiments conducted in the absence of water vapor. A summary of the experimental conditions, after conditioning the sample, are presented in Table 4.9.

Table 4.9 Experimental Conditions for the Baseline Experiments Above $WO_3(s)$

Condensed Phase	Amb. Press. (atm)	Amb. Temp (°C)	Boats Temp (°C)	P_{O2} (atm)	Run Time (hrs)	Wt. Change (gm)
$WO_3(s)$	0.82	22	902	0.26	14.5	+0.00002

It is clear from Table 4.9 that no appreciable weight loss occurred in a run of 14.5 hrs. Moreover, no evidence of vapor transport of tungsten was found in the condenser system. These results corroborate the data reported in the literature that the contribution of volatile oxides to the total vapor pressure is insignificant. As in the case of the studies on $V_2O_5(s)$, this null contribution allowed for the direct measurements of the volatile hydroxides from the measured vapor pressures.

4.4.2 Measurements on $WO_3(s)$ in the Presence of Water Vapor

It was found in the literature, that $WO_3(s)$ reacts with water according to the reaction:

$$WO_3(s) + H_2O(g) = Wo_2(OH)_2(g) \qquad (4.29)$$

As in the case of molybdenum trioxide, although the different investigators mentioned in the literature agreed on the molecularity of the species, they did not agree in the vapor pressures of the volatile hydroxides formed. Again, a thorough investigation on this system was undertaken to resolve these discrepancies.

If the equilibrium constant for the above reaction were linearized and graphed, in a similar fashion as in the case of $MoO_2(OH)_2(g)$, the Log $P_{WO2(OH)2}$ would be a linear function of Log P_{H2O} with a theoretical slope of 1. A plot of Log $P_{WO2(OH)2}$ vs. Log P_{H2O} was constructed at two different O_2 potentials (see Figure 4.18). From this figure, it was determined that the experimental slope of 1.05 agreed extremely well with the theoretical slope of 1. Also, it was appreciated that, as expected, there was no dependence on the O_2 potential.

In Figures 4.19 and 4.20, the attainment of equilibrium was demonstrated by showing the independence of the equilibrium constant from both the water pressure and the carrier gas flowrate. Also, these figures were utilized to obtain an average value of the equilibrium constant, at 902 °C, of 3.49 X 10^{-4}.

As in the case of the molybdenum studies, a check of the consistency of the data was obtained by plotting $P_{WO2(OH)2}$ vs. P_{H2O} and forcing the linear regression through zero (see Figure 4.21). Again, the slope should give the equilibrium constant for the reaction. From Figure 4.21, it was observed that the slope of 3.52 X 10^{-4} agreed very well with the average value of 3.49 x 10^{-4} obtained in Figures 4.19 and 4.20.

Once the molecularity of the volatile hydroxide had been established, measurements at different temperatures were conducted. A summary of the experimental results on the formation of $WO_2(OH)_2(g)$ is presented in Figure 4.22.

It can be seen that $WO_3(s)$ was studied in both the alpha and the beta regions. The free energy equations, obtained through separate linear regressions at each phase were:

$$Wo_3(\alpha,\beta) + H_2O(g) = WO_2(OH)_2(g)$$

$$\Delta G^\circ_\alpha = 39{,}733 - 18.00\ T \quad (\pm\ 239\ \text{cal/mol}) \tag{4.31}$$

$$\Delta G^\circ_\alpha - 166{,}243 - 75.31\ T \quad (\pm\ 1000\ \text{J/mole})$$

$$\Delta G^\circ_\beta = 40{,}162 - 18.40\ T \quad (\pm\ 315\ \text{cal/mol}) \tag{4.32}$$

$$\Delta G^\circ_\beta = 168{,}038 - 76.99\ T \quad (\pm\ 1318\ \text{J/mole})$$

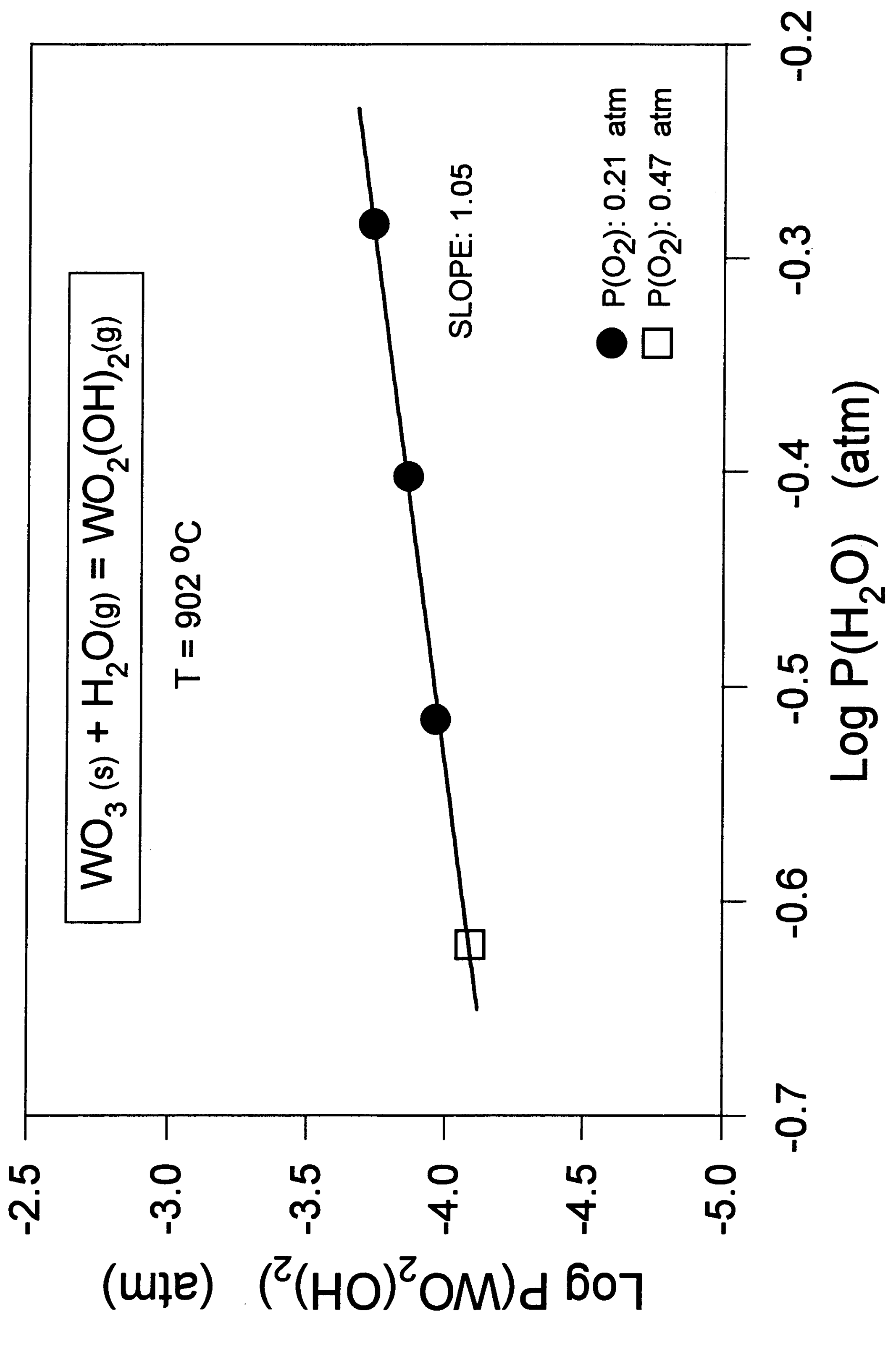

Figure 4.18 Vapor pressure of $WO_2(OH)_2$ as a function of water potential.

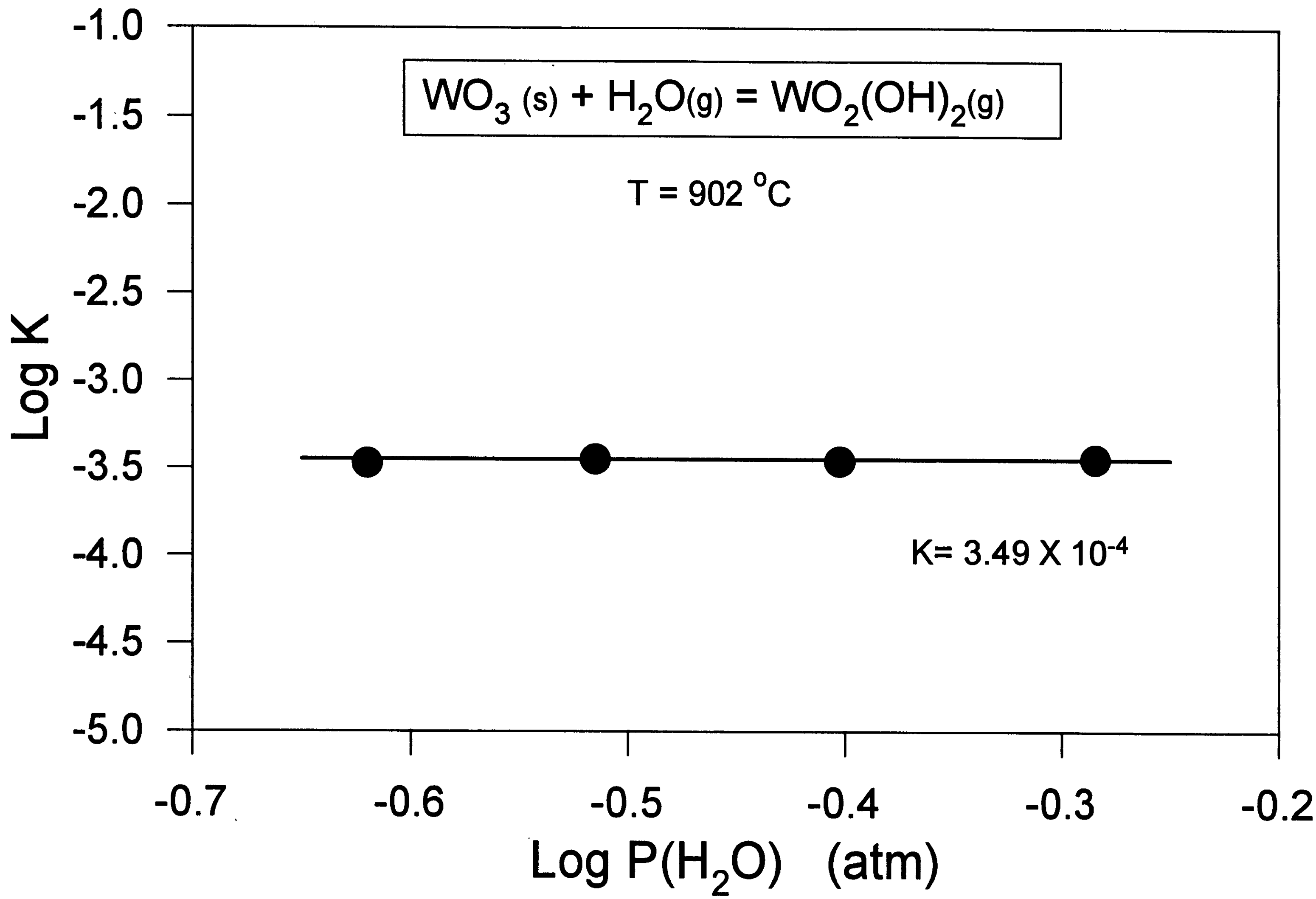

Figure 4.19 Equilibrium constant for the reaction (4.29) as a function of water potential.

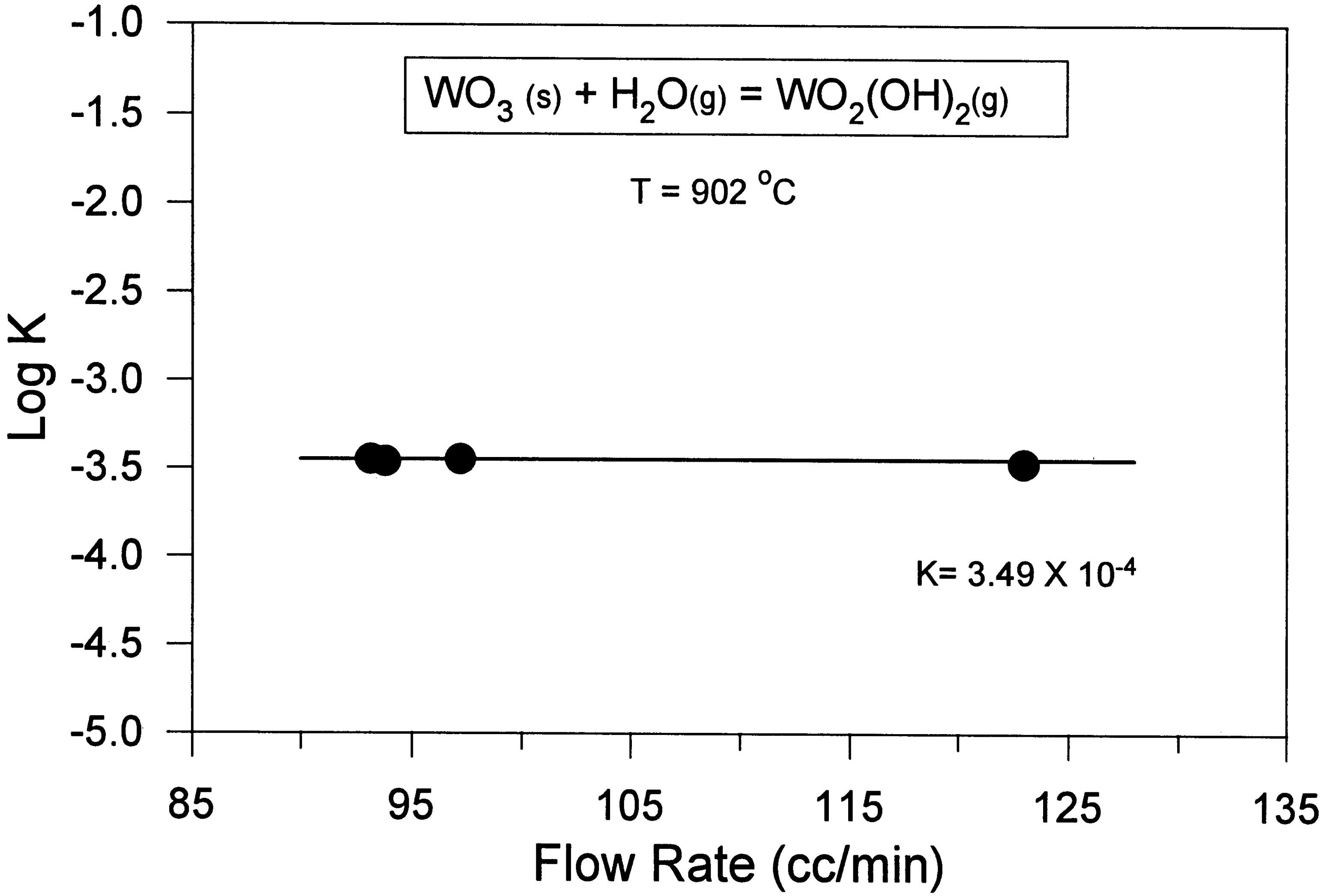

Figure 4.20 Equilibrium constant for the reaction (4.29) as a function of flow rate.

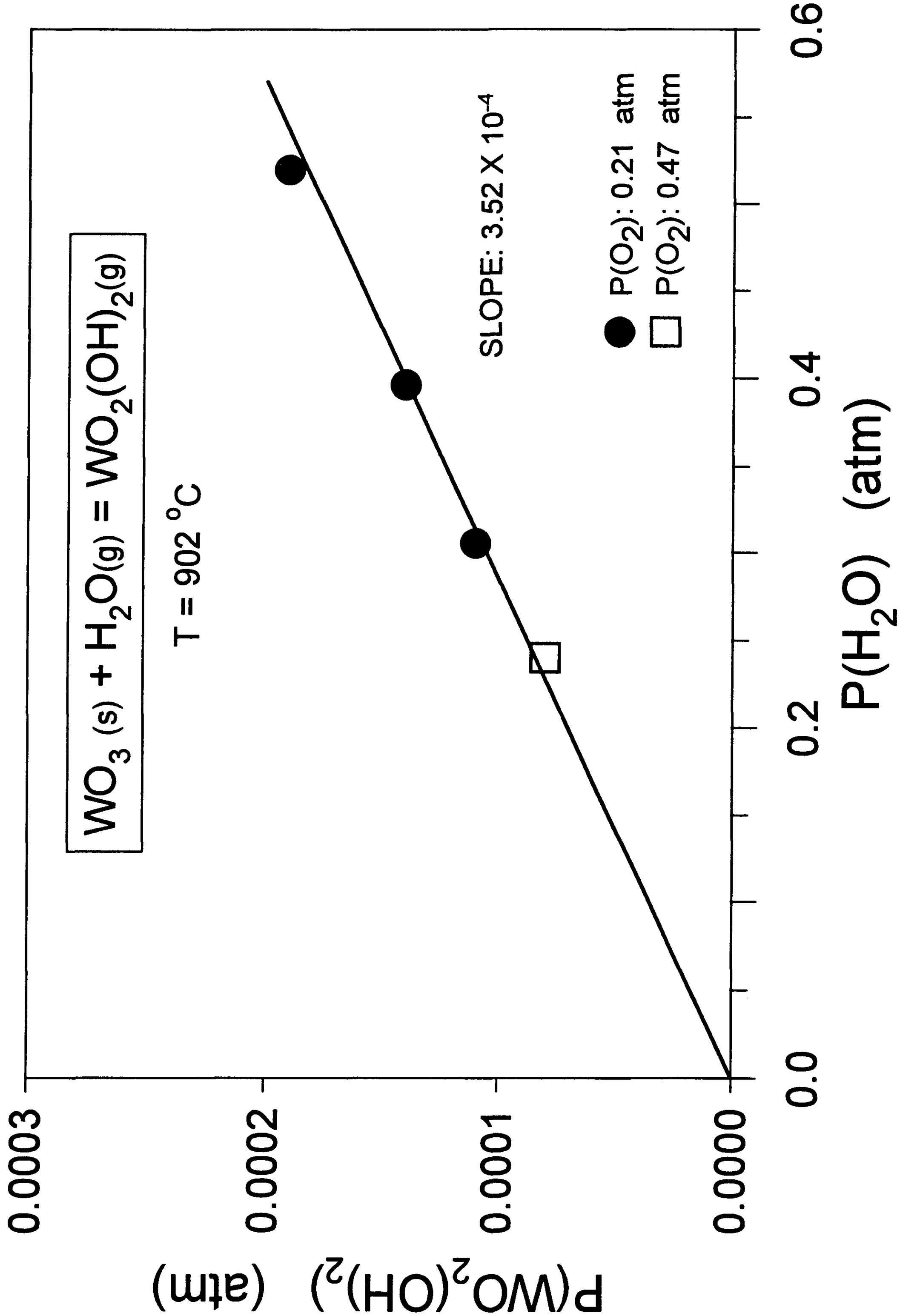

Figure 4.21 Partial pressure of $Wo_2(OH)_2$ as a function of water potential.

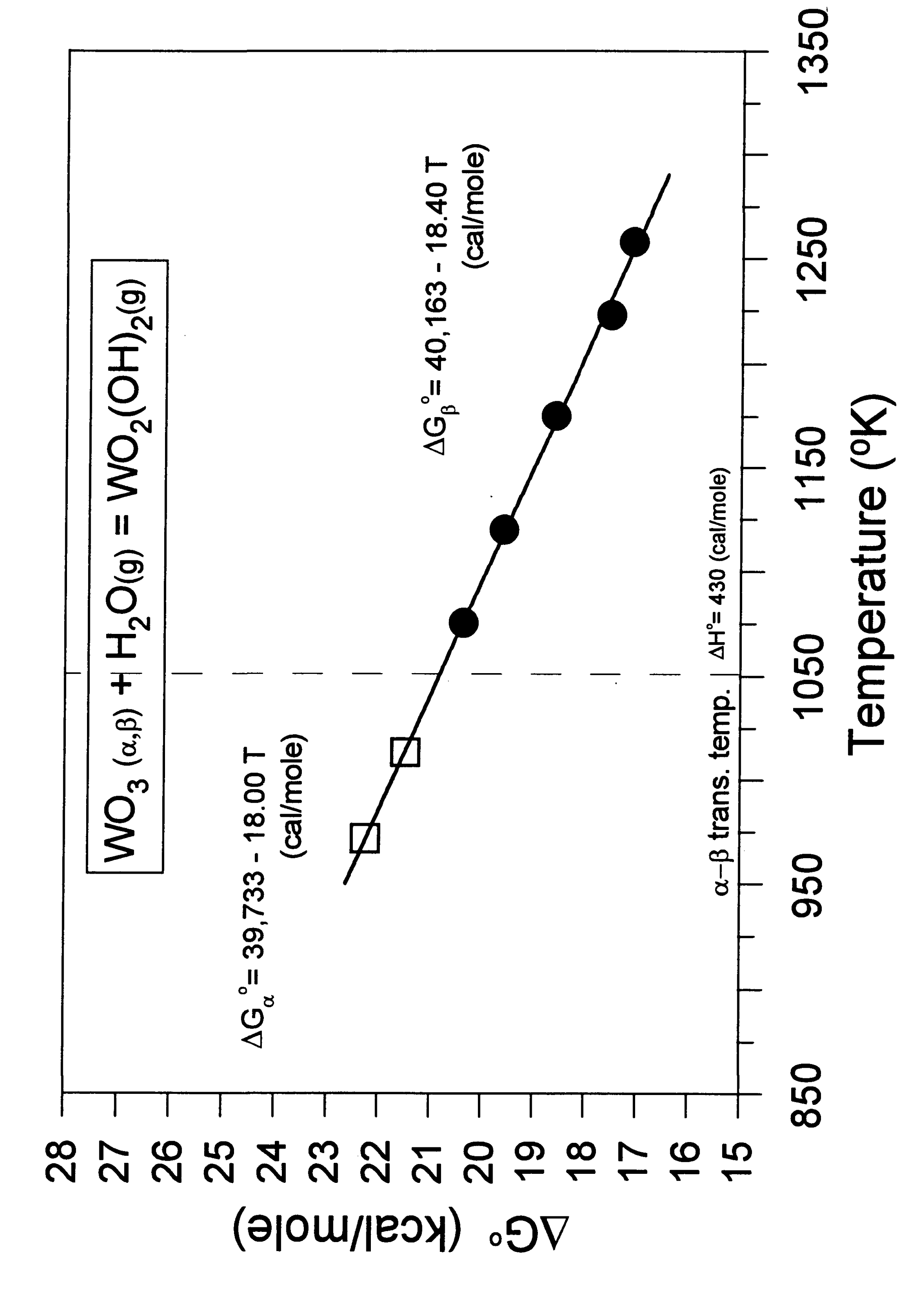

Figure 4.22 Gibbs free energy for reactions (4.31) and (4.32) as a function of temperature.

where the stated errors are the 95% confidence range of the regressions evaluated at the temperature where the error was the largest within the temperature ranges studied.

As in the cases of $V_2O_5(s)$ and $MoO_3(s)$ studies, the ΔC_p^o's for these reactions were considered equal to zero because C_p^o values for $WO_2(OH)_2(g)$ were not available.

It is important to note that although measurements at only two temperatures in the alpha phase were conducted, a third point, at the transition temperature, was calculated using the equation for the beta phase. Using these three points, the regression in the alpha phase was obtained. Although it is true that measurements at only two temperatures cannot describe the trends in the alpha phase from a statistical point of view, the accuracy of the measurements was evaluated by subtracting the ΔH^o obtained in the alpha phase from the ΔH^o in the beta phase. The difference should give the ΔH^o of transition for $WO_3(s)$. The obtained experimental value for the ΔH^o of transition was 430 cal/mole. This value agreed very well with the value reported in the literature[1] of 410 cal/mole, thus validating the accuracy of the measurements.

Equation (4.32) was combined with the Gibbs free energy of formation of WO_3 (β) reported in USBM # 672[1] to obtain the free energy of formation of $WO_2(OH)_2$:

$$W(\beta) + 2O_2(g) + H_2(g) = Wo_2(OH)_2(g) \tag{4.33}$$

$$\Delta G^o_f = -220{,}120 - 1.755\ T\ \mathrm{Ln}\ T - 0.812 \times 10^{-3}\ T^2 + 1.617 \times 10^5 / T + 69.060\ T \quad \text{(cal/mole)} \tag{4.34}$$

$$\Delta G^o_f = -920{,}982 - 7.343\ T\ \mathrm{Ln}\ T - 3.397 \times 10^{-3}\ T^2 + 6.766 \times 10^5 / T + 288.947\ T \quad \text{(cal/mole)}$$

Equation (4.32) was used for the above derivation because, since more measurements were conducted with $WO_3(\beta)$, this equation was more accurate.

4.4.3 Discussion of the Results

A comparison of the results of this investigation with the work of other investigators is presented in Figure 4.23. As in the case of the molybdenum studies, the work of Belton and McCarron, who worked with W metal as the condensed phase, was recalculated to $WO_3(s)$ using data from USBM bulletin # 672.

When the present work was extrapolated to the temperature range of the other investigators, it was observed that the obtained free energy equation fell between the two energy equations reported by Glemser. Also, when the present work was further extrapolated to the recalculated values of Belton and McCarron, there was a difference of 721 cal/mole at 1500 °K which was within the experimental and extrapolating error mentioned by Belton and McCarron.

Given the analysis of the results presented above, especially the excellent agreement of the obtained $\Delta H°$ of transition with that reported in the literature, it was believed that the discrepancies in the vapor chemistry of $WO_3(s)$ in the presence of water vapor were finally resolved.

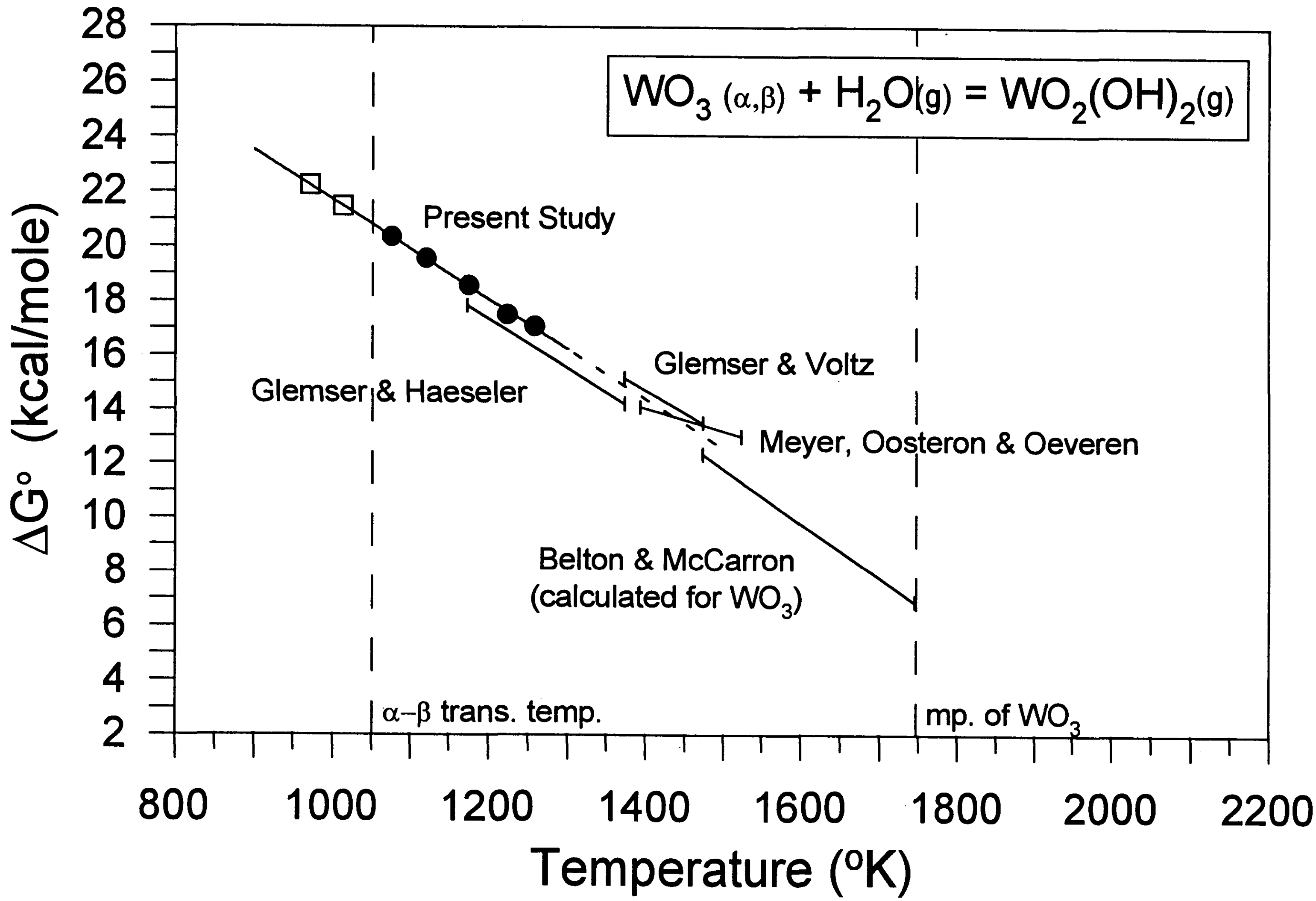

Figure 4.23 Comparison of the Gibbs free energy of the reactions obtained in the present investigation with those of the other investigators.

4.4.4 Industrial Applications of the Generated Knowledge

The results of the present investigation were used to determine process conditions for the extraction of tungsten from tungsten containing wastes. Table 4.10 shows the calculated vapor pressures for $WO_2(OH)_2$ under different processing conditions.

It can be concluded from Table 4.10, that the extraction of WO_3 by vapor transport, through the formation of volatile hydroxides, is not viable at temperatures below 1100 °C and for water vapor pressures of 1 atm . More significant extractions, however are realized at higher temperatures. At 1200 °C and 1 atm of water vapor for example, the vapor pressure of the volatile hydroxide is almost 9 Torr. This pressure increases linearly with water pressure by a factor of one. Significantly higher vapor pressures are obtained if the operating temperature is increased to 1300 °C. At this temperature and a water potential of 1 atm, the vapor pressure of the volatile hydroxide is 21 Torr. Again, the pressure increases linearly with the pressure of water by a factor of one.

Similar to the case of the extraction of molybdenum, a thorough cost-benefit analysis must be conducted in order to assess the optimal operating conditions for the recovery of tungsten by vapor transport. It is the preference of the author, however, to work under atmospheric pressures to facilitate the design of a continuous process.

In order to minimize losses of $WO_3(s)$ containing materials, such as catalysts, it is recommended to operate at temperature below 700 °C. At this temperature and at a water vapor pressures of 1 atm, the vapor pressure of the volatile hydroxide is 0.01 Torr.

Table 4.10 Calculated Vapor Pressures for $WO_2(OH)_2$ Above $WO_3(\alpha,\beta)$ Under Different Process Conditions

Temperature °C	P_{H2O} (atm)	$P_{WO2(OH)2}$ (Torr)
900	0.5	0.13
	1	0.26
	5	1.31
	10	2.63
1100	0.5	1.62
	1	3.23
	5	16.17
	10	32.33
1200	0.5	4.39
	1	8.78
	5	43.91
	10	87.82
1300	0.5	10.50
	1	21.01
	5	105.03
	10	210.07

4.5 Mass Closures and X-Ray Analysis

As mentioned in the section of the data analysis, the vapor pressures can be calculated based on the weight loss or on the moles of material transported to the condenser system.

In the present investigation, excellent agreement between the weight loss and the moles reported at the condenser was obtained in the vanadium pentoxide and molybdenum trioxide experiments. In these cases the mass closures were between 95 to 105%; thus demonstrating that within the experimental error, either method could be used to calculate the resulting vapor pressures. In the case of the studies of tungsten trioxide, however, the recovery was only good up to 93%. This was probably due to the difficulty in dissolving the transported material. The condenser tubes had to be stripped with a warm solution of NaOH 1N for at least 12 hours until no visible left material was observed. Increasing the temperature to accelerate the dissolution did not seem to improve the dissolution rate significantly. Moreover, the handling of the condenser sheath was more involved due to the necessity of keeping it hot. It is believed that the recoveries were not complete, mainly for the inability of properly dissolving the sample, rather than experimental errors in weighing or analyzing the samples.

A summary of the stripping conditions for $V_2O_5(s)$, $V_2O_3(s)$, $MoO_3(s)$, and $WO_3(s)$ is presented in Table 4.11.

Another important consideration in the transpiration technique is the integrity of the condensed phase. The x-ray diffraction patterns taken before and after the

Table 4.11 Summary of the Stripping Conditions for $V_2O_5(s)$, $V_2O_3(s)$, $MoO_3(s)$, and WO_3.

Sample	Stripping Solutions		Recoveries
$V_2O_5(s)$	H_2SO_4	1.8 N	95 - 105%
$V_2O_3(s)$	HNO_3	conc.	no vanadium was detected
$MoO_3(s)$	NaOH	1 N	95 - 105%
$WO_3(s)$	NaOH	1 N	81 - 93%

experiments indicated that no phase change of the condensed sample had occurred. Thus, no weight losses could be attributed to disproportionation (reduction) of the sample.

Based on the good mass closures obtained and the fact that the integrity of the condensed phases was maintained throughout the experiments, it was concluded that the experimental technique employed was reliable in measuring the vapor pressures of the volatile hydroxides in equilibrium with $V_2O_5(s)$, $MoO_3(s)$, and $WO_3(s)$.

V. SUMMARY AND CONCLUSIONS

5.1 Vanadium Pentoxide

The results of the present investigation confirmed the formation of volatile hydroxide of vanadium above $V_2O_5(s)$ in the presence of water vapor. The molecularity of the species was determined to be $VO(OH)_3(g)$, according to:

$$V_2O_5(s) + 3H_2O(g) = 2VO(OH)_3(g)$$

$$\Delta G^\circ = 57{,}938 - 14.46\ T \quad (\pm\ 328\ \text{cal/mol})$$

$$\Delta G^\circ = 242{,}413 - 60.50\ T \quad (\pm\ 1004\ \text{J/mole})$$

Combining the ΔG° of fusion reported in USBM bulletin # 672 with this equation, the Gibbs free energy equation, considering liquid vanadium pentoxide as the standard state, was calculated:

$$V_2O_5(l) + 3H_2O(g) = 2VO(OH)_3(g)$$

$$\Delta G^\circ = 48{,}482 + 11.435\,T\ln T - 0.004844T^2 + \frac{286{,}850}{T} - 78.625\ T \quad (\text{cal/mole})$$

The equation for the Gibbs free energy change considering solid vanadium pentoxide obtained in the present study was also combined with the Gibbs free energies of formation for both $H_2O(g)$ and $V_2O_5(s)$ to obtain the expression for the $\Delta G°$ of

$$V(s) + \frac{3}{2}H_2(g) + 2O_2(g) = VO(OH)_3(g)$$

formation of the established volatile hydroxide:

$$\Delta G°_f = -243{,}300.50 + 1.88\,T\ln T - 0.001838T^2 + \frac{100{,}450}{T} + 50.911\,T \quad \text{(cal/mole)}$$

$$\Delta G°_f = -1{,}018{,}655.2 + 7.866\,T\,\mathrm{Ln}\,T - 0.007790\,T^2 + 420{,}283\,/\,T + 213.011\,T \quad \text{(J/mole)}$$

For the investigated temperature range the vapor pressures were determined to be too low for commercial extractive applications. However, at higher temperatures (1250 °C) and under pressurized conditions (5 atm of H_2O), significnat vapor transport is achieved through the formation of volatile hydroxides.

Finally, another important finding, concerning industrial applications, was the fact that the vanadium hydroxide formed in equilibrium with $V_2O_5(s)$ significantly attacks silica and, to a lesser extent, alumina. So, if these materials are used, as catalysts for example, in the presence of vanadium and water vapor, the hydroxide formed will deteriorate the silica substrate; reducing the service life of the catalyst. Thus, silica substrates are not recommended when V_2O_5 and water vapor are both expected to be present in a given catalytic process.

5.2 Vanadium Trioxide

In the present investigation no evidence of enhanced volatility of $V_2O_3(s)$ in the presence of water vapor was observed. Thus it was concluded that $V_2O_3(s)$ does not form volatile hydroxides detectable with the transpiration technique in the temperature range of 600 to 950 °C at atmospheric pressures.

5.3 Molybdenum Trioxide

The results of the present investigation confirm the high volatility of $MoO_3(s)$. This volatilization was primarily attributed to the formation of the polymeric species $Mo_3O_9(g)$ according to:

$$3MoO_3(s) = Mo_3O_9(g)$$

$$\Delta G^\circ = 83{,}684 - 68.07\ T \quad (\pm\ 673\ \text{cal/mol})$$

$$\Delta G^\circ = 350{,}134 - 284.80\ T \quad (\pm\ 2117\ \text{J/mole})$$

Combining the above equation with the ΔG° of fusion, derived from the $C_p{}^\circ$ values for $MoO_3(s)$ and $MoO_3(l)$ reported by Cosgrove and Snyder[57], the Gibbs free energy equation, considering liquid molybdenum trioxide as the standard state, was calculated:

$$3MoO_3(l) = Mo_3O_9(g)$$

$$\Delta G^\circ = -49{,}183.28 + 1586.615\,T + 0.14484\,T^2 - 1.16667\text{x}10^{-5}T^3$$

$$+\ 5.52 \times 10^5 / T - 239.784\ T \ln T \quad (\text{cal/mole})$$

Finally, the Gibbs free energy of formation of the established hydroxide was established using the $C_p°$ data for $MoO_3(s)$ reported by Cosgrove and Snyder, and the $C_p°$ data for O_2 and Mo(s) reported in USBM bulletin # 672:

$$3M(s) + \frac{9}{2}O_2 = Mo_3O_9(g)$$

$$\Delta G°_f = -488{,}778.07 + 14.544\,T\ln T - 3.033\times10^{-3}T^2 + 5.391\times10^5 / T + 222.549\,T \quad \text{(cal/mole)}$$

$$\Delta G°_f = -2{,}045{,}047.4 + 60.852\,T\,\mathrm{Ln}\,T - 12.690\times10^{-3}\,T^2 + 22.556\times10^5 / T + 931{,}145\,T \quad \text{(J/mole)}$$

The results of the present study also confirmed the formation of volatile hydroxides above $MoO_3(s)$. The molecularity of the species was determined to be $MoO_2(OH)_2(g)$ according to:

$$MoO_3(s) + H_2O(g) = MoO_2(OH)_2(g)$$

$$\Delta G° = 31{,}143 - 19.57\,T \quad (\pm\ 61 \text{ cal/mol})$$

$$\Delta G° = 130{,}302 - 81.88\,T \quad (\pm\ 167 \text{ J/mole})$$

Combining the above equation with the $\Delta G°$ of fusion based on the work of Cosgrove and Snyder[57], the Gibbs free energy, considering liquid MoO_3 as the standard state, was calculated:

$$MoO_3(l) + H_2O(g) = MoO_2(OH)_2(g)$$

$$\Delta G^\circ = -101{,}724.28 + 1635.11\,T + 0.14484\,T^2 - 1.16667\text{x}10^{-5}T^3$$
$$+ 5.52 \text{ x } 10^5 / T - 239.784\, T \ln T \quad \text{(cal/mole)}$$

In a similar fashion as in the case of the free energy of formation of $Mo_3O_9(g)$, the free energy of formation of $MoO_2(OH)_2(g)$ was calculated to be:

$$\Delta G^\circ_f = -206{,}493.69 - 1.6720\, T \ln T - 1.782\text{x}10^{-3}T^2$$
$$+ 1.6465 \text{ x } 10^5 / T + 66.925\, T \quad \text{(cal/mole)}$$

$$\Delta G^\circ_f = -863{,}969.59 - 6.9956\, T \text{ Ln } T - 7.456 \text{ x } 10^{-3}\, T^2$$
$$+ 6.8890 \text{ x } 10^5 / T + 280.014\, T \quad \text{(J/mole)}$$

It was determined that extraction processes, based on the formation of volatile hydroxides of molybdenum, are important at temperature below the melting point. Specifically around 780 °C. The recommended conditions for the extraction of molybdenum in the presence of water vapor were:

T = 780 °C

P_{H2O} = 1 atm

$P_{MoO2(OH)2}$ = 7.41 Torr

Higher vapor pressures could be obtained by increasing the water pressure.

At temperatures above the melting point, the vapor pressure of $Mo_3O_9(g)$ is significantly higher than that of $MoO_2(OH)_2$. Thus the role of volatilization enhancement with water vapor is less important at these temperatures.

Finally, in order to minimize losses of molybdenum trioxide based materials in the presence of water vapor, it was recommended that the temperature did not exceed 500 °C. At this temperature, and at a water vapor pressure of 1 atm, the total apparent vapor pressure is 0.02 Torr.

5.4 Tungsten Trioxide

The results of the present investigation also confirmed the formation of volatile hydroxides above $WO_3(s)$. The molecularity of the species was determined to be $WO_2(OH)_2(g)$ according to:

$$WO_3(\alpha,\beta) + H_2O(g) = WO_2(OH)_2(g)$$

$$\Delta G^\circ_\alpha = 39{,}733 - 18.00\ T \quad (\pm\ 321\ \text{cal/mol})$$

$$\Delta G^\circ_\alpha = 166{,}243 - 75.31\ T \quad (\pm\ 1000\ \text{J/mole})$$

$$\Delta G^\circ_\beta = 40{,}163 - 18.40\ T \quad (\pm\ 400\ \text{cal/mol})$$

$$\Delta G^\circ_\beta = 168{,}038 - 76.99\ T \quad (\pm\ 1318\ \text{J/mole})$$

The calculated $\Delta H^\circ_{\alpha\text{-}\beta}$ was 430 cal/mole which was in excellent agreement with the value reported in the literature of 410 cal/mole.

The calculated Gibbs free energy of formation for $WO_2(OH)_2$, using the Gibbs free energy equation for the β phase and the Gibbs free energy of formation for $WO_3(\beta)$ reported in USBM bulletin # 672 was:

$$W(\beta) + 2O_2(g) + H_2(g) = WO_2(OH)_2(g)$$

$$\Delta G^\circ_f = -220{,}120 - 1.755\,T\ln T + 0.812\times10^{-3}T^2 + 1.617 \times 10^5 / T + 69.060\,T \quad \text{(cal/mole)}$$

$$\Delta G^\circ_f = -920{,}982 - 7.343\,T\,\mathrm{Ln}\,T - 3.397 \times 10^{-3}\,T^2 + 6.766 \times 10^5 / T + 288.947\,T \quad \text{(J/mole)}$$

It was determined that viable extraction processes, based on the formation of volatile hydroxides, are attractive for industrial applications at temperatures at least at 1150 °C and at water vapor pressures of 1 atm.

Finally, in order to minimize losses of tungsten trioxide based materials in the presence of water vapor, it was recommended that operating temperatures did not exceed 700 °C. At this temperature and a water pressure of 1 atm, the vapor pressure of the volatile hydroxide is 0.01 Torr.

REFERENCES CITED

1. L. B. Pankratz, "Thermodynamic Properties of Elements and Oxides", U.S. Bureau of Mines Bulletin 672, (1982), 454-460.

2. M. W. Chase et al., "JANAF Thermochemical Tables, 1975 Supplement", J. Phys. and Chem., Ref. Data, 10, (1975), 1-175.

3. T. Matsui and K. Naito, "Thermodynamic Properties of the Phases in the V-O and Nb-O Systems at High Temperatures", Netsu Sokutei, 15(1), (1988), 21-41

4. R. E. Reed-Hill, Physical Metallurgy Principles, 2^{nd} Ed. , PWS Publishers, (1973), 327-328

5. R. Dziembaj, "Oxygen Equilibrium Pressure Above V_2O_{5-x} and Thermodynamic Properties of this Oxide System", J. Solid State Chemistry, 26, 1978, pp 159-165

6. J. Stringer, "The Vanadium-Oxygen System - A Review", Journal of Less Common Metals, 8, (1965), 1-14

7. R. Dziembaj and J. Piwowarczyk, "Oxygen Equilibrium Pressure Above V_2O_{5-x} Oxide System at 600 °C ($x < 0.43$)", Journal of Solid State Chemistry, 21, 1977, 387-392

8. Y. Polyakov, "Vapor Pressure of Liquid Vanadium Pentoxide", J. Phys. Chem. (USSR), 20, (1978), 1021-1024

9. J. Berkowitz, W.A. Chupka and M.G. Inghram, "Thermodynamics of the V-O system: Dissociation Energies of VO and VO_2", The Journal of Chemical Physics, 27, N. 1, (1957), 87-90

10. K.E. Frantseva and G.A. Semenov, "Mass-Spectrometer Study of the Evaporation of Certain Vanadium Oxides", Leningrad State University, translated from Teplofizika Vysokikh Temperatur, 7, N. 1, (1969), 55-61

11. M. Farber, M. Uy and R.D. Srivastava, "Effusion-Mass Spectrometric Determination of the Heats of Formation of the Gaseous Molecules V_4O_{10}, V_4O_8, VO_2 and VO", The Journal of Chemical Physics, 56, N. 11, (1972), 5312-5315

12. L. N. Yannopoulos, "The Thermodynamics of the Vanadium Pentoxide (Solid or Liquid)-Water Vapor System", The Journal of Physical Chemistry, 27, N. 9, (1968), 3293-3296.

13. G.A. Semenov, K.E. Frantseva and E.K. Shalkova, Reports of the University of Leningrad, 16, (1970), 82-86

14. H. Suito and D. R. Gaskell, "The Reaction of Water Vapor with Melts in the System VO_2-V_2O_5", Metal-Slag-Gas Reactions and Processes, Electrochemical Society Incorporated, (1975), 251-266, Princeton, N.J., P.O. Box 2071, Princeton, N.J., 08540.

15. O. Glemser and A. Muller, Z. Anorg. Allgem. Chem. , 325, (1963), 220-22

16. M. Taniguchi and M. Ooue, 23rd Annual Conf. of the Chem. Soc. of Japan (1970), Reprint 2, 1112.

17. G. H. Chambers, "Process of Extracting Vanadium", U.S. Patent 3,607,005, 1971.

18. T.P. McNulty: Letter of October 4, 1988 to J.P. Hager, Hazen Research Incorporated (copy attached)

19. Kirk and Othomer, Encyclopedia of Chemical Technology, 3rd Ed., John Wiley and Sons Inc., 23, (1983), 673-703

20. M. Wakihara and T. Katsura, "Thermodynamic Properties of V_2O_3-V_4O_7 System at Temperatures from 1400 to 1700 °K", Metallurgical Transactions, 1, (1970), 363-366

21. J.S. Anderson and A.S. Khan, "Phase Equilibria in the Vanadium-Oxygen System", Journal of Less Common Metals, 22, (1970), 209-218

22. S. Killingbeck, Ph.D. Thesis, University of Kansas (1964)

23. Kirk and Othomer, Encyclopedia of Chemical Technology, 3rd Ed., John Wiley and Sons Inc., 15, (1983), 684.

24. A. Magnéli, Acta Chem. Scand. 2, (1948), 501

25. Ibid, 861

26. L. Kihlborg, "The Crystal Chemistry of Molybdenum Oxides", Advances in Chemistry Series 39, American Chemical Society, (1963), 37

27. L. Kihlborg, Acta Chem. Scand. 13, (1959), 954

28. L.L. Chang and B. Phillips, J. Amer. Chem. Soc. 52, (1969), 527

29. B. Phillips and L.L. Chang, AIME 233, (1965), 1433

30. Binary Alloy Phase Diagrams, edited by T.B. Massalski, H. Okamoto, P.R. Subramanian, and L. Kacprzak, ASM International, 1990

31. O. Glemser, and R. Haeseler, Z. Anorg. Allgem. Chem., 316, (1962), 168-181

32. J. Feiser Metall u. Erz, 29, (1931), 297

33. J. Berkowitz, M.G Inghram and W.A. Chupka, "Polymeric Gaseous Species in the Sublimation of Molybdenum Trioxide", The Journal of Chemical Physics, 26, N.4, (1957), 842-846

34. Y. Ikeda, H. Ito, T. Mizuno, K. Amioka, G. Matsumoto, "Sublimation Behavior of Molybdenum Oxides", High Temperature Science, 16, (1983), 1-22

35. E.K. Kazenas and U.V. Tsuvetkov, Zh. Neorg. Khim., 14, (1969), 11

36. L.A. Aleshko-Ozhevskaya, M.K. Ilin, A.V. Makarov, O.T. Nikitin, Vestn. Mosk. Univ. Ser. 2, Khim., 19, (1978), 681

37. P.E. Blackburn, M. Hoch and H.L. Johnston, "The Vaporization of Molybdenum and Tungsten Oxides", The Journal of Physical Chemistry, 62, N.7, (1958), 769-773

38. K. Ueno, J. Chem. Soc. Japan, 62, (1941), 990

39. E.A. Gulbransen, K.F. Andrew and F.A. Brassart, "Vapor Pressure of Molybdenum Trioxide", Journal of the Electrochemical Society, 3, (1963), 242-243

40. R. Horbe, O. Knacke and K.E. Prescher, Metall u. Erz., 14, (1961), 232

41. A.N. Selikman, N.N. Gorowitsch and T.J. Prosenkowa, Z. Anorg. Chem., USSR, 1, (1956), 632

42. R.J. Ackermann, R.J. Thorn, C. Alexander, M. Tetenbaum, "Free Energies of Formation of Gaseous Uranium, Molybdenum and Tungsten Trioxides", J. Physic. Chem., 64, (1960), 350-355

43. S.M. Ariya, S.A. Schukarev u., V.B. Glushkova, Zhur. Obshchei Khim., 23, (1953), 2063

44. L. Brewer and G.R.B. Elliot, U.C.R.L., report 1831, (1952)

45. T. Millner and J. Neugebauer, Nature, 163, (1949), 601

46. H.G. Wendlant and O. Glemser, Angew. Chem., 75, (1963), 949

47. G.R. Belton and A.S. Jordan, "The Volatilization of Molybdenum in the Presence of Water Vapor, The Journal of Physical Chemistry, 69, N.6, (1965), 2065-2071

48. B. Phillips, L.L.Y. Chang and M.G. Scroger, Tech. Doc. Rept. No. ML-TDR-64-230, Part I, Contract N. AF 33(657)-11235, Tem-Pres Research, Inc., State College, Pa., (1964)

49. L. Grossweiner and R.L. Seifert, U.S. Atomic Energy Commission Unclassified Paper AECU-1573

50. O. Glemser u. H.G. Volz, Naturwiss. 43, (1956), 33

51. G. Meyer, J.F. Oosterom u. and W.J. Van Oeveren, Rec. Trav. Chim. Pays-Bas 78, (1959), 417

52. G.R. Belton, R.L. McCarron, "The Volatilization of Tungsten in the Presence of Water Vapor", The Journal of Physical Chemistry, 68, N.7, (1964), 1852-1856

53. "Selected Chemical Thermodynamic Properties", Series III, Vol. 1, National Bureau of Standard, Washington 25 D.C.

54. C.B. Alcock and G.W. Hooper, "Measurement of the Vapor Pressures at High Temperatures by the Transpiration Method", Physical Chemistry of Process Metallurgy, 7(1), ed. G.R. St. Pierre, (N.Y., NY: Interscience Publishers), (1959), 324-340

55. V. Annamalai, "A Thermodynamic Study of the Formation of Vapor Complexes in the System Mn-Fe-Cl", (M.S. Thesis, Colorado School of Mines, 194-203, (1972)

56. Lange's Handbook of Chemistry, 6th Edition, Handbook Publisher Inc., Sandusky, Ohio, 1946

57. L.A. Cosgrove and P.E. Snyder, J. Am. Chem. Soc., 75, (1953), 1227

APENDIX I

(SUMMARY OF EXPERIMENTAL CONDITIONS FOR $V_2O_5(S)$)

VANADIUM-OXYGEN-HYDROGEN SYSTEM (WT. LOSS)

RUN#	RUN#	(m/d/yr) DATE	(cm Hg) AMB.PRESS.	(Deg. C) AMB.TEMP.	(cm) REACTOR DH	(cm) O2 DH	(cm) AR DH	H2O SET	(Deg. C) BOAT TEMP.
16	16	07/12/91	62.82	23.50	0.10	25.28	23.28	0.03971	641.5
?17	?17	07/15/91	62.46	24.20	0.05	25.33	23.33	0.03731	640.8
&19	&19	07/24/91	62.73	21.88	0.38	31.11	28.86	0.04489	644.4
*20	*20	07/25/91	62.50	22.25	0.35	31.12	28.81	0.04490	644.4
*21	*21	09/16/91	62.60	20.87	0.40	27.73	25.50	0.04157	642.5
*22	*22	09/18/91	62.84	18.75	0.30	55.35	11.75	0.04426	644.3
*23	*23	09/18/91	62.59	19.50	0.24	43.33	20.25	0.04367	644.3
24	24	09/21/91	62.44	21.00	0.68	40.81	0.00	0.05550	644.5
*25	*25	09/22/91	62.66	19.00	0	49	0	0.05879	644.5
*28	*28	11/06/91	62.74	21.18	0.05	37.8	24.06	0.04413	644.5
*29	*29	11/27/91	61.67	20.50	2.69	63.63	31.31	0.04724	645.21
30	30	12/04/91	62.27	19.50	0.76	41.92	65.63	0.04738	645.5
*33	*33	02/08/92	61.76	20.00	1.43	41.87	65.83	0.04690	647.2
*34	*34	02/10/92	62.05	20.83	1.98	42.02	65.86	0.04942	646.4
*35	*35	02/13/92	61.40	20.33	0.92	63.79	28.92	0.04634	647.8
&36	&36	02/18/92	62.23	17.00	0.75	34.58	28.76	0.06374	645.8
*37	*37	02/21/92	62.07	21.25	-0.40	34.75	29.57	0.06565	645.8
&38	&38	02/26/92	62.66	20.17	-0.22	34.79	38.38	0.04059	645.8
*39	*39	03/13/92	62.35	20.00	-0.23	34.83	33.63	0.04706	645.8
*40	*40	03/18/92	61.76	19.98	-0.33	34.86	62.88	0.05545	645.7
*42	*42	03/26/92	61.94	20.15	-0.25	49.40	70.60	0.04242	645.7
*43	*43	03/30/92	62.39	20.50	-0.26	49.62	24.72	0.05881	645.7
*44	*44	04/09/92	61.78	20.76	-0.38	34.82	29.42	0.06807	604.9
*45	*45	04/13/92	62.18	21.42	-0.28	34.85	69.21	0.05221	605.3
&46	&46	04/16/92	61.79	21.11	-0.25	34.83	38.51	0.03806	605.3
*48	*48	04/20/92	61.80	22.17	-0.25	34.81	33.78	0.06408	605.3
*50	*50	06/08/92	62.37	21.00	-0.20	34.82	33.65	0.04435	605.3
&51	&51	06/10/92	62.37	23.28	-0.20	34.82	38.77	0.03913	605.3
*52	*52	06/11/92	62.46	22.00	-0.35	34.83	30.00	0.06741	605.3
*53	*53	06/15/92	61.64	22.32	-0.31	30.64	26.75	0.05834	605.3
*54	*54	06/19/92	62.49	24.38	-0.30	30.56	26.62	0.05781	560.4
*55	*55	06/22/92	62.53	23.00	-0.30	34.70	29.94	0.06429	560.4
*57?	*57?	06/29/92	61.86	21.83	-0.30	32.66	28.25	0.06003	561.3
*59	*59	07/03/92	62.39	23.00	-0.37	32.82	28.42	0.06475	561.3
60	60	07/06/92	62.39	26.58	-0.26	32.94	37.48	0.03525	561.3
*62	*62	07/16/92	62.39	26.54	-0.50	22.48	19.88	0.03978	561.3
*63	*63	07/22/92	62.48	26.48	-0.30	34.77	29.78	0.06543	561.3
*64	*64	07/24/92	62.59	27.82	-0.36	34.66	29.93	0.06676	561.3
*65	*65	07/27/92	62.66	28.37	-0.27	34.65	29.62	0.06771	561.3
&67	&67	08/03/92	62.54	27.63	-0.24	34.83	39.80	0.03915	561.3
68	68	08/06/92	62.55	29.25	-0.28	34.84	39.87	0.03720	561.3
69	69	08/10/92	62.87	26.88	-0.34	34.79	39.74	0.03948	561.0
*70	*70	08/25/92	62.73	21.68	-0.44	34.83	66.38	0.04748	561.0
*102	*102	06/07/93	61.59	22.16	-0.71	21.07	28.61	0.04819	625.2
*103	*103	06/14/93	62.37	27.00	-0.59	19.48	26.24	0.04501	625.2
*104	*104	06/16/93	62.30	25.13	-0.63	19.25	26.02	0.04059	625.2

VANADIUM-OXYGEN-HYDROGEN SYSTEM (WT. LOSS)

RUN#	(Deg. C) BOILER	(Deg. C) DEOX.FUNR.	(min) RUN TIME	(g) WT. LOSS	(atm) Pt	(cc/min) FO2	(cc/min) FAr	(cc/min) FH2O(v)	(cc/min) Tot.Flow
16	385	246	1297	0.00078	0.82668	27.20	37.81	64.95	129.97
?17	381	241	1300	0.00076	0.82189	27.25	37.89	61.53	126.67
&19	384	244	1448	0.00109	0.82577	33.55	46.47	73.11	153.13
*20	386	242	1403	0.00115	0.82272	33.56	46.40	73.49	153.44
*21	374	240	1448	0.00079	0.82408	29.86	41.26	67.61	138.73
*22	368	233	1446	0.00088	0.82714	59.92	19.91	71.20	151.03
*23	376	244	1470	0.00108	0.82379	46.84	33.11	70.72	150.67
24	375	20	1242	0.00120	0.82226	44.10	0.00	90.51	134.61
*25	393	20	1320	0.00149	0.82447	53.01	0.00	94.97	147.98
*28	377	231	1432	0.00110	0.82558	40.82	39.02	71.73	151.57
*29	390	18	1512	0.00123	0.81414	63.43	17.53	77.68	158.63
30	389	18	1507	0.00105	0.82010	40.97	38.89	77.07	156.93
*33	390	20	1446	0.00108	0.81406	40.92	39.01	76.99	156.92
*34	390	20	1564	0.00129	0.81843	41.07	39.03	80.93	161.03
*35	401	20	1448	0.00105	0.80881	63.59	16.04	76.65	156.28
&36	407	17	1434	0.00155	0.81957	33.38	15.94	102.87	152.19
*37	407	21	1450	0.00164	0.81631	33.55	16.44	107.93	157.93
&38	421	20	1547	0.00091	0.82426	33.60	61.25	65.85	160.70
*39	437	20	1685	0.00113	0.82017	33.64	53.88	76.68	164.20
*40	434	20	1450	0.00126	0.81230	33.67	37.17	91.22	162.06
*42	421	20	1464	0.00084	0.81475	48.71	41.98	69.61	160.30
*43	423	20	1527	0.00155	0.82066	48.94	13.42	95.93	158.29
*44	425	21	1428	0.00112	0.81252	33.63	16.35	112.25	162.22
*45	421	21	1494	0.00060	0.81787	33.66	41.11	85.72	160.50
&46	437	21	1566	0.00042	0.81278	33.63	61.45	62.82	157.90
*48	430	22	1445	0.00071	0.81291	33.62	19.06	106.12	158.80
*50	418	21	1452	0.00051	0.82046	33.63	53.91	72.49	160.02
&51	426	23	1472	0.00040	0.82046	33.63	61.86	64.45	159.93
*52	426	22	1442	0.00085	0.82149	33.63	16.71	110.41	160.75
*53	424	22	1450	0.00074	0.81074	29.30	14.69	96.93	140.92
*54	420	24	1505	0.00034	0.82194	29.22	14.61	95.40	139.22
*55	418	23	1459	0.00037	0.82246	33.50	16.67	105.53	155.71
*57?	432	22	1416	0.00034	0.81365	31.39	15.62	99.21	146.23
*59	432	23	1534	0.00037	0.82056	31.56	15.73	106.53	153.82
60	436	26	2804	0.00020	0.82066	31.68	59.85	58.69	150.23
*62	436	27	2441	0.00012	0.82042	20.86	10.41	66.24	97.52
*63	433	26	1514	0.00056	0.82181	33.58	16.57	108.75	158.90
*64	435	28	1456	0.00010	0.82319	33.46	16.67	111.27	161.40
*65	431	28	2862	0.00074	0.82421	33.45	16.47	112.92	162.85
&67	432	28	4207	0.00005	0.82266	33.64	63.46	65.25	162.35
68	435	30	4635	0.00003	0.82275	33.65	63.56	62.33	159.54
69	434	27	4210	0.00023	0.82690	33.60	63.36	65.30	162.26
*70	438	22	3612	0.00057	0.82495	33.64	39.35	77.36	150.35
*102	446	22	1494	0.00088	0.80968	22.53	18.90	80.12	121.56
*103	440	27	1453	0.00085	0.82007	20.75	17.31	75.10	113.16
*104	435	25	1483	0.00080	0.81911	20.49	17.16	67.38	105.04

VANADIUM-OXYGEN-HYDROGEN SYSTEM (WT. LOSS)

RUN#	(g.mol) NO2(ini.)	(g.mol) NAr(ini.)	(g.mol) NH2O(ini.)	(g.mol) N'VO(OH)3	(g.mol) N'V2O3(OH)4	(g.mol) N'VO2(OH)2	(atm) PVO(OH)3	Log PVO(OH)3	(atm) PV2O3(OH)4	Log PV2O3(OH)4	(atm) PVO2(OH)2	Log PVO2(OH)2	(atm) PO2
16	1.19821	1.66542	2.86105	8.58E-06	4.29E-06	8.58E-06	1.24E-06	-5.9071	6.19E-07	-6.2081	1.24E-06	-5.9071	0.1730
?17	1.19336	1.65910	2.69461	8.36E-06	4.18E-06	8.36E-06	1.24E-06	-5.9072	6.19E-07	-6.2082	1.24E-06	-5.9072	0.1768
&19	1.65684	2.29532	3.61115	1.20E-05	5.99E-06	1.20E-05	1.31E-06	-5.8832	6.54E-07	-6.1842	1.31E-06	-5.8832	0.1809
*20	1.59793	2.20930	3.49971	1.26E-05	6.32E-06	1.26E-05	1.42E-06	-5.8466	7.12E-07	-6.1476	1.42E-06	-5.8466	0.1799
*21	1.47700	2.04052	3.34408	8.69E-06	4.34E-06	8.69E-06	1.04E-06	-5.9816	5.22E-07	-6.2826	1.04E-06	-5.9816	0.1774
*22	2.99193	0.99422	3.55555	9.68E-06	4.84E-06	9.68E-06	1.06E-06	-5.9742	5.31E-07	-6.2752	1.06E-06	-5.9742	0.3281
*23	2.36205	1.66948	3.56638	1.19E-05	5.94E-06	1.19E-05	1.29E-06	-5.8902	6.44E-07	-6.1912	1.29E-06	-5.8902	0.2561
24	1.86582	0.00000	3.82950	1.32E-05	6.60E-06	1.32E-05	1.91E-06	-5.7201	9.53E-07	-6.0211	1.91E-06	-5.7201	0.2694
*25	2.40645	0.00000	4.31127	1.64E-05	8.19E-06	1.64E-05	2.01E-06	-5.6966	1.01E-06	-5.9977	2.01E-06	-5.6966	0.2953
*28	1.99832	1.91007	3.51110	1.21E-05	6.05E-06	1.21E-05	1.35E-06	-5.8710	6.73E-07	-6.1720	1.35E-06	-5.8710	0.2224
*29	3.24034	0.89532	3.96833	1.35E-05	6.76E-06	1.35E-05	1.36E-06	-5.8669	6.79E-07	-6.1679	1.36E-06	-5.8669	0.3255
30	2.10861	2.00132	3.96666	1.15E-05	5.77E-06	1.15E-05	1.17E-06	-5.9309	5.86E-07	-6.2320	1.17E-06	-5.9309	0.2141
*33	2.00240	1.90901	3.76763	1.19E-05	5.94E-06	1.19E-05	1.26E-06	-5.9000	6.29E-07	-6.2010	1.26E-06	-5.9000	0.2123
*34	2.17951	2.07099	4.29405	1.42E-05	7.09E-06	1.42E-05	1.36E-06	-5.8669	6.79E-07	-6.1679	1.36E-06	-5.8669	0.2088
*35	3.09269	0.77995	3.72780	1.15E-05	5.77E-06	1.15E-05	1.23E-06	-5.9106	6.14E-07	-6.2116	1.23E-06	-5.9106	0.3291
&36	1.64766	0.78675	5.07795	1.70E-05	8.52E-06	1.70E-05	1.86E-06	-5.7306	9.30E-07	-6.0317	1.86E-06	-5.7306	0.1798
*37	1.64408	0.80563	5.28847	1.80E-05	9.02E-06	1.80E-05	1.90E-06	-5.7207	9.51E-07	-6.0217	1.90E-06	-5.7207	0.1734
&38	1.77986	3.24501	3.48849	1.00E-05	5.00E-06	1.00E-05	9.69E-07	-6.0138	4.84E-07	-6.3148	9.69E-07	-6.0138	0.1723
*39	1.93251	3.09533	4.40534	1.24E-05	6.21E-06	1.24E-05	1.08E-06	-5.9664	5.40E-07	-6.2675	1.08E-06	-5.9664	0.1680
*40	1.64867	1.82037	4.46681	1.39E-05	6.93E-06	1.39E-05	1.42E-06	-5.8483	7.09E-07	-6.1493	1.42E-06	-5.8483	0.1688
*42	2.41403	2.08056	3.45016	9.24E-06	4.62E-06	9.24E-06	9.47E-07	-6.0235	4.74E-07	-6.3246	9.47E-07	-6.0235	0.2476
*43	2.54501	0.69812	4.98905	1.70E-05	8.52E-06	1.70E-05	1.70E-06	-5.7698	8.50E-07	-6.0708	1.70E-06	-5.7698	0.2537
*44	1.61779	0.78655	5.40022	1.23E-05	6.16E-06	1.23E-05	1.28E-06	-5.8921	6.41E-07	-6.1931	1.28E-06	-5.8921	0.1684
*45	1.70147	2.07841	4.33343	6.60E-06	3.30E-06	6.60E-06	6.65E-07	-6.1771	3.33E-07	-6.4782	6.65E-07	-6.1771	0.1715
&46	1.77285	3.23939	3.31122	4.62E-06	2.31E-06	4.62E-06	4.51E-07	-6.3458	2.25E-07	-6.6469	4.51E-07	-6.3458	0.1731
*48	1.62951	0.92403	5.14420	7.81E-06	3.90E-06	7.81E-06	8.24E-07	-6.0838	4.12E-07	-6.3849	8.24E-07	-6.0838	0.1721
*50	1.65970	2.66071	3.57757	5.61E-06	2.80E-06	5.61E-06	5.83E-07	-6.2347	2.91E-07	-6.5357	5.83E-07	-6.2347	0.1724
&51	1.66962	3.07126	3.19996	4.40E-06	2.20E-06	4.40E-06	4.54E-07	-6.3425	2.27E-07	-6.6435	4.54E-07	-6.3425	0.1725
*52	1.64501	0.81731	5.40029	9.35E-06	4.67E-06	9.35E-06	9.77E-07	-6.0103	4.88E-07	-6.3113	9.77E-07	-6.0103	0.1719
*53	1.42082	0.71213	4.69961	8.14E-06	4.07E-06	8.14E-06	9.66E-07	-6.0152	4.83E-07	-6.3163	9.66E-07	-6.0152	0.1686
*54	1.48053	0.74006	4.83356	3.74E-06	1.87E-06	3.74E-06	4.36E-07	-6.3609	2.18E-07	-6.6619	4.36E-07	-6.3609	0.1725
*55	1.65435	0.82328	5.21106	4.07E-06	2.03E-06	4.07E-06	4.35E-07	-6.3613	2.18E-07	-6.6623	4.35E-07	-6.3613	0.1770
*57?	1.49425	0.74352	4.72236	3.74E-06	1.87E-06	3.74E-06	4.37E-07	-6.3595	2.19E-07	-6.6605	4.37E-07	-6.3595	0.1747
*59	1.63464	0.81460	5.51814	4.07E-06	2.03E-06	4.07E-06	4.19E-07	-6.3778	2.10E-07	-6.6788	4.19E-07	-6.3778	0.1684
60	2.96426	5.60007	5.49117	2.20E-06	1.10E-06	2.20E-06	1.28E-07	-6.8914	6.42E-08	-7.1924	1.28E-07	-6.8914	0.1731
*62	1.69898	0.84785	5.39461	1.32E-06	6.60E-07	1.32E-06	1.36E-07	-6.8654	6.82E-08	-7.1665	1.36E-07	-6.8654	0.1755
*63	1.69909	0.83868	5.50339	6.16E-06	3.08E-06	6.16E-06	6.29E-07	-6.2011	3.15E-07	-6.5022	6.29E-07	-6.2011	0.1736
*64	1.62394	0.80885	5.40014	1.10E-06	5.50E-07	1.10E-06	1.16E-07	-6.9372	5.78E-08	-7.2382	1.16E-07	-6.9372	0.1707
*65	3.18924	1.57058	10.76589	8.14E-06	4.07E-06	8.14E-06	4.32E-07	-6.3645	2.16E-07	-6.6656	4.32E-07	-6.3645	0.1693
&67	4.71684	8.89819	9.15023	5.50E-07	2.75E-07	5.50E-07	1.99E-08	-7.7018	9.93E-09	-8.0029	1.99E-08	-7.7018	0.1705
68	5.17104	9.76874	9.57900	3.30E-07	1.65E-07	3.30E-07	1.11E-08	-7.9559	5.53E-09	-8.2569	1.11E-08	-7.9559	0.1735
69	4.75053	8.95962	9.23393	2.53E-06	1.26E-06	2.53E-06	9.11E-08	-7.0403	4.56E-08	-7.3413	9.11E-08	-7.0403	0.1712
*70	4.14299	4.84699	9.52765	6.27E-06	3.13E-06	6.27E-06	2.79E-07	-6.5540	1.40E-07	-6.8551	2.79E-07	-6.5540	0.1846
*102	1.12475	0.94364	3.99977	9.68E-06	4.84E-06	9.68E-06	1.29E-06	-5.8890	6.46E-07	-6.1901	1.29E-06	-5.8890	0.1501
*103	1.00398	0.83740	3.63331	9.35E-06	4.67E-06	9.35E-06	1.40E-06	-5.8539	7.00E-07	-6.1549	1.40E-06	-5.8539	0.1504
*104	1.01715	0.85170	3.34417	8.80E-06	4.40E-06	8.80E-06	1.38E-06	-5.8594	6.91E-07	-6.1605	1.38E-06	-5.8594	0.1598

VANADIUM-OXYGEN-HYDROGEN SYSTEM (WT. LOSS)

RUN#	Log PO2	(atm) PH2O	Log PH2O	LOG K	AVG(LOGK)	DG (cal/mol)
16	-0.7619	0.4132	-0.3839	-10.66250	-10.63	44625.38
?17	-0.7525	0.3993	-0.3988	-10.61814		44408.14
&19	-0.7426	0.3943	-0.4042	-10.55376		44312.74
*20	-0.7449	0.3940	-0.4045	-10.47974		44001.96
*21	-0.7511	0.4016	-0.3962	-10.77465		45146.53
*22	-0.4839	0.3900	-0.4090	-10.72139		45009.25
*23	-0.5916	0.3867	-0.4126	-10.54248		44258.18
24	-0.5696	0.5529	-0.2574	-10.66808		44797.63
*25	-0.5297	0.5291	-0.2764	-10.56392		44360.25
*28	-0.6530	0.3907	-0.4082	-10.51745		44165.13
*29	-0.4874	0.3987	-0.3994	-10.53554		44275.29
30	-0.6694	0.4028	-0.3949	-10.67706		44884.21
*33	-0.6731	0.3994	-0.3986	-10.60423		44658.61
*34	-0.6804	0.4113	-0.3858	-10.57624		44505.38
*35	-0.4827	0.3967	-0.4015	-10.61651		44741.42
&36	-0.7453	0.5540	-0.2565	-10.69173		44960.09
*37	-0.7609	0.5579	-0.2535	-10.68104		44915.62
&38	-0.7637	0.3378	-0.4714	-10.61332		44630.33
*39	-0.7746	0.3830	-0.4168	-10.68255		44921.47
*40	-0.7727	0.4572	-0.3399	-10.67690		44893.79
*42	-0.6063	0.3538	-0.4512	-10.69343		44962.81
*43	-0.5957	0.4974	-0.3033	-10.62956	-10.63	44694.28
*44	-0.7736	0.5622	-0.2501	-11.03381		44331.94
*45	-0.7657	0.4368	-0.3597	-11.27521		45323.51
&46	-0.7617	0.3233	-0.4903	-11.22066		45104.24
*48	-0.7643	0.5432	-0.2650	-11.37264		45715.17
*50	-0.7634	0.3716	-0.4299	-11.17969		44940.57
&51	-0.7632	0.3306	-0.4807	-11.24303		45194.17
*52	-0.7648	0.5642	-0.2485	-11.27498		45322.58
*53	-0.7732	0.5576	-0.2536	-11.26955	-11.23	45300.76
*54	-0.7632	0.5632	-0.2493	-11.97376		45669.70
*55	-0.7521	0.5574	-0.2538	-11.96117		45621.65
*57?	-0.7578	0.5520	-0.2580	-11.94487		45610.85
*59	-0.7738	0.5683	-0.2454	-12.01930		45894.51
60	-0.7618	0.3206	-0.4940	-12.30078		46969.33
*62	-0.7557	0.5573	-0.2539	-12.96918		49521.56
*63	-0.7603	0.5624	-0.2499	-11.65249		44493.91
*64	-0.7679	0.5675	-0.2460	-13.13632		50159.76
*65	-0.7713	0.5715	-0.2430	-12.00020		45822.69
&67	-0.7684	0.3307	-0.4806	-13.96183		53311.89
68	-0.7607	0.3214	-0.4929	-14.43302		55111.07
69	-0.7665	0.3328	-0.4778	-12.64701		48275.19
*70	-0.7338	0.4245	-0.3722	-11.99158	-12.19	45773.32
*102	-0.8237	0.5337	-0.2727	-10.95992		45055.20
*103	-0.8228	0.5442	-0.2642	-10.91508		44870.87
*104	-0.7964	0.5255	-0.2795	-10.88046	-10.92	44728.53

VANADIUM-OXYGEN-HYDROGEN SYSTEM (CONDENSER)

RUN#	(m/d/yr) DATE	(cm Hg) AMB.PRESS.	(Deg. C) AMB.TEMP.	(cm) REACTOR DH	(cm) O2 DH	(cm) AR DH	H2O SET	(Deg. C) BOAT TEMP.	(Deg. C) BOILER	(Deg. C) DEOX.FUNR.	(min) RUN TIME	(g) WT.COND	(atm) Pt
*63	07/22/92	62.48	26.48	-0.30	34.77	29.78	0.06543	561.3	433	26	1514	0.00034	0.822
*64	07/24/92	62.59	27.82	-0.36	34.66	29.93	0.06676	561.3	435	28	1456	0.00036	0.823
*65	07/27/92	62.66	28.37	-0.27	34.65	29.62	0.06771	561.3	431	28	2862	0.00079	0.824
&67	08/03/92	62.54	27.63	-0.24	34.83	39.80	0.03915	561.3	432	28	4207	0.00048	0.823
68	08/06/92	62.55	29.25	-0.28	34.84	39.87	0.03720	561.3	435	30	4635	0.00054	0.823
69	08/10/92	62.87	26.88	-0.34	34.79	39.74	0.03948	561.0	434	27	4210	0.00039	0.827
*70	08/25/92	62.73	21.68	-0.44	34.83	66.38	0.04748	561.0	438	22	3612	0.00054	0.825
*71	08/28/92	62.53	24.23	-0.41	34.62	32.79	0.04438	561.0	435	24	4446	0.00057	0.822
*72	09/01/92	62.35	25.28	-0.35	34.73	33.26	0.04341	561.0	435	25	5757	0.00075	0.820

VANADIUM-OXYGEN-HYDROGEN SYSTEM (CONDENSER)

RUN#	(cc/min) FO2	(cc/min) FAr	(cc/min) FH2O(v)	(cc/min) Tot.Flow	(g.mol) NO2(ini.)	(g.mol) NAr(ini.)	(g.mol) NH2O(ini.)	(g.mol) N'VO(OH)3	(g.mol) N'V2O3(OH)4	(g.mol) N'VO2(OH)2	(atm) PVO(OH)3	% REC	Log PVO(OH)3	(atm) PV2O3(OH)4
*63	33.58	16.57	108.75	158.90	1.69909	0.83868	5.50339	3.74E-06	1.87E-06	3.74E-06	3.82E-07	60.7	-6.4178	0.0000
*64	33.46	16.67	111.27	161.40	1.62394	0.80885	5.40014	3.96E-06	1.98E-06	3.96E-06	4.16E-07	360.0	-6.3809	0.0000
*65	33.45	16.47	112.92	162.85	3.18924	1.57058	10.76589	8.69E-06	4.34E-06	8.69E-06	4.61E-07	106.8	-6.3362	0.0000
&67	33.64	63.46	65.25	162.35	4.71684	8.89819	9.15023	5.28E-06	2.64E-06	5.28E-06	1.91E-07	960.0	-6.7196	0.0000
68	33.65	63.56	62.33	159.54	5.17104	9.76874	9.57900	5.94E-06	2.97E-06	5.94E-06	1.99E-07	1800.0	-6.7006	0.0000
69	33.60	63.36	65.30	162.26	4.75053	8.95962	9.23393	4.29E-06	2.14E-06	4.29E-06	1.55E-07	169.6	-6.8109	0.0000
*70	33.64	39.35	77.36	150.35	4.14299	4.84699	9.52765	5.94E-06	2.97E-06	5.94E-06	2.65E-07	94.7	-6.5775	0.0000
*71	33.42	52.57	73.16	159.16	5.00738	7.87715	10.96186	6.27E-06	3.13E-06	6.27E-06	2.16E-07	172.7	-6.6653	0.0000
*72	33.53	53.30	72.02	158.85	6.46490	10.27614	13.88396	8.25E-06	4.12E-06	8.25E-06	2.21E-07	136.4	-6.6559	0.0000

VANADIUM-OXYGEN-HYDROGEN SYSTEM (CONDENSER)

RUN#	Log PV2O3(OH)4	(atm) PVO2(OH)2	Log PVO2(OH)2	(atm) PO2	Log PO2	(atm) PH2O	Log PH2O	Log K	DG (CAL/MO
*63	-6.7189	0.0000	-6.4178	0.1736	-0.7603	0.5624	-0.2499	-12.0859	46149
*64	-6.6819	0.0000	-6.3809	0.1707	-0.7679	0.5675	-0.2460	-12.0237	45911
*65	-6.6372	0.0000	-6.3362	0.1693	-0.7713	0.5715	-0.2430	-11.9434	45606
&67	-7.0206	0.0000	-6.7196	0.1705	-0.7684	0.3307	-0.4806	-11.9973	45810
68	-7.0016	0.0000	-6.7006	0.1735	-0.7607	0.3214	-0.4929	-11.9225	45525
69	-7.1119	0.0000	-6.8109	0.1712	-0.7665	0.3328	-0.4778	-12.1883	46524
*70	-6.8786	0.0000	-6.5775	0.1846	-0.7338	0.4245	-0.3722	-12.0385	45953
*71	-6.9663	0.0000	-6.6653	0.1727	-0.7628	0.3780	-0.4225	-12.0631	46046
*72	-6.9570	0.0000	-6.6559	0.1731	-0.7617	0.3718	-0.4297	-12.0227	45892

APENDIX II

(SUMMARY OF EXPERIMENTAL CONDITIONS FOR MoO_3(S))

MOLYBDENUM-OXYGEN SYSTEM

Run	Date	Amb.Press.	Amb. Tem	Dh(react.)	Dh(O2)	Dh(Ar)	Boat Tem	Wt. Loss(g)	Time(min)
1	08/25/93	62.26	27.50	-0.60	23.40	39.70	648	0.00699	378
2	08/26/93	62.74	26.52	-0.60	23.40	39.76	648	0.00672	390
3	08/27/93	62.88	23.81	-0.60	27.11	46.95	648	0.00750	373
12	09/24/93	62.47	23.50	-0.55	59.10	34.95	648	0.00637	360
13	09/28/93	62.87	23.72	-0.64	35.27	61.97	648	0.02088	1491
4	08/28/93	62.38	25.25	-0.60	23.40	39.78	702	0.08590	391
5	08/29/93	62.18	27.00	0.20	43.35	26.98	739	0.20144	205
14	10/01/93	62.33	24.50	-0.25	47.43	50.10	674	0.02978	533

MOLYBDENUM-OXYGEN SYSTEM

Run	Pt(atm)	F(O2)	F(Ar)	F(tot)	n(o2)	n(Ar)	n(Mo3O9)	n(tot)	P(Mo3O9)	P(O2)	10^4/T
1	0.81860	25.58481	62.03383	87.6186	0.32091	0.77809	0.00002	1.09902	1.21E-05	0.23903	10.85600
2	0.82492	25.58481	62.12758	87.7124	0.33475	0.81286	0.00002	1.14762	1.12E-05	0.24062	10.85600
3	0.82676	29.64121	73.36243	103.0036	0.37513	0.92846	0.00002	1.30361	1.102E-05	0.23791	10.85600
12	0.82142	64.61805	54.61165	119.2297	0.78501	0.66345	0.00001	1.44847	8.37E-06	0.44517	10.85600
13	0.82659	38.56309	41.31980	79.8829	1.95108	2.09055	0.00005	4.04168	9.89E-06	0.39903	10.85600
4	0.82018	25.58481	62.15884	87.7436	0.33510	0.81413	0.00020	1.14942	1.42E-04	0.23911	10.25483
5	0.81836	47.39750	42.15800	89.5555	0.32286	0.28717	0.00047	0.61050	6.25E-04	0.43279	9.87996
14	0.81988	51.85298	33.40523	85.2582	0.92778	0.59770	0.00007	1.52555	3.71E-05	0.49862	10.55799

MOLYBDENUM-OXYGEN SYSTEM

Run	LogP(Mo3O9)	DG (cal/mol)	T(k)	LnPi
1	-4.91876	20730.01	921.15	-11.3259
2	-4.95132	20867.24	921.15	-11.4008
3	-4.95801	20895.43	921.15	-11.4162
12	-5.07751	21399.06	921.15	-11.6914
13	-5.00484	21092.81	921.15	-11.5241
			avg:	-11.4717
4	-3.84788	17167.47	975.15	-8.8601
5	-3.20390	14836.69	1012.15	-7.3772
14	-4.43106	19201.69	947.15	-10.2029

MOLYBDENUM-OXYGEN-HYDROGEN SYSTEM

Run	Date	Amb.Pres	Amb. Te	Dh(react.)	Dh(O2)	Dh(Ar)	F(H2O) (l)	Boat Temp. (C)	Wt. Loss(g)
6	08/30/93	62.78	22.50	0.33	23.35	53.08	0.02183	702	0.14994
7	08/31/93	62.59	23.00	-0.17	23.35	34.75	0.02706	702	0.16778
8	09/01/93	62.23	24.00	-0.20	23.35	13.20	0.03485	702	0.20433
9	09/01/93	62.19	23.50	-0.07	39.33	35.68	0.01988	702	0.17759
16	10/04/93	62.55	23.00	-0.10	30.73	71.55	0.02876	702	0.44422
10	09/02/93	62.74	22.50	-0.43	23.40	35.73	0.02701	647	0.08105
11	09/03/93	62.65	21.50	-0.40	23.35	34.68	0.02741	609	0.06857
15	10/03/93	62.65	22.50	-0.23	20.05	30.58	0.02868	579	0.03609

MOLYBDENUM-OXYGEN-HYDROGEN SYSTEM

Run	Time(min)	Pt(atm)	F(O2)	F(Ar)	F(H2O)	F(tot)	Nini(O2)	Nini(Ar)
6	252	0.83	25.53	35.39	35.60	96.52	0.21916	0.30382
7	255	0.82	25.53	23.17	44.37	93.07	0.22059	0.20020
8	264	0.82	25.53	8.80	57.67	92.00	0.22629	0.07801
9	332	0.82	43.00	23.79	32.86	99.65	0.47980	0.26548
16	619	0.82	33.59	47.71	47.18	128.48	0.70420	1.00006
10	448	0.83	25.58	23.82	44.12	93.52	0.38984	0.36296
11	839	0.82	25.53	23.12	44.69	93.34	0.72991	0.66110
15	802	0.82	21.92	20.39	46.90	89.21	0.59726	0.55543

MOLYBDENUM-OXYGEN-HYDROGEN SYSTEM

Run	Nini(H2O)	Nini(tot)	Nini(MoO3)	K1	N(H2O)	N(Mo3O9	N[MoO2(OH)2]	N(TOT)	P[O2]	P[H2O]
6	0.30562	0.82860	0.00104	0.00013	0.30498	0.00013	0.00064	0.82873	0.21854	0.30411
7	0.38335	0.80414	0.00117	0.00013	0.38257	0.00013	0.00078	0.80427	0.22583	0.39166
8	0.51113	0.81543	0.00142	0.00013	0.51011	0.00013	0.00102	0.81556	0.22713	0.51202
9	0.36668	1.11196	0.00123	0.00013	0.36598	0.00018	0.00069	1.11214	0.35297	0.26924
16	0.98902	2.69329	0.00309	0.00013	0.98724	0.00043	0.00179	2.69372	0.21513	0.30160
10	0.67225	1.42505	0.00056	0.00001	0.67174	0.00002	0.00051	1.42506	0.22571	0.38893
11	1.27761	2.66862	0.00048	0.00000	1.27715	0.00000	0.00046	2.66863	0.22534	0.39429
15	1.27785	2.43054	0.00025	0.00000	1.27760	0.00000	0.00025	2.43054	0.20251	0.43319

MOLYBDENUM-OXYGEN-HYDROGEN SYSTEM

Run	P[Mo3O9]	P[MoO2(OH)2]	Pt(app.)	K2	Log [K2]	Log P[hyd]	Log P[H2O]	LnP[hyd]	DG(cal/mol)
6	0.00013	0.00064	0.00077	0.00211	-2.67541	-3.19238	-0.51696	-6.16037	11936.47
7	0.00013	0.00080	0.00093	0.00203	-2.69161	-3.09870	-0.40709	-6.19766	12008.73
8	0.00013	0.00103	0.00116	0.00201	-2.69719	-2.98790	-0.29072	-6.2105	12033.61
9	0.00013	0.00051	0.00064	0.00190	-2.72169	-3.29156	-0.56987	-6.26692	12142.93
16	0.00013	0.00055	0.00068	0.00181	-2.74208	-3.26265	-0.52057	-6.31387	12233.89
10	0.00001	0.00030	0.00031	0.00076	-3.11856	-3.52869	-0.41013	-7.18075	13128.85
11	0.00000	0.00014	0.00014	0.00036	-3.4408	-3.84499	-0.40419	-7.92274	13887.24
15	0.00000	0.00008	0.00008	0.00019	-3.71118	-4.07450	-0.36332	-8.54532	14469.12

APENDIX III

(SUMMARY OF EXPERIMENTAL CONDITIONS FOR WO_3(S))

TUNGSTEN-OXYGNEN-HYDROGEN SYSTEM

Run	Date	Amb.Pres	Amb. Te	Dh(react.)	Dh(O2)	Dh(Ar)	F(H2O) (l)	Boat Temp. (C)	Wt. Loss(g)	Time(min
3	09/07/93	62.68	23.00	-0.37	23.35	34.79	0.02753	902	0.04729	385
4	09/08/93	62.55	23.00	-0.35	23.33	53.38	0.02201	902	0.06426	636
5	09/09/93	62.59	23.00	-0.40	23.35	13.15	0.03588	902	0.09282	563
12	10/10/93	62.44	22.50	0.00	65.15	23.75	0.02189	902	0.0773	813
6	09/10/93	62.77	23.50	-0.35	23.35	34.70	0.02626	950	0.13956	556
7	09/15/93	62.29	24.50	-0.40	23.43	34.78	0.02902	985	0.17707	441
8	09/21/93	62.25	25.91	-0.40	23.43	34.88	0.02879	847	0.03299	587
9	10/06/93	62.09	24.79	-0.15	20.01	23.48	0.02885	740	0.01157	1338
10	10/07/93	62.04	23.45	-0.19	34.87	0.00	0.02885	802	0.03051	1130
13	10/12/93	62.34	23.06	-0.25	34.27	0.00	0.02781	699	0.01018	2869

TUNGSTEN-OXYGNEN-HYDROGEN SYSTEM

Run	Pt(atm)	F(O2)	F(Ar)	F(H2O)	F(tot)	Nini(O2)	Nini(Ar)	Nini(H2O)	Nini(tot)
3	0.82	25.53	23.20	45.09	93.81	0.33343	0.30296	0.58884	1.22522
4	0.82	25.51	35.59	36.12	97.22	0.54921	0.76632	0.77769	2.09321
5	0.82	25.53	8.77	58.85	93.15	0.48687	0.16721	1.12225	1.77632
12	0.82	71.23	15.84	35.91	122.98	1.96122	0.43600	0.98870	3.38592
6	0.83	25.53	23.14	43.02	91.68	0.48142	0.43629	0.81114	1.72885
7	0.82	25.61	23.19	48.07	96.87	0.37884	0.34302	0.71099	1.43284
8	0.82	25.62	23.26	47.94	96.82	0.50166	0.45544	0.93887	1.89598
9	0.82	21.88	15.66	47.97	85.51	0.97803	0.69986	2.14452	3.82241
10	0.82	38.13	0.00	47.80	85.92	1.44466	0.00000	1.81114	3.25580
13	0.82	37.47	0.00	45.80	83.27	3.62671	0.00000	4.43261	8.05931

TUNGSTEN-OXYGNEN-HYDROGEN SYSTEM

Run	Nini(WO3)	N(H2O)	N[WO2(OH)2]	N(TOT)	P[O2]	P[H2O]	P[WO2(OH)2]	K2	Log [K2]
3	0.00020	0.58863	0.00020	1.22522	0.22434	0.39605	0.00014	0.00035	-3.46028
4	0.00028	0.77741	0.00028	2.09321	0.21585	0.30554	0.00011	0.00036	-3.44792
5	0.00040	1.12185	0.00040	1.77632	0.22561	0.51986	0.00019	0.00036	-3.44750
12	0.00033	0.98836	0.00033	3.38592	0.47588	0.23982	0.00008	0.00034	-3.47194
						0.00000	0.00000	avg(logk):	-3.45190
6	0.00060	0.81054	0.00060	1.72885	0.22989	0.38705	0.00029	0.00074	-3.12922
7	0.00076	0.71023	0.00076	1.43284	0.21659	0.40606	0.00044	0.00108	-2.96846
8	0.00014	0.93873	0.00014	1.89598	0.21662	0.40534	0.00006	0.00015	-3.81937
9	0.00005	2.14447	0.00005	3.82241	0.20900	0.45826	0.00001	0.00002	-4.63319
10	0.00013	1.81101	0.00013	3.25580	0.36213	0.45396	0.00003	0.00007	-4.13869
13	0.00004	4.43256	0.00004	8.05931	0.36900	0.45100	0.00000	0.00001	-5.00411

TUNGSTEN-OXYGNEN-HYDROGEN SYSTEM

Run	Log P[hyd]	Log P[H2O]	Ln Pi	DG(cal/mol)
3	-3.86254	-0.40225	-7.96759	18604.51
4	-3.96285	-0.51494	-7.93912	18538.03
5	-3.73161	-0.28411	-7.93816	18535.79
12	-4.09206	-0.62011	-7.99445	18667.22
6	-3.54145	-0.41223	-7.20530	17511.75
7	-3.35987	-0.39141	-6.83513	17087.44
8	-4.21155	-0.39218	-8.79442	19574.07
9	-4.97208	-0.33889	-10.66832	21476.71
10	-4.48167	-0.34298	-9.52967	20358.46
13	-5.34994	-0.34583	-11.52240	22257.38

BIOGRAPHICAL NOTE

The author was born in México city on June 21, 1962. He moved to São Paulo, Brasil at the age of 9 where he lived until the age of 19.

The author received his B.S. degree in Chemical Engineering from the Monterrey Institute of Technology (ITESM) in Monterrey, México in June 1986.

In August of 1989, after having worked as process superintendent with Rohm and Haas Co. in the production of acrylic sheets for three years, the author enrolled at the Colorado School of Mines to pursue his doctoral degree in Metallurgical and Materials Engineering.

The author is a member of The Minerals, Metals, and Materials Society (TMS) and the Society for Mining, Metallurgy, and Exploration Inc. (SME).